Université du Québec
Institut national de la recherche scientifique
Centre Armand-Frappier Santé Biotechnologie

Development of rolling circle amplification based biosensing technologies

Par

Seyed Vahid Hamidi

Présenté pour l'obtention du grade
de Philosophiae Doctor (Ph.D.)
en Biologie

Jury d'évaluation

Président du jury et examinateur interne	Prof. Richard Villemur INRS - Centre Armand-Frappier Santé Biotechnologie
Examinateur externe	Prof. Alexis Vallée-Bélisle Université de Montréal
Examinateur externe	Prof. Yingfu Li McMaster University
Directeur de recherche	Prof. Jonathan Perreault INRS - Centre Armand-Frappier Santé Biotechnologie

ACKNOWLEDGEMENTS

This thesis was done under supervision of Professor Jonathan Perreault INRS - Centre Armand-Frappier Santé Biotechnologie, to whom I am grateful for his guidance, support, and inspiring discussions.

I would like to thank professors Prof. Wojtek J Bock, Prof. Ana Tavares, for sharing their labs and instruments and having constructive collaborations with us.

I would also like to thank my Ph.D. evaluation committee members, professors Richard Villemur, Alexis Vallée-Bélisle and Yingfu Li for their constructive comments and also the financial support from Fonds de Recherche du Québec – Nature et technologies and Armand-Frappier Foundation.

I would like to take the chance to thank all Jonathan Perreault's lab members, including Reza, Ryan, Emilie, Sabrine, Vanessa, Aurelie, Kamar, Nour, Philip, Pierre-Luc, Samia, Emre, Vesta, Jay, Gerald, Rehab, Quetia and all scientists at INRS for their help and supports during this journey.

RÉSUMÉ

Les maladies infectieuses sont l'une des principales causes de mortalité humaine et animale. La propagation de maladies infectieuses parmi la faune et les animaux domestiques menace la production animale, l'approvisionnement alimentaire et a également un impact sur la biodiversité environnementale et mondiale. Les gouvernements dépensent beaucoup d'argent pour les soins de santé publics et à ce titre, la surveillance des maladies peut avoir un rôle majeur pour la prévention afin de réduire les risques pour la santé et aussi pour réduire les dépenses publiques en santé. Un exemple actuel evident de l'importance d'un tel suivi est bien illustré par le coronavirus 2 du syndrome respiratoire aigu sévère (SRAS-CoV-2), responsable de la COVID-19.

La méthode standard pour la détection et l'identification des maladies infectieuses telles que le virus de la grippe et le coronavirus est la PCR quantitative (qPCR). La qPCR est une méthode de laboratoire qui nécessite un thermocycleur en temps-réel, qui est coûteux et sophistiqué, ainsi que du personnel de laboratoire formé pour effectuer de tels tests. D'autres méthodes alternatives, y compris le dosage immuno-enzymatique conventionnel (ELISA) et les méthodes basées sur la culture cellulaire, nécessitent également des laboratoires équipés pour effectuer les tests. Par conséquent, le développement d'une méthode simple, sensible, portable, rapide et surtout sans instrumentation, pour la surveillance des maladies infectieuses sur le terrain est très important pour le dépistage rapide des virus et la gestion de la situation en cas de pandémie.

L'amplification en cercle roulant (RCA) est une technique d'amplification d'ADN isotherme biomimétique et en raison de sa robustesse et de sa simplicité, elle peut rivaliser avec les autres méthodes d'amplification isotherme de l'ADN, comme l'amplification isotherme à médiation en boucle (LAMP). La RCA est une réaction de polymérisation d'ADN isotherme qui génère un ADN simple brin à partir d'une courte matrice d'ADN circulaire. Contrairement à la réaction en chaîne par polymérase (PCR) qui nécessite un thermocycleur et une ADN polymérase thermostable, la technique RCA est isotherme et la polymérisation se produit à une température plus basse (25-65 ° C selon les enzymes choisies). La technique a d'abord été menée pour la détection ultra-sensible de cibles ADN et a aussi été combinée à toutes sortes de plates-formes pour la détection très sensible des cibles diverses.

Ici, plusieurs biocapteurs basés sur RCA ont été développés pour la détection de maladies infectieuses en utilisant différentes plates-formes, y compris des plates-formes colorimétriques et optiques. En outre, une nouvelle méthode a été proposée pour la génération d'ADN linéaire et

circulaire monocaténaire *in vitro* en raison des vastes applications dans le domaine de la biologie moléculaire, en particulier dans la procédure du SELEX (*Systematic Evolution of Ligands by EXponential enrichment*). De plus, cette nouvelle technique est utilisée pour la sélection d'aptamères linéaires et circulaires contre le coronavirus du Moyen-Orient (MERS CoV). Voici les principaux objectifs de cette thèse: i) développer une nouvelle technologie colorimétrique basée sur RCA pour la détection simple des maladies infectieuses en utilisant le rouge de phénol comme colorant sensible au pH. ii) Couplage de RCA avec d'autres plates-formes sensibles, y compris la technologie de microcavité optique, comme nouveau moyen de détection sensible des biomarqueurs. iii) Développer une nouvelle technique de préparation *in vitro* d'ADN simple brin linéaire et circulaire (ADNsb). Dans le cadre de l'objectif iii, cette nouvelle technique a été utilisée pour la sélection d'aptamères linéaires et circulaires contre le MERS-CoV.

Le premier objectif de cette thèse, une méthode colorimétrique simple est développée pour la détection spécifique du virus de la grippe H5N1 en utilisant le rouge de phénol comme colorant sensible au pH. Tout d'abord, suite à l'optimisation les paramètres expérimentaux, la performance de la réaction de ligature dans une solution sans tampon (sans Tris-HCl), a été évaluée avec succès, de même que sa sélectivité. Ces travaux ont été publiée dans le journal Talanta. Cette technique conviviale a l'avantage d'être simple, portable et de ne requérir aucune instrumentation due à nature isotherme.

Le deuxième objectif a été réalisé en collaboration avec le laboratoire de photonique de l'Université du Québec en Outaouais. Dans cette étude en couplant deux techniques puissantes, y compris l'interféromètre de Mach Zehnder en ligne à microcavité optique (μIMZI), une plateforme de détection ultra-sensible a été développée pour la surveillance en temps réel des maladies infectieuses et en particulier du virus de la grippe H5N1 (l'objet de cette étude). Ce biocapteur à base de uIMZI fournit une amplification d'ADN dans un volume aussi bas que le picolitre où la réaction RCA est initiée à partir des amorces immobilisées dans la cavité. Cela a conduit à la large plage linéaire de 283 et 2 830 000 copies cibles H5N1 et à une limite de détection (LOD) très basse de 6 copies. Ce travail est publié dans le journal Lab on a Chip.

Dans le cas de l'objectif 3, une nouvelle méthode de préparation in vitro d'ADNsb linéaire et circulaire a été introduite. Bien qu'il existe plusieurs méthodes pour préparer l'ADNsb linéaire à partir de produits, la production d'ADNsb circulaire est toujours un défi. Dans ce travail, en utilisant des modifications dérivées du phosphore, à savoir des liaisons phosphorothioate et des modifications de phosphorylation et en utilisant l'enzyme exonucléase Lamda conventionnelle, la préparation d'ADNsb circulaire à partir d'un produit de PCR a été simplifiée. Cette méthode peut

servir pour des applications telles que le SELEX ou la préparation de PLP basée sur PCR, la préparation de bibliothèque pour séquençage, etc. Les résultats de ce travail seront soumis prochainement pour un troisième article. De plus, pour vérifier les performances de la méthode proposée, 15 cycles de SELEX ont été effectués pour la sélection des aptamères linéaires et circulaires par rapport au MERS CoV.

Mots clés : Amplification en cercle roulant, Biocapteurs, détection colorimétrique, Microcavités optiques, préparation ADNsb circulaire, SELEX.

ABSTRACT

One of the leading causes of human and animal death is infectious diseases. The propagation of infectious diseases among wildlife and domestic animals threatens animal production, food supply and have impacts on the environmental and global biodiversity as well. Governments are spending lots of money on the public healthcare and, in that regard, monitoring of diseases and pathogens can have a major role in prevention to reduce risks for health and decrease the governments' expenses on the public health-care. Also, viral infection of animal population endangers the global public health by introduction of new versions of pandemic viral strain and sporadic human zoonotic infections in view of the fact that animals are regarded to be the cause of about 70% of all emerging infections. An obvious current example of the importance of such monitoring is illustrated by the pandemic of Severe Acute Respiratory Syndrome Corona Virus 2 (SARS-CoV-2).

The gold standard method for detection and identification of infectious diseases such as influenza virus and coronavirus is quantitative PCR (qPCR). qPCR is a lab-based method and it needs an expensive and sophisticated real-time thermal cycler machine as well as trained lab staff members to do such tests. Other alternative methods including conventional enzyme-linked immunosorbent assay (ELISA) and cell culture-based methods also lab need equipped labs to perform the tests. Therefore, developing a simple, sensitive, portable, rapid and more importantly instrumentation-free method for in field infectious disease monitoring is very important for fast screening of the viruses and managing of the situation in case of pandemic.

Rolling circle amplification (RCA) is a biomimetic isothermal DNA amplification technique and because of its robustness and simplicity, it can compete with the other isothermal DNA amplification methods, like loop mediated isothermal amplification (LAMP). RCA is an isothermal DNA polymerization reaction that generate single strand DNA from short circular DNA template. In contrast to PCR which needs thermal cycler and thermostable DNA polymerases, the RCA technique is isothermal, and polymerization occurs at lower temperature (25-65˚C depending on chosen enzymes). The technique was first conducted to ultra-sensitive detection of DNA targets and also combined to all sorts of platform for highly sensitive detection of targets.

Herein, several RCA based biosensors have been developed for detection of infectious disease using different platforms including colorimetric and optical platforms. In addition, a novel method was proposed for in vitro single stranded linear and circular DNA generation due to the broad applications in molecular biology field especially in SELEX procedure. Moreover, this novel

technique is used for linear and circular aptamer selection against middle east corona virus (MERS CoV). Here are the main objectives for this PhD thesis: i) developing a new RCA based colorimetric technology for simple detection of infectious diseases using phenol red as a pH sensitive dye. ii) Coupling RCA with other sensitive platforms including optical microcavity technology as a novel way for sensitive detection of biomarkers. iii) Developing a new technique for in vitro preparation of linear and circular single stranded DNA (ssDNA). As a part of objective iii, this novel technique was used for selection of linear and circular aptamers against MERS-CoV.

In the first objective of this thesis, a simple colorimetric method was developed for specific detection of H5N1 influenza virus using phenol red as a pH sensitive dye. Following optimization, performance of ligation reaction in buffer free solution (without Tris-HCl) was successful and showed excellent selectivity. This work was published in Talanta. This user-friendly technique is simple, portable and does not require instrumentation due to its isothermal nature.

The second objective was performed in collaboration with the photonics lab at Université du Québec en Outaouais. In this study by coupling two powerful techniques including RCA and optical microcavity in-line Mach Zehnder interferometer (μIMZI), an ultra-sensitive detection platform was developed for real-time monitoring of infectious disease and particularly H5N1 influenza virus (the focus of this study). This μIMZI based biosensor provides DNA amplification in a volume of as low as picoliter where RCA reaction is initiated from the immobilized primers in the cavity. This led to the wide linear range form 283 and 2 830 000 H5N1 target copies and very low limit of detection (LOD) of 6 copies. This work was published in Lab on a Chip.

In case of objective 3, a novel method for *in vitro* preparation of linear and circular ssDNA was introduced. Although there are several methods for preparing linear ssDNA from products, producing circular ssDNA is still challenging. In this work by employing phosphor derived modifications namely phosphorothioate bonds and phosphorylation modifications and using conventional Lamda exonuclease enzyme, circular ssDNA preparation from PCR product have been simplified. This method can be used for applications such as SELEX, PLP preparation, library preparation for sequencing, etc. The results of this work will be submitted for a third article. In addition, to verify the performance of the proposed method 15 cycles of SELEX have been done for linear and circular aptamer selection against MERS-CoV.

Keywords: Rolling circle amplification, Biosensors, colorimetric detection, Optical microcavities, circular ssDNA preparation, SELEX.

TABLE OF CONTENTS

LIST OF FIGURES

LIST OF TABLES

LIST OF EQUATION

LIST OF ABBREVIATIONS

(Azidopropyl)triethoxysilane	(AzPTES)
3-ethylbenzothiazoline-6-sulfonic acid	($ATBS^{2-}$)
Ammonium Persulfate	(APS)
Bovine serum albumin	(BSA)
Circle to Circle Amplification	(C2CA)
Circularized DNA	(circDNA)
Triethoxysilylpropyl Succinic Anhydride	(TESPSA)
Clustered regularly interspaced short palindromic repeats	(CRISPR)
Coronavirus disease 2019	(COVID-19)
Deoxynucleotide triphosphate	(dNTP)
Dissociation constant	(K_D)
Double-strand DNA	(dsDNA)
Exonuclease III-Assisted Cascade Signal Amplification	(Exo III)-aided
Glutamate dehydrogenase	(GDH)
Gold nanoparticle	(AuNP)
Helicase-dependent amplification	(HAD)
Hemagglutinin	(HA)
Hybridization chain reaction	(HCR)
Hydrofluoric acid	(HF)
Hydroxy naphthol blue	(HNB)
Hyperbranched RCA	(HRCA)
Limit of detection	(LOD)
Linear RCA	(LRCA)
Long period fiber grating	(LPFG)

Loop mediated isothermal amplification	(LAMP)
Microcavity in-line Mach Zehnder interferometer	(μIMZI)
Middle east respiratory syndrome corona virus	(MERS CoV)
Molecular Inversion Probes	(MIP)
N,N,N',N'-tetramethylethane-1,2-diamine	(TEMED)
Neuraminidase	(NA)
Next generation sequencing	(NGS)
Nucleic acid amplification tests	(NAATs)
Nucleic acid sequence-based amplification	(NASBA)
Oligonucleotide Ligation Assay	(OLA)
Padlock probe	(PLP)
Point of care	(POC)
Polymerase chain reaction	(PCR)
Pyrophosphate	(PPi^{-})
quantitative PCR/Real time PCR	(qPCR)
RCA products	(RCPs)
Receptor Binding Domain	(RBD)
Refraction index unit	(RIU)
Rolling circle amplification	(RCA)
Recombinase polymerase amplification	(RPA)
Severe acute respiratory syndrome coronavirus 2	(SARS-CoV-2)
Severe Acute Respiratory Syndrome	(SARS)
Signal mediated amplification of RNA technology	(SMART)
Single nucleotide polymorphism	(SNP)
Single stranded DNA	(ssDNA)
Single stranded PCR products	(ssPCRPs)

Strand displacement amplification	(SDA)
Surface plasmon resonance	(SPR)
Systematic Evolution of Ligands by Exponential Enrichment	(SELEX)
T4 Polynucleotide Kinase	(PNK)
WarmStart	(WS)
World Health Organization	(WHO)

1 INTRODUCTION

1.1 Biosensors

Analytical methods are techniques by which the study of separation, identification, purification and quantification of components (biological or chemical) become possible. These techniques have wide applications in different fields including medicinal, industrial and environmental analysis, quality control, forensics, etc. With the quantification and qualification of biological samples, physicians are able to evaluate different parameters of patient states, make a diagnostic and prescribe care accordingly. A biosensor is composed of three different parts including the sensitive layer, transducer and driving circuit. The sensitive layer, which is usually the immobilized layer, has selective interactions with a specific target molecule. Transducer converts the microscopic signal that happens because of interactions among bio-receptors and targets into macroscopic signal. The third part is a driving circuit which amplifies this signal to a stable electrical signal (Fig. 1.1) (Tsouti *et al.*, 2011). Biosensors are used in different fields including general healthcare monitoring, screening for disease, veterinary and agricultural applications, industrial processing and environmental pollution control. Among these applications, health care technology has witnessed most improvements in the field of biosensors during these years. Improvements are continuously made to design fast, cheap and portable devices which can analyze genetic profiles or other analytes easily and precisely. They aim to relinquish the classical ways of medical diagnosis and start to design miniaturized and label free systems. Therefore, about 10 years ago the world health organization (WHO) came up with a new idea of ASSURED (affordable, sensitive, specific, user-friendly, rapid, equipment-free, delivered) to describe an ideal test to meet all the demands for all developing and developed countries.

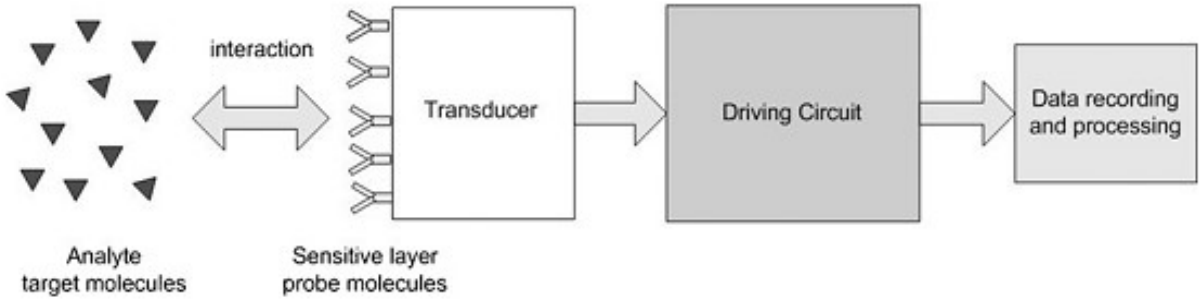

Figure 1.1 Schematic illustration of biosensors. Adapted from (Tsouti *et al.*, 2011) with permission.

Biosensors are categorized in different types depending on the type of the transducer into optical, electrochemical, acoustic, mechanical, etc. In addition, each biosensor is classified based on the platform that is used in developing of the biosensor. For instance, optical biosensors are classified into the chemiluminescence, UV-visible, electrochemiluminescence, fluorescence as well as optical fiber-based biosensors including long period fiber grating (LPFG) and microcavity one. In fluorescent biosensors, fluorescence is emitted when the electron goes back to the lower energy orbitals from the orbitals with higher energy levels. However, LPFG and microcavity are based on the diffraction of the light from the core area into the cladding area depending on the changes in refractive index (RI) of sensing area (Chen *et al.*, 2020, Eftimov *et al.*, 2019). Electrochemical transducers used in biosensors have different categories such as potentiometric, voltametric, etc. In potentiometric sensors, the potential of a cell is measured when the current is zero. However, in the voltametric, by applying the appropriate potential to electrodes in an electrochemical cell, the electroactive species in the solution are oxidized or reduced which results in changes of the current (Cho *et al.*, 2020).

1.1.1 Commercialized biosensors

The biosensor market has substantially expanded and will be growing during the next decade. The total biosensor market worth is estimated to be $36.7 billion by 2026 and so many different biosensors have been commercialized for POC purposes that each works based on a specific technology.[1] Among commercialized biosensors glucometers and pregnancy tests are popular examples that are working based on electrochemistry and lateral flow systems, respectively. Lateral flow tests can be performed by a healthcare professional in clinics or by patients at home, Lateral flow tests use immunoassay-based technology that is generally comprised of nitrocellulose membrane, nanoparticles, and antibodies. Once the sample is added, it flows through the strip by passing along the conjugate pad and then nitrocellulose membrane and finally absorbent pad. The sample pad acts as a filter, for accurate flow of the sample. In the presence of specific target, they are bounded with immobilised antibodies and label antibodies that are all stored in the conjugate pad to finally lined up at the test line to form a coloured line. The density of the colored lines is dependent on the quantity of targets in the sample. Therefore, sometimes it is necessary to combine this rapid test with a reader to get quantitative results (Koczula *et al.*, 2016).

[1] www.marketsandmarkets.com

Glucometers come with strips that have a capillary to take the blood to the test strip where glucose oxidase enzyme is immobilized on an electrode. Catalyzing of the glucose by oxidase enzyme causes electrical current which is read by glucose meter. The created current in the electrode is proportional to the quantity of the glucose in the blood. It is necessary to evaluate glucose meters before use since several factors can affect the accuracy of results such as environmental exposure, operator technique, physiologic of patient and effects of medication. Therefore sometime the results given by glucose meter are not matched with clinical ones (Tonyushkina *et al.*, 2009).

1.1.2 Optical biosensors

Optical biosensors are one of the common types of analytical devices that are produced by integration of an optical transducer with biorecognition elements. This type of biosensor is categorized in two general categories including label-free and label-based ones. In label-free optical biosensors, signal is generated by direct interaction of analytes with optical transducers. On the other hand, in the label-based modes signal is created by integrating fluorescent or luminescent molecules with optical transducers. So far several types of optical biosensors such as LPFG, SPR, evanescent wave fluorescence as well as bioluminescent optical fibre biosensors have been developed (Damborský *et al.*, 2016). Although LPFG, SPR, evanescent wave fluorescence and bioluminescent ones are still very popular biosensors for pathogens, cancers, and infectious diseases detection, they are labeled based sensors which needs time consuming and costly process of integration of transducer with fluorophore molecules. In addition, LPFG based sensors are temperature sensitive which can cause variation of signal during detection process. The recent optical microcavity based biosensors are label free, temperature insensitive biosensor and highly reproducible biosensors which covers all deficient that happen in other optical sensors. Furthermore, very minute a mount of targets at the scales of few copy numbers can be detected by microcavities which has not been achievable by former biosensors (Janik, 2019, Neumann *et al.*, 2007).

1.1.2.1 Microcavity based biosensors

Due to the advancements in surface micromachining technology, including femtosecond laser technology, new ways for sensing approaches have been introduced. These advances allowed in-fiber microcavities as a new classes of sensing platform. In this platform a tiny microcavity in the order of tens of micrometers is fabricated in an optical fiber. Although this new platform has

been frequently used for different purposes so far, biosensors development using microcavity-based platforms have been rarely reported in the literature. However, due to the sensitivity, miniaturized feature, and design to quantify samples as low as picoliters, compatibility with biological samples as well as temperature insensitivity, microcavity-based platforms are good candidates for development of highly sensitive biosensors (Janik, 2019, Zhao *et al.*, 2019)

So far, many techniques have been employed for microholes or microchannels fabrication in optical fibers. The most efficient and user-friendly technique for this is femto-second laser micromachining (Donlagic, 2011). The other alternatives for microcavity fabrication use long and multistep procedures of wet etching (using hydrofluoric acid (HF) or other etchants) (Pevec *et al.*, 2014) and fusion splicing (Hu *et al.*, 2012). However, these methods are time-consuming and acquired reflective index (RI) sensitivity through these procedures hardly surpasses 1000 nm/RIU (Liao *et al.*, 2012, Wei *et al.*, 2008).

Microcavity in-line Mach-Zehnder interferometer (μIMZI) is adapted from microcavity systems and fabricated by well controlled optical fiber cladding and partial ablation of core areas in dimensions of about one hundred micrometers. When the incoming light into the optical fiber reaches the cavity, it is splitted into two beams, where the beam in the fiber core stays in the core, meanwhile the one in the cladding area is propagated throughout the cavity (Fig. 1.2). It is worth to note that the optical characteristics of μIMZI are controlled by shape, size as well as microcavity position. Due to the size at micrometer scales, this platform is able to evaluate sub-nanoliter volumes of samples. One of the main advantages of μIMZI is that the fiber core can directly interact with the external media which in turn leads to RI sensitivity of the system over 20,000 nm/RIU (one of the RI based sensitive platform to date (Janik *et al.*, 2017)). Unlike the long period fiber grating (LPFG) technique, this system is not temperature sensitive and due to its precise fabrication, this device is small, highly sensitive and also reproducible (Janik, 2019).

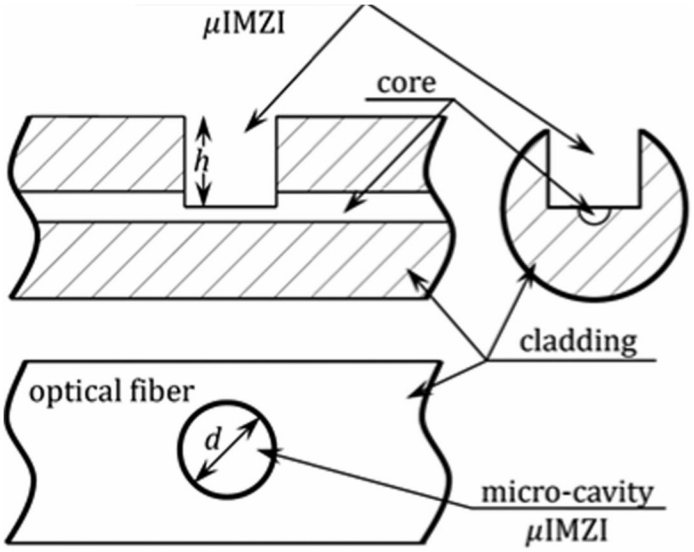

Figure 1.2 Schematic illustration of μIMZI structure. Adapted from (Eftimov *et al.*, 2019) with permission.

Although so far, many biosensors and detection platforms have been developed for selective targeting of biomarkers, detection of very low a mounts of targets or even a few copy numbers are still challenging. In most of the time the clinical samples matrix have a low abundance of biomarker/targets which means that in some cases some sorts of nucleic acid amplification may be demanded to get enough concentration of target molecules to be used for point-of-care testing (POC). Nucleic Acid Testing (NAT) are sensitive, rapid, and selective ways for detection of infectious, congenital diseases and pathogens. Among NAT techniques, isothermal DNA amplification method much simpler and more user-friendly since they can perform DNA amplification at moderate temperature, and they do not rely on thermal cycler machines (Craw *et al.*, 2012). Here we introduce several popular isothermal amplification methods that have been utilized for specific biomarkers/targets monitoring.

1.2 Isothermal nucleic acid amplification technologies

Isothermal nucleic acid amplification techniques are powerful molecular tools that have been widely used in the fields of nano-biotechnology and molecular diagnostics. Although polymerase chain reaction (PCR) is the gold standard technique for molecular tests including detection, identification and quantification of nucleic acids, it needs sophisticated and expensive thermal cycler devices for DNA denaturation, annealing and amplification steps. In contrast, isothermal DNA amplification techniques do not require thermocyclers and are able to perform DNA amplification at constant temperature. Identification of DNA polymerase enzymes with DNA

displacement activity make it possible to do DNA amplification at isothermal condition. So far, several DNA polymerases with displacement activities have been discovered, such as Φ29 DNA polymerase, Sequenase, Klenow and Vent (exo-) enzymes, and the large fragment of Bst DNA polymerase (Demidov, 2002). So far, several types of isothermal nucleic acid amplification techniques have been developed including nucleic acid sequence-based amplification (NASBA), signal mediated amplification of RNA technology (SMART), recombinase polymerase amplification (RPA), strand displacement amplification (SDA), rolling circle amplification, loop-mediated isothermal amplification (LAMP), helicase-dependent amplification (HDA) (Demidov, 2002, Gill *et al.*, 2008, Leonardo *et al.*, 2021, Obande *et al.*, 2020).

Table 1.1 compares different aspects of these isothermal nucleic acid amplification techniques which clearly depicts advantages and disadvantages each method over the others. NASBA and SMART technique are categorized in the first group of Table 1.1 which use transcription to amplify the sample target. In the second group (RPA and HDA) helicase enzyme is used to unwind the double stranded DNA in the target molecule to let the primer to hybridize and find the target site. The third group is working based on the strand displacement activity of the DNA polymerase such as Phi29 and Bst DNA polymerases, so that in this type of amplifications (RCA and LAMP) there is no need for helicase enzymes. The fourth group is working based on the same principle as the third group, however in this case the hyperbranched form of the product caused by SDA amplification is digested by restriction enzyme to purify a specific target site or gene.

Numerous of the isothermal DNA amplification presented in the Table 1.1 have DNA amplification efficiency, sensitivity, and specificity equal to the conventional molecular PCR/qPCR methods. Therefore, one may conclude that due to the possibility for miniaturisation (because of their isothermal nature), such strategies will be popular in the next generation of POC diagnostic devices. Especially for the purpose of personalised healthcare using mobile and electronic healthcare (mHealth/eHealth). However, after about 20 years of introduction of isothermal amplification techniques, the filed of isothermal NAT has not witnessed obvious applications in the market. This is not because of their technical deficiency, but it is more about the complicated engineering fine tuning challenges that are needed to be addressed to automate and integrate of these technologies in portable devices. This requires multidisciplinary approaches and knowledge to meet all the obstacles and challenges that cause delay the development of these devices (Craw *et al.*, 2012).

In this thesis the aim is to use rolling circle amplification (RCA) as an isothermal DNA amplification technique to develop biosensors using different platforms. In the following section we first

introduce some prevalent isothermal amplification methods that have been employed in POC including, nucleic acid sequence-based amplification (NASBA) and loop mediated isothermal reaction (LAMP). Thereafter, we explain the basic mechanism, principle, and modes of RCA technologies since RCA is a central signal amplification method that is used in this work. Then a summary on approaches employed to visualize and detect RCA product is given which provides readers a short overview on works that are done in this area. This part is then followed by a subsection on padlock probes (PLPs) and applications in medical diagnosis in combination with RCA techniques. Finally, we describe some of the applications of PLP based RCA in POC (using colorimetric strategies), nanotechnology and biomaterials.

Table 1.1 Comparing different features of isothermal nucleic acid amplification methods.

Method	Reaction temperature (˚C)	Reaction duration (min)	NO of primers	Multiplex[a]	Rapid detection format[b]	Target	Amplification product	Refs
1. RNA based transcription methods								
NASBA	41	105	2	Y	RTF, NALF	DNA, RNA	RNA, DNA	(Gracias *et al*., 2007)
SMART	41	180	1	N/A	RTF	DNA, RNA	RNA	(Wharam *et al*., 2007)
2. DNA based amplification methods with enzymatic duplex melting/primer annealing								
RPA	30-42	60	2	Y	RTF, NALF	DNA	DNA	(Lutz *et al*., 2010)
HDA	65	90	2	Y	RTF, NALF	DNA	DNA	(Jeong *et al*., 2009)
3. DNA-polymerase-mediated strand displacement methods based on targeting linear or circular targets								
LAMP	65	90	6	N/A	RTF, NALF, RTT, TE	DNA, RNA	DNA	(Curtis *et al*., 2009)
RCA	25, 37, 65	60-90	1, 2	Y	RTF, NALF, RTT, TE	DNA, RNA	DNA	(Johne *et al*., 2009)
4. Isothermal methods based on polymerase extension and a single strand cutting event								
SDA	37	120	4	Y	RTF, NALF	DNA	DNA	(Hellyer *et al*., 2004)

[a] Multiplexing is defined as an ability to amplify different targets simultaneously, yes (Y) or data not available (N/A).
[b] nucleic acid lateral flow (NALF), real-time fluorescence (RTF), real-time turbidity (RTT), turbidity related endpoint (TE).

1.2.1 Nucleic acid sequence-based amplification (NASBA)

NASBA is an isothermal DNA amplification technology that targets RNA and DNA. The NASBA reaction is composed of repeating steps including annealing of primer, double-stranded DNA (dsDNA) production, and finally exponential transcription from the dsDNA target produced by a reverse transcriptase enzyme. Thus, at the beginning of NASBA reaction, a complementary DNA strand is produced from the RNA target using the first primer and AMV reverse transcriptase

enzyme, then the RNA strand is degraded by RNase H enzyme. Thereafter, the double-stranded DNA is produced by annealing of the secondary primer and the action of reverse transcriptase enzyme. Then, the embedded T7-RNA-polymerase-promoter overhang is utilized as a starting point for exponential RNA production using T7 RNA polymerase. This results in exponential production of RNA targets that are used as templates for further NASBA cycles (Böhmer *et al.*, 2009) (Fig. 1.3). It is worth to note that NASBA is performed isothermally which means that this type of amplification can be done in a simple incubator, however PCR needs a thermal cycler machine. In addition, because NASBA is based on the transcription of RNA, a huge amount of RNA is generated in each cycle. Therefore, the efficiency of NASBA is supposed to be much better than PCR amplification which is restricted to dual increases in each cycle (Uyttendaele *et al.*, 1999).

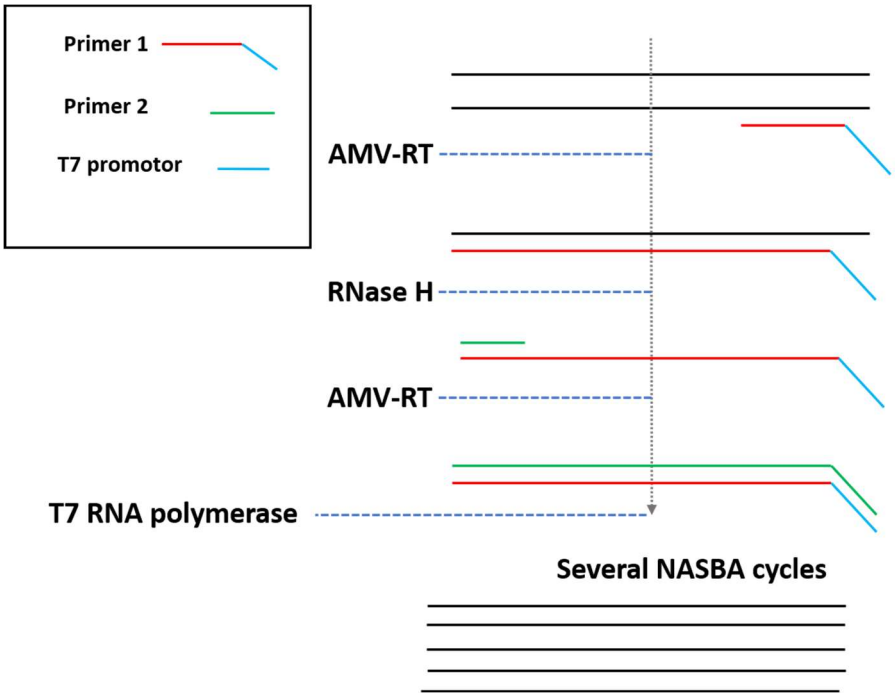

Figure 1.3 **Visual illustration of NASBA reaction.**

1.2.2 Loop mediated isothermal reaction (LAMP)

LAMP is an isothermal DNA amplification reaction that targets DNA/RNA sequence with elevated specificity and sensitivity. LAMP reaction is consisting of three major steps including initial step for primers hybridization, amplification step, and elongation step. LAMP reaction now typically uses the Bst DNA polymerase enzyme which has a strong strand-displacement activity enabling this reaction to be performed at isothermal condition. In this isothermal DNA amplification reaction two inner primers (FIP, BIP) and outer primers (F3, B3) are designed to recognize six different

sequences in the target (Fig. 1.4). This highly increases the specificity, since LAMP reaction can only occur when all selected 6 sequences within the target are properly detected and hybridized by inner and outer primers. In addition, it is possible to target RNA sequence using reverse transcription LAMP (RT-LAMP) strategy by employing reverse transcriptase enzyme. Although PCR has a broad application as a basic tool in molecular biology and is the gold standard method in molecular diagnostics, the selectivity and isothermal nature of LAMP reaction makes it a user-friendly rapid test for nucleic acid testing. In contrast with PCR technique, isothermal LAMP reaction does not need any thermal cycle device to do DNA amplification and also using three pairs of primers (instead of one primer pair in PCR), highly increases the selectivity of LAMP process (Table. 1.1) (Mori *et al.*, 2009, Tomita *et al.*, 2008).

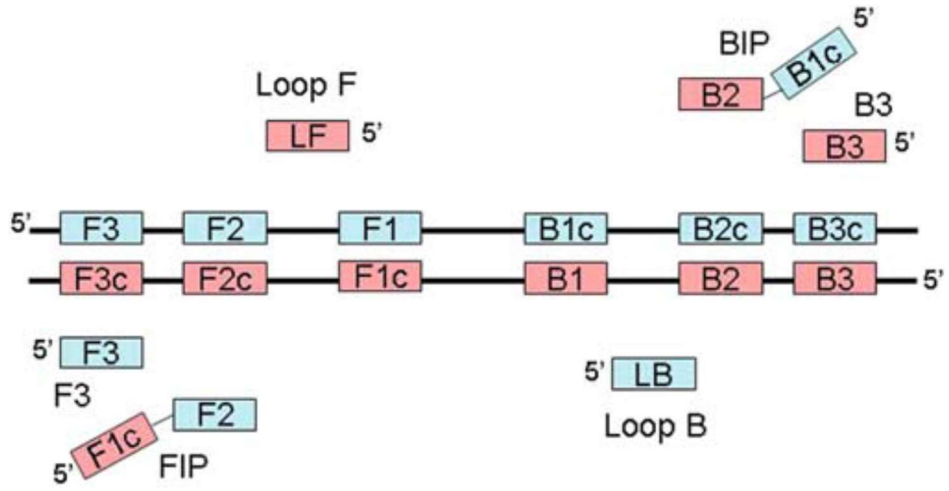

Figure 1.4 Schematic visualization of LAMP reaction. Adapted from (Mori *et al.*, 2009) with permission

1.2.3 Rolling circle replication is a bio mimetic technique

Many phages use rolling circle replication mechanism to replicate their genomes. The genome of the phage φX174 is a single-stranded circular DNA which is called plus (+) strand and a complementary strand DNA (minus (-) strand) is synthesized during genome replication. This produces the covalently closed circular dsDNA which is then amplified by a rolling circle replication reaction (Fig. 1.5). The protein A, which is coded by the phage genome, cleaves the plus strand of the dsDNA at the origin of replication and remains attached to the 5' end of the nicked site. This generates the 3' OH used as a primer by the DNA polymerase enzyme for DNA amplification (Lewin, 2004). It is worth to note that the structure of the DNA is very important in this process since only the negatively super coiled DNA is cleaved by the A protein.

Thereafter, rolling circle replication is initiated by extending the DNA from the 3'-OH end by using the minus circular strand as a template and it amplifies DNA by displacing the downstream DNA until it reaches the starting point. At this point, protein A functions again by sealing the head to tail of newly synthesized DNA and making new single strand circular DNA genomes. It remains connected with the rolling circle as well as to the 5' end of the displaced tail, and it is therefore in the vicinity as the growing point returns past the origin. Therefore, the same protein A is available again to recognize the origin and nick it, now attaching to the end generated by the new nick. The cycle repeats in order to produce further φX174 phage genomes (Fig. 1.5) (Lewin, 2004).

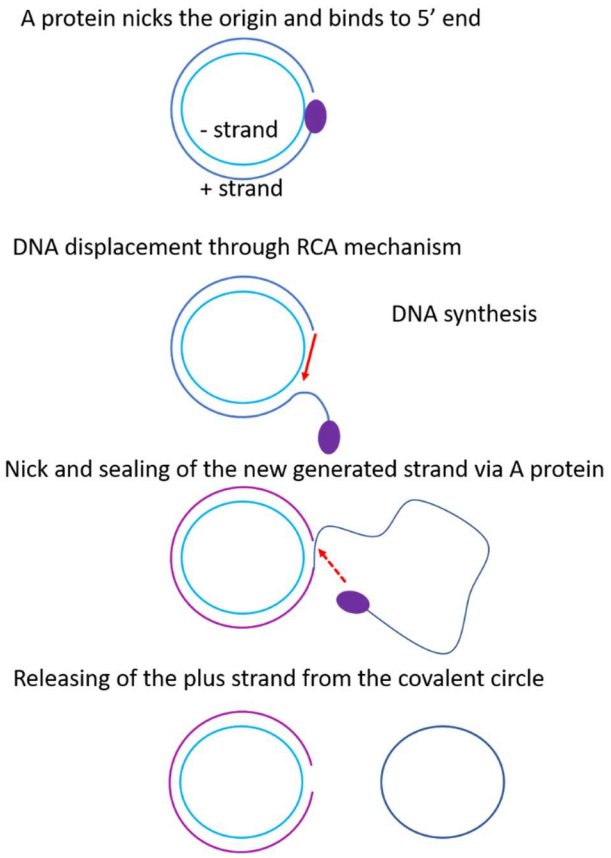

Figure 1.5 Rolling circle replication in φX174 phage.

1.2.4 Principle of rolling circle amplification

Rolling circle amplification (RCA) is an isothermal amplification method and is simpler and more robust than other isothermal amplification techniques such as loop mediated isothermal amplification. As compared with LAMP method where six sophisticated primers are used, designing RCA primers is much simpler and can perform exponential amplification in the presence of just two primers. In addition, RCA can perform DNA reaction at moderate temperature (37 ˚C)

or even at room temperature (compared to LAMP where the reaction is done at 65 ˚C) which makes RCA much more compatible with other platforms including electrochemistry, Surface Plasmon Resonance (SPR) and optical ones (Table. 1.1) (Ali *et al.*, 2014, Xu *et al.*, 2021). This technique is based on the fundamental property of a circular DNA and it is divided in two models: Linear RCA (LRCA) and Hyperbranched RCA (HRCA). In LRCA, one primer is used for starting the RCA reaction and produces long ssDNA (Fig 1.6. A). The products of this mode of RCA generally exhibit a wide, continuous distribution of DNA length and as a result they have a broad smear of the high molecular weight DNAs on gel electrophoresis (Demidov, 2002, Lizardi *et al.*, 1998). HRCA is also called double-primed, geometric, hyperbranched, ramification or cascade RCA and in this DNA amplification reaction two primers are used, including sense primer and anti-sense primer. Therefore, in this mode of RCA, the long multimeric DNA produced by RCA also serves as a template for multiple primer extensions, because of strand displacement, these also serve as templates for primer extensions, and so on (Fig 1.6. B). Consequently, high molecular weight of dsDNA is produced which is similar to the ladder type bands in the gel electrophoresis. In case of the potential of the amplification reaction, HRCA is more robust in comparison with LRCA technique and has the ability to produce more than 10^9 copies of the initially circular DNA template in less than one hour. Therefore, due to the power of HRCA in amplifying DNA, it can detect less than 10 circular DNA molecules (Demidov, 2002, Li *et al.*, 2019, Lizardi *et al.*, 1998).

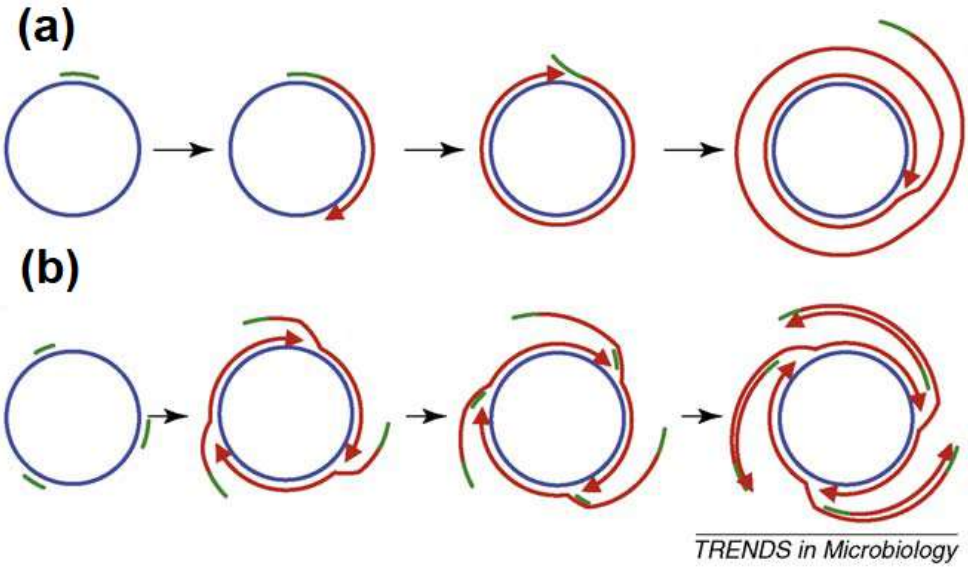

Figure 1.6 **Principle of rolling circle amplification. (a) and (b) show the LRCA and HRCA, respectively. Arrows show the direction of DNA amplification. Adapted from (Johne *et al.*, 2009) with permission.**

1.2.5 Methods that are used for detection of RCA products

The are several ways for monitoring RCA products (RCPs) such as detection in real-time, RCP monitoring using solid support, gel-based visualization and *in situ* detection. Some of the most frequently used methods are described.

Polyacrylamide or agarose gel: Due to the high molecular weight of RCPs, most of the time RCPs do not go through the gel and stay in gel wells or get a huge DNA smear which is consistent with the nature of RCPs (Baner *et al.*, 1998) (Fig. 1.7. A). Therefore, in order to avoid DNA smear in gel electrophoresis, sometimes restriction enzymes are used which cleave repetitive sequences that are produced during RCA reaction and give specific band after running the gel (Hamidi *et al.*, 2015b, Liu *et al.*, 1996).

Solid support detection: RCPs can also be detected using solid support strategy, where RCA primers for RCA initiation are immobilized on a solid surface such as on a tissue or a microscope glass slide. Thereafter, during RCA reaction fluorophore labeled oligonucleotides are hybridized to the tandemly repeated single stranded RCPs that are visible as shiny fluorescent dots under a fluorescent microscope. Because RCPs form localized structures due to their coiled structures, they are seen as individual dots under the microscope (Goo *et al.*, 2016, Nallur *et al.*, 2001) (Fig. 1.7. B).

Single RCPs detection through microfluidic systems: unlike solid support detection, in microfluidic based detection format RCPs are not fixed to a surface but are loaded in a flow micro channel that is coupled to a microscope. This detection format allows single RCP detection when each RCP passes the microscope's objective (Gu *et al.*, 2018, Jarvius *et al.*, 2006).

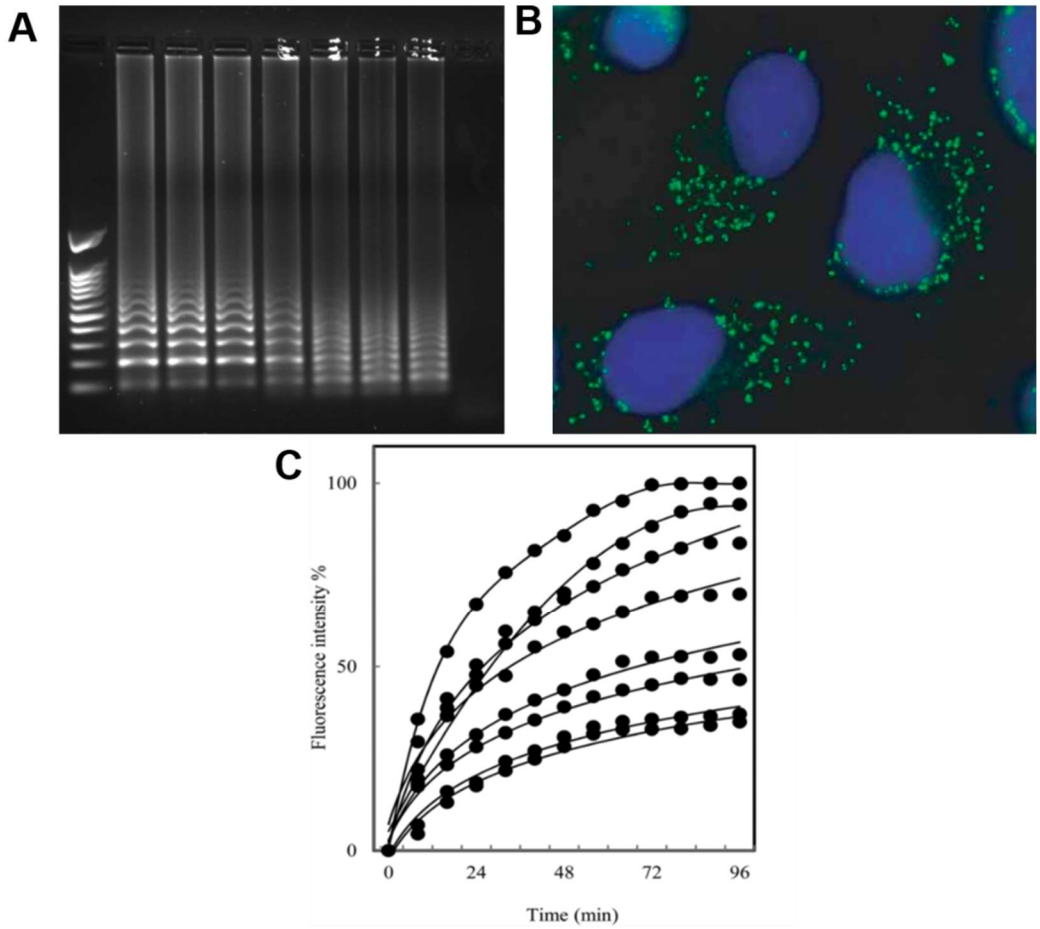

Figure 1.7 **Different method for detection of RCPs. (A) RCA product visualization using agarose gel and Gel red dye. (B) RCPs illustration on solid support and utilizing fluorophore labeled oligonucleotides. (C) Real time monitoring of RCA using DNA intercalating dyes. Adapted from (Hamidi *et al.*, 2015b, Jarvius *et al.*, 2006) with permission.**

Real-time RCP detection: DNA synthesis through RCA can be tracked in real-time via DNA intercalating molecules such as SYBR Green (Fig. 1.7. C) or using molecular beacons (Hamidi *et al.*, 2015b) (Fig. 1.8. A). It is reported that molecular beacons can fold in a structure which quench the fluorescence even after binding to the single stranded RCPs (Fig. 1.8. B). It could be prevented by designing the molecular beacon in a way that one of the arms and the backbone hybridize with the RCPs (Fig. 1.8. C). Another challenge is that some enzymes that are used for rolling DNA synthesis process have some 3' to 5' exonuclease activity on single stranded DNA that leads to degradation of molecular beacon structures and production of false negative signal. This problem has been solved by imbedding 2-O-Me-RNA modification at 3' end of molecular beacon to protect it from degradation (Ali *et al.*, 2014, Nilsson *et al.*, 2002) . In addition, SYBR Gold and SYBR Green have been widely used for monitoring of RCPs, however such detection is not suggested for multiplexing purposes.

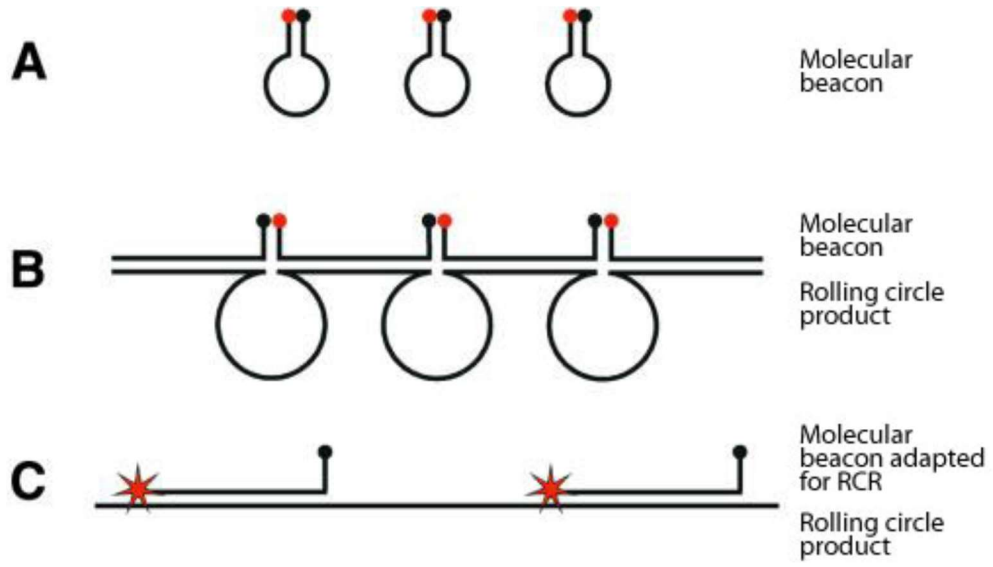

Figure 1.8 **RCP monitoring using molecular beacons (A) Schematic representation of molecular beacons. (B) Secondary structures in RCPs cause molecular beacon quenching. (C) Adapted molecular beacons for rolling circle DNA synthesis. Adapted from (Nilsson *et al.*, 2002) with permission.**

1.3 Padlock probe is adapted from Oligonucleotide Ligation Assay method

Oligonucleotide Ligation Assay (OLA) was proposed by Landegren et al. in 1988 for multiplex detection of single nucleotide polymorphism (SNP) by using the PCR method. This technique is based on the exact hybridization of the two oligonucleotides next to each other followed by ligation reaction in case the two oligonucleotides are fully hybridized at the site of ligation. Because this reaction relies on the exact hybridization of two oligonucleotides at the site of ligation, this method has potential to detect SNPs (Fig. 1.9. A) (Landegren *et al.*, 1988).

Padlock probe (PLP) was developed based on the principle of the OLA technology, however in this technique a single oligonucleotide is circularized upon specific detection of the target. This type of probe was first introduced by Nilsson et al., in 1994 for detection of linear targets by using the RCA method. The PLP is a circularizable probe that has two specific sequences in order to distinguish and hybridize the target and also a linker part to help formation of a circular template and provide room for hybridization of additional primers (Fig. 1.9. B). PLPs have several advantages over OLA including: i) PLPs are topologically linked to the target after ligation which makes it possible to use stringent washing after ligation step if the target is attached to some solid-support; ii) in this method one probe is used, therefore this technique is simpler in comparison with the OLA procedure; and iii) using PLPs makes it possible to amplify the signal by using the RCA technique (Nilsson *et al.*, 1994, Xu *et al.*, 2021).

It is reported that RCA can be suppressed if the PLP is topologically locked to the target sequence. However, this problem can be solved if the ligation sequence of the PLP is located in the vicinity of the free ends of the target molecule (3´ or 5´ ends) which enables the circular PLP to be freed from the target after starting the RCA reaction (Koch, 2003, Larsson *et al.*, 2004b). On the other hand, other studies claimed that topological hindrance does not impede the DNA polymerase from amplifying the circular PLP. One may conclude that the difference in these publications is the use of two different DNA polymerases (Baner *et al.*, 1998, Hamidi *et al.*, 2015a, Kuhn *et al.*, 2002).

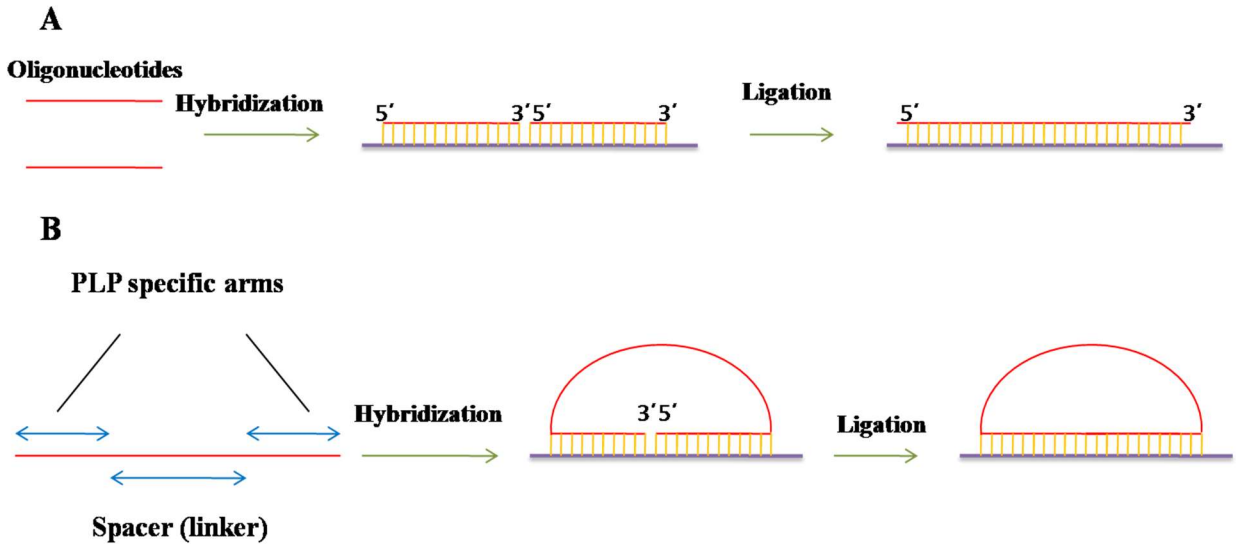

Figure 1.9 Schematic visualization of the (A) OLA and (B) PLP methodologies.

1.3.1 Application of PLPs in pathogen detection

As previously mentioned, PLPs have the advantage of combination with RCA method for exponential signal amplification. Due to simplicity and isothermal nature of RCA based PLP, various works have been done for detection of DNA and RNA viruses using this isothermal DNA amplification technique (Ciftci *et al.*, 2020, Gyarmati *et al.*, 2008, Hamidi *et al.*, 2015a, Ke *et al.*, 2011, Neumann *et al.*, 2018). In addition, because of the potential of RCA based PLP to monitor targets in multiplex format, this method has been used to detect viruses with several subtypes such as seasonal influenza (Neumann *et al.*, 2018). In addition, HRCA based PLP methods have been employed with colorimetric strategies for H5N1 influenza virus detection. This strategy not only offers an instrumentation-free detection method due to its isothermal nature but

also further simplifies the detection process by monitoring the sample via a naked eye (Hamidi *et al.*, 2015a).

1.3.2 Application of PLPs in SNP detection

As well as specific detection of the targets, PLPs have been also utilized for the recognition of SNPs. Therefore, a new type of probe was developed based on the PLP which is called Molecular Inversion Probes (MIP). An optimized version of the MIP has been used by ParAllele BioScience and Affymetrix companies (now part of ThermoFisher Scientific) to do multiplex assays in a chip based format (Fig. 1.10). This procedure is different from the OLA assay because a single nucleotide gap between the 5´ and 3´ ends of the PLP is produced after hybridization of the PLP to the target. These hybridized probes are introduced to the tubes where each of the tube contains one of the deoxynucleotides (dNTP) including dATP, dTTP, dGTP and dCTP. As a result, the PLP is ligated in the tube for which the gap is filled with the proper dNTP and non-ligated PLPs are removed by adding an exonuclease enzyme into the tubes. Thereafter, the ligated PLPs become circular and are amplified by PCR and finally the amplified probes are hybridized to the array for visualization (Hardenbol *et al.*, 2003, Hardenbol *et al.*, 2005, Krzywkowski *et al.*, 2018) (Fig. 1.10). One of the main advantages of using this strategy is that one probe is needed instead of four probes for detecting one SNP.

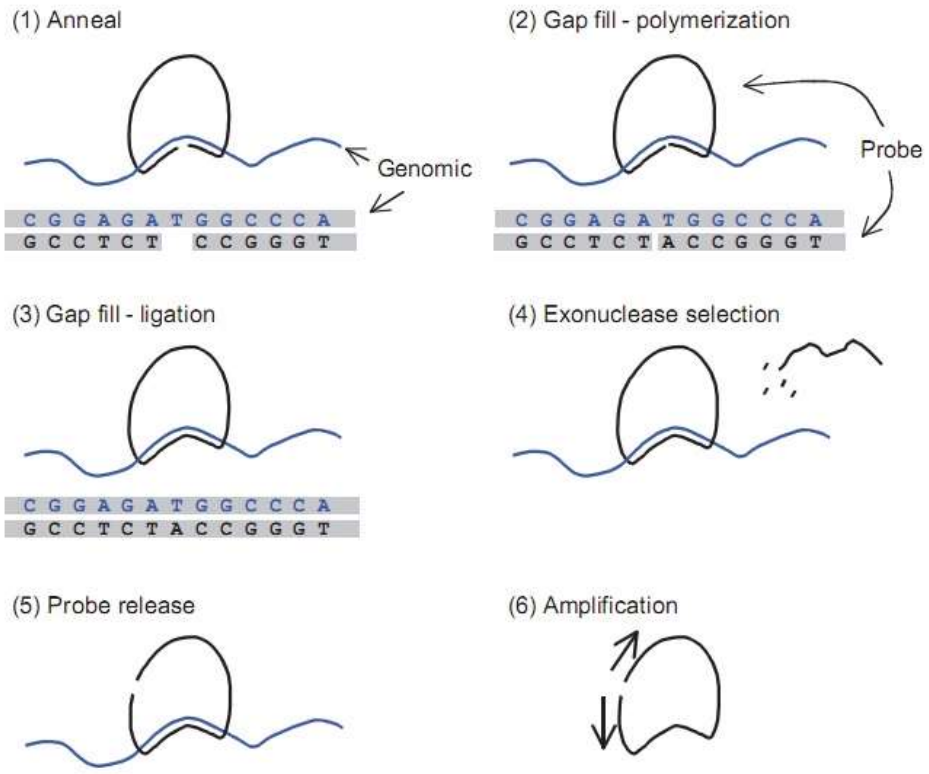

Figure 1.10 **Detailed procedure of specific detection of SNPs using a molecular inversion probe. Adapted from (Hardenbol *et al.*, 2003) with permission.**

1.3.3 PLP based RCA technique applications in diagnostic, nanotechnology, and biomaterials

1.3.3.1 RCA based diagnosis using colorimetric strategies

So far, various methods have been used to detect RCPs, including fluorescence, bioluminescence, electrochemiluminescence, electrophoresis, electrochemistry, as well as colorimetric strategies. Fluorophore-labeled probes, molecular beacons, and intercalating DNA molecules have been used extensively for real-time monitoring of RCA reaction (Hamidi *et al.*, 2015a, Hamidi *et al.*, 2015b, Li *et al.*, 2010, Liang *et al.*, 2014, Long *et al.*, 2011, Wu *et al.*, 2010). To simplify the whole RCA based detection process, in 2015 pH shock was used instead of heat shock for DNA denaturation. Using this strategy not only simplifies the whole detection process, but also it prevents possible DNA breaks that may happen at high temperatures (95 ˚C). In this study, signal intensity in HRCA reaction was monitored for real-time detection of H5N1 influenza virus using SYBR Green as an intercalating DNA dye and phi29 DNA polymerase for isothermal DNA polymerisation (Hamidi *et al.*, 2015b) (Fig. 1.11. A). In another study a new colorimetric method was developed for monitoring of HRCA reaction using hydroxy naphthol blue

(HNB) as a metal indicator. HNB in a metal sensitive indicator dye which has dark blue color at high concentration of metal ion including Mg^{2+} and sky-blue color at low concentrations of metal ions. During RCA reaction using Bst DNA polymerase enzyme, pyrophosphate (PPi^{4-}) releases as a by-product, as a result, because Mg^{2+} and PPi^{4-} have opposite charges, they can be chelated through ionic bonds and consequently change the color of sample solution containing HNB from dark blue to sky blue (Hamidi *et al.*, 2015a) (Fig. 1.11. B).

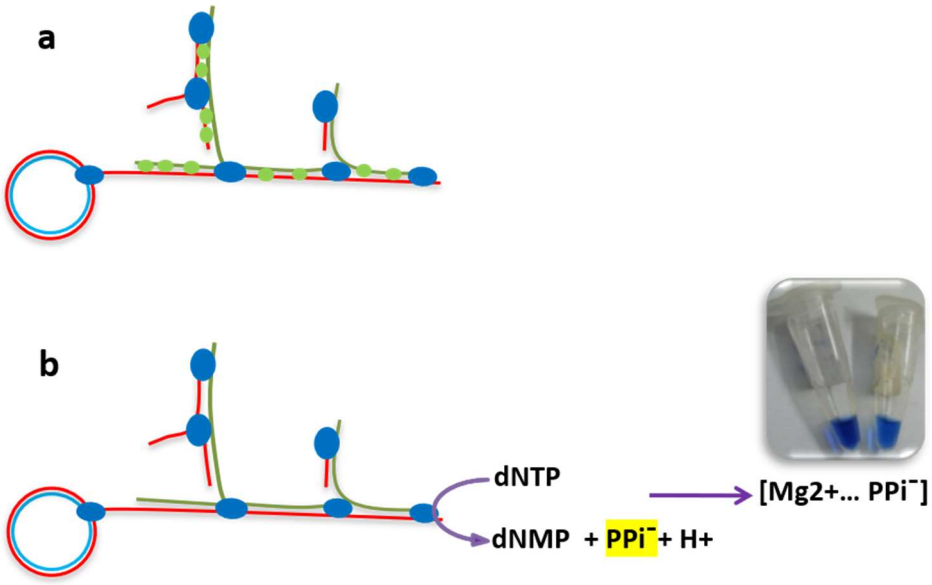

Figure 1.11 **Schematic representation of the methods used for simple monitoring of the RCA reaction. (A) Real-time monitoring of RCA using SYBR Green and employing pH shock for DNA denaturation. (B) colorimetric approaches for monitoring of RCA using HNB. Blue circle, blue oval and green dots are circularized PLP, DNA polymerase enzymes and SYBR Green, respectively.**

Another simple and colorimetric strategy that has been used for colorimetric detection assays using isothermal DNA amplification techniques including LAMP and RCA is based on calcein (Goto *et al.*, 2009, Tomita *et al.*, 2008). This colorimetric method was first reported by Tomita et al. in 2008 and works based on the change in the concentration of metal ions during the LAMP procedure. As mentioned before, one of the by-products during DNA amplification is the PPi^{4-} ion. Due to the fact that PPi^{4-} has a strong negative charge it can easily chelate metal ions and produce insoluble salt (Hamidi *et al.*, 2015a, Tomita *et al.*, 2008). As it can be seen from Fig. 1.12, calcein is quenched when it binds to Mn^{2+} and it starts to fluoresce when coupled with Mg^{2+}. Therefore, before the DNA amplification reaction, the Calcian is quenched since the Mn^{2+} is the dominant ion in the reaction mixture. However, during the reaction and chelating of Mn^{2+} by PPi^{4+}, there are more metal-free calcein molecules available for binding Mg^{2+} and as a result Calcian becomes

unquenched and thus fluorescent (Fig. 1.12) (Tomita *et al.*, 2008). This phenomenon can also be observed with the naked eye (Fig. 1.13).

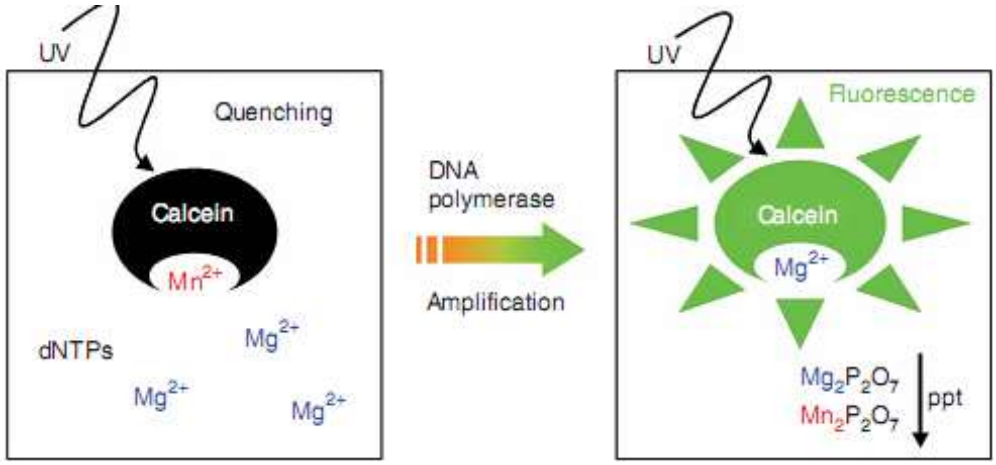

Figure 1.12 **Mechanism of visual detection via calcein. Adapted from (Tomita *et al.*, 2008) with permission.**

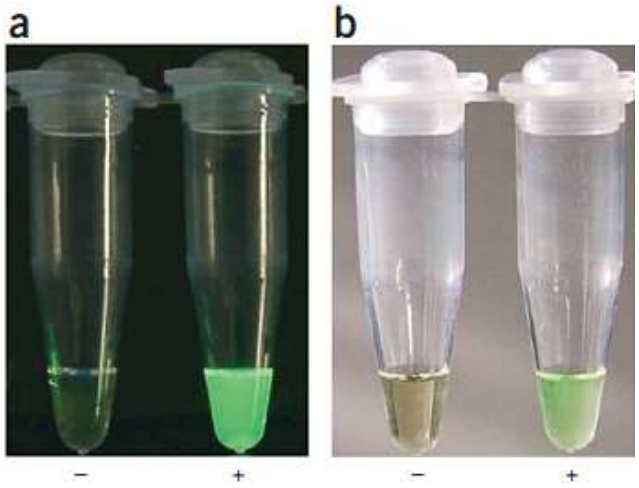

Figure 1.13 **Monitoring of the isothermal reaction by calcein. (a) Visualization of tubes under the UV lamp (wavelength: 365 nm). (b) Visualization without using UV lamp. (-) and (+) show the sample in the absence and presence of the target, respectively. Adapted from (Tomita *et al.*, 2008) with permission.**

The tandemly repeated DNA-sequence in RCPs is an excellent template and programmable building block to make nano- or micro-scale structure. It is also possible to manipulate the properties of RCPs by changing the length and sequence of template circular DNA. Therefore, the technique has been frequently used for different propose in nano-biotechnology and biomaterial (Ali *et al.*, 2014, Li *et al.*, 2020). Therefore, in this section, we give a short overview about applications of RCA in these fields.

1.3.3.2 RCA application in biomaterials and nanotechnology

DNA nanotubes have become popular tools in different materials and biological purposes, due to their porosity and rigidity as well as the possibility for drug encapsulation and release once they are exposed to specific external stimuli. Therefore, in an attempt a new approach for DNA nanotubes construction was developed using RCPs. In this strategy the DNA nanotubes used tandemly repeated ssDNA produced by RCA, triangular rungs, linking strands and external stimuli sensitive co-polymers (Fig. 1.14). Fluorescent labeling of such nanotubes show that they are more nuclease-resistant and their efficiency to entering cell have highly improved (compared to dsDNA). Also, they are more efficient for drug encapsulation and releasing purposes (Fig. 1.14, I–IV) (Hamblin *et al.*, 2012).

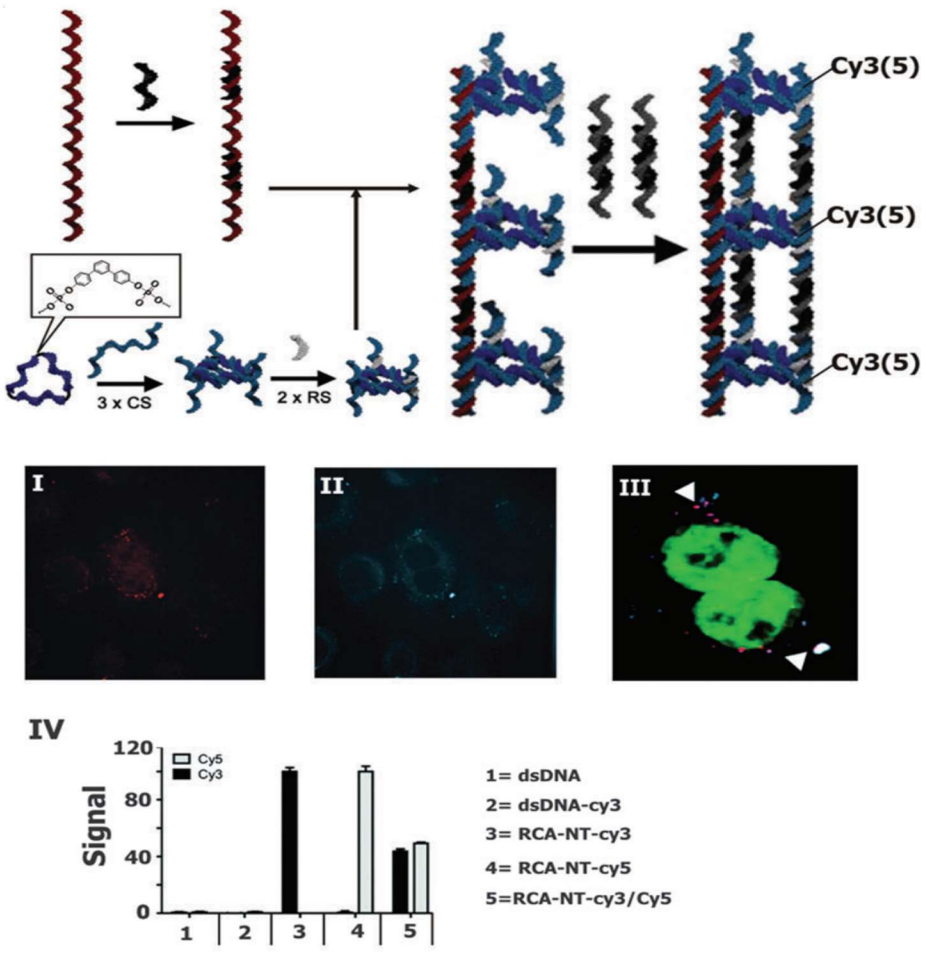

Figure 1.14 **Assembling of DNA nanotube using ssDNA produced by RCA. Assembly of DNA nano rings on RCPs for DNA tube production. (I, II, III) Fluorescent labeling of nanotubes with Cy3, Cy5, and mixture of Cy3–Cy5 confirms their improved capability for cell internalization. (IV) Cell internalization of nanotubes produced by RCA compared to dsDNA. Adapted from (Hamblin et al., 2012) with permission.**

In another study by employing RCA and a self-assembly DNA mechanism, a new approach for drug delivery was introduced. In this work a DNAzyme-driven system for drug delivery that is composed of self-degraded DNAzyme-substrate scaffolds, aptamers, targeting drug molecules as well as pH-responsive ZnO nanoparticles has been developed. In this strategy Zn^{2+} ions released as a result of dissolving of ZnO particles in acidic lysosomal microenvironment. These ions are then served as cofactors for DNAzymes activity to degrade DNA scaffolds for specific release of drugs in targeting cells (Fig. 15). The produced Multivalent DNAzymes via RCA has the advantages of being resistant to degradation by exonucleases and more importantly highly efficient DNA scaffold degradation activity due to the local concentration of DNAzymes (Li *et al.*, 2020, Wang *et al.*, 2019).

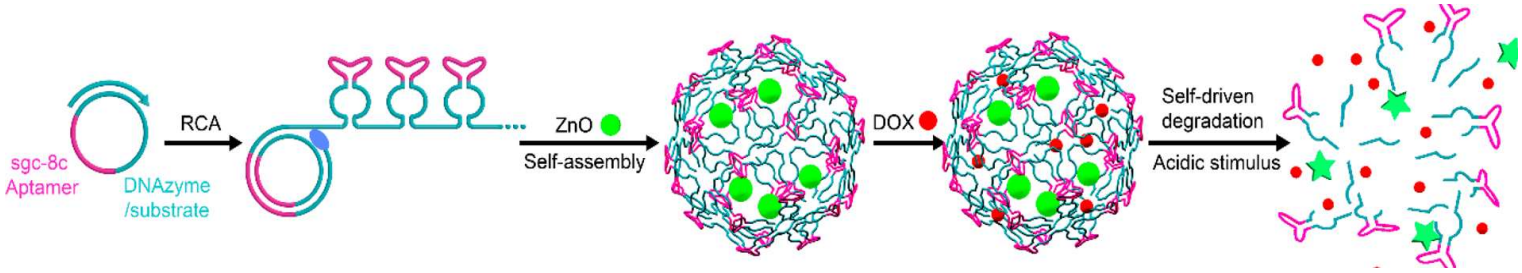

Figure 1.15 **Schematic illustration of a multivalent DNAzyme-driven based RCA drug delivery system that is composed of aptamer, encapsulated drug molecules, substrate for self degradation of DNA scaffolds, and ZnO nanoparticles. Adapted from (Wang *et al.*, 2019) with permission.**

1.4 Aptamer

The word “Aptamer” is adapted from a Greek root including *aptus* and *merus* which mean “to fit” and “particle”, respectively. These short DNA (or RNA) molecules were first introduced in the 1990s and due to their versatility, they have been used for different applications such as therapy and diagnosis (Darmostuk *et al.*, 2015, Ellington *et al.*, 1990, Tuerk *et al.*, 1990). Such small ssDNA or RNA molecules can be folded into a well-defined three-dimensional structure and they have shown a high affinity and selectivity for their specific target (Fig. 1.16). As compared with antibodies, aptamers are cheaper and have more thermal stability, they can also serve in other applications (Li *et al.*, 2014, Shen *et al.*, 2015, Wang *et al.*, 2014).

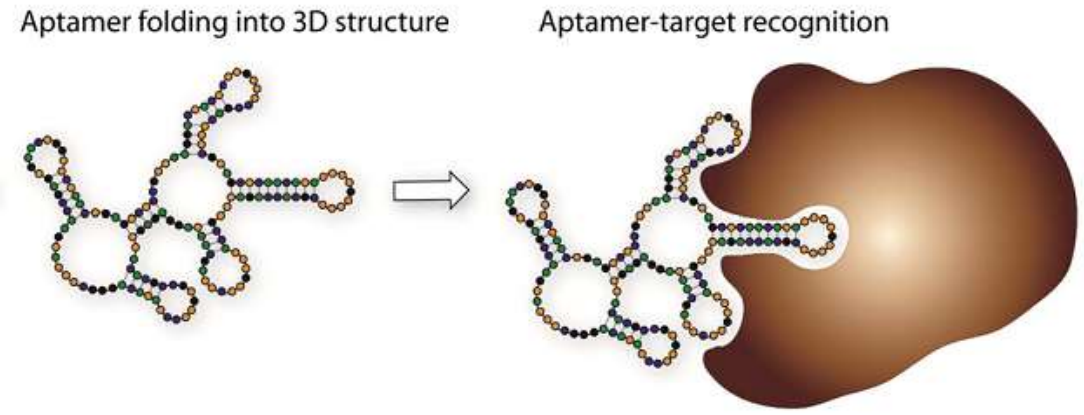

Figure 1.16 **Schematic representation of an interaction between an aptamer and its target. Adapted from (Darmostuk *et al.*, 2015) with permission.**

1.4.1 Systematic evolution of ligands by exponential enrichment (SELEX)

The SELEX approach was first introduced in early 1990s in the laboratories of Szostack and Gold. Since then, this technique was enhanced in many ways and for numerous applications (Ellington *et al.*, 1990, Tuerk *et al.*, 1990). Selecting aptamers by using conventional SELEX requires a chemically synthesized oligonucleotide library and can take from a few weeks to a few months. These synthesized oligonucleotides are designed to have a random region (e.g. 50 nucleotides, "Ns") bordered with two defined sequences for primer hybridization during the PCR (Darmostuk *et al.*, 2015, Mallikaratchy, 2017). For selection using DNA aptamers, synthesized oligonucleotides are first mixed with the targets (a protein immobilized on beads for example) and then the un-bound oligonucleotides are separated from the bound ones by performing several washing steps. Following this, the bound oligonucleotides are enriched via PCR and these steps are repeated several times to obtain the desired aptamer. After several selection iterations, the potential aptamers are sequenced, and their binding affinities are evaluated using different strategies. RNA aptamer selection is similar to their DNA aptamer selection counterpart, but further steps are needed, including reverse transcription and *in vitro* transcription. In this type of selection, a RNA library is produced by transcribing the DNA library and then this library is used for the selection steps. The bound RNA sequences are reverse transcribed into DNA and then amplified by PCR (Darmostuk *et al.*, 2015) (Fig. 1.17). It is worth saying that 15, and up to 20, rounds of selections are usually required to reach aptamers that have high affinity to specific targets.

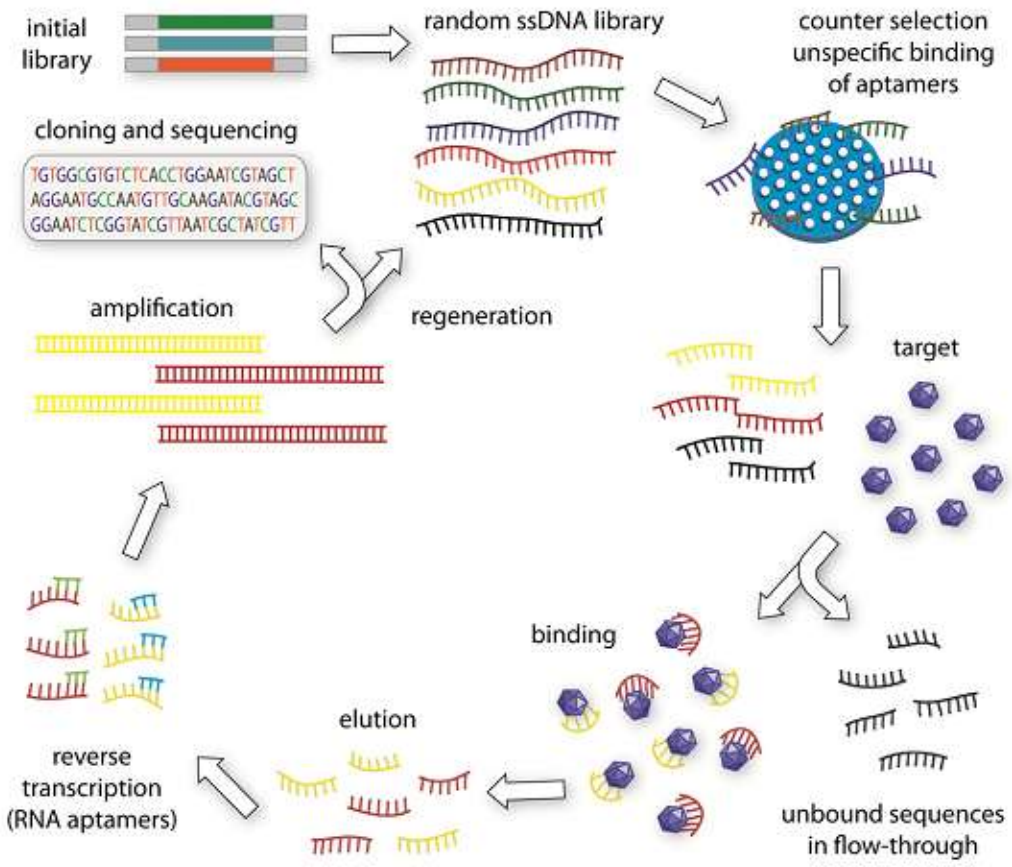

Figure 1.17 **The fundamental principle of aptamer selection by using conventional SELEX. Adapted from (Darmostuk *et al.*, 2015) with permission.**

1.4.1.1 Positive and negative selections in SELEX

To achieve aptamer selectivity with SELEX, we need to do positive selection for collecting the oligonucleotides that have affinity to the specific target and also negative selection to remove oligonucleotides that have affinity for other ligands from the library. In positive selections, the library is exposed to the target in the binding buffer and thereafter the sample is centrifuged for collection of the bound oligonucleotides. Therefore, if the target is big enough, like mammalian cells or bacteria, it can be easily separated from supernatant. However, in the case of small targets, they need to be modified and attached to the solid support for separation. Next the supernatant is removed, and the pellet is washed with the washing buffer for several times, the resulting pellet is eluted by using denaturing conditions to recover the bound sequences. After elution, the sample is centrifuged and in this part the supernatant is gathered in view of the fact that after elution the bound sequences have gone to the supernatant (Sefah *et al.*, 2010). In the next step the remaining oligonucleotides are exposed to the non-specific targets for negative

selection and as a result those oligonucleotides that have affinity to these ligands attach to them. After centrifuging the sample the pellet is removed and the supernatant is kept for further negative selections steps (Darmostuk *et al.*, 2015).

1.4.1.2 Enrichment by PCR

Enrichment via PCR is one of the most important parts of the SELEX procedure. It is essential to optimize PCR, including the concentration of primers and annealing temperature, before starting the selection. After the first round of the selection, different PCRs can be carried out both for preparative and analytic purposes. Amplification of the selected pool is necessary to prepare single strand nucleic acids for the next iteration of selection. Moreover, qPCR can be used to optimize the number of PCR cycles for preparative PCR to determine the plateau of amplification and avoid over-amplification, which increases chances of getting PCR artefacts (Darmostuk *et al.*, 2015, Sefah *et al.*, 2010).

1.4.1.3 Single strand DNA preparation

Asymmetric PCR: Asymmetric PCR has been widely used for producing ssDNA in DNA aptamer selection and in this procedure the ssDNA is produced because of uneven concentration of the sense and antisense primers in the PCR reaction. Therefore, in the asymmetric PCR the first dsDNA production proceeds exponentially followed by ssDNA production and this step continues until the amplification reaches a plateau (Fig. 1.18). The most important parameter in this type of PCR is the proportion of primer quantities (Marimuthu *et al.*, 2012).

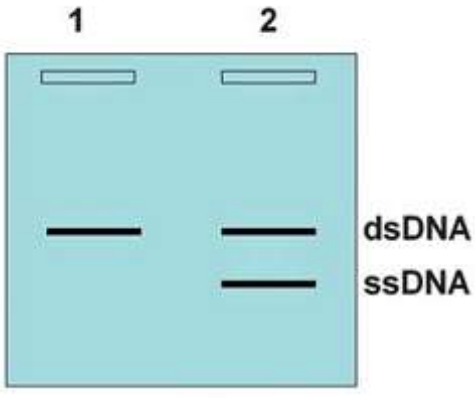

Figure 1.18 **Asymmetric PCR investigation on agarose gel electrophoresis. Lane 1 shows symmetric PCR in the presence of the same concentration of sense and antisense primers. Lane 2 refers to asymmetric PCR where different concentrations of primers are used. Adapted from (Marimuthu *et al.*, 2012) with permission.**

Separation via biotin–streptavidin interaction: Biotin–streptavidin is one of the most powerful biological interactions, with a dissociation constant (K_D) of 4×10^{-14} M, and thus it is one of the methods that is used to generate ssDNA from the PCR product. In this method, one of the primers of the PCR is biotinylated and thus this primer can be then captured by streptavidin coated magnetic beads. This captured oligo can be separated from the other strand by alkaline treatment (NaOH) and via a magnet (Green, 1990, Marimuthu *et al.*, 2012) (Fig. 1.19).

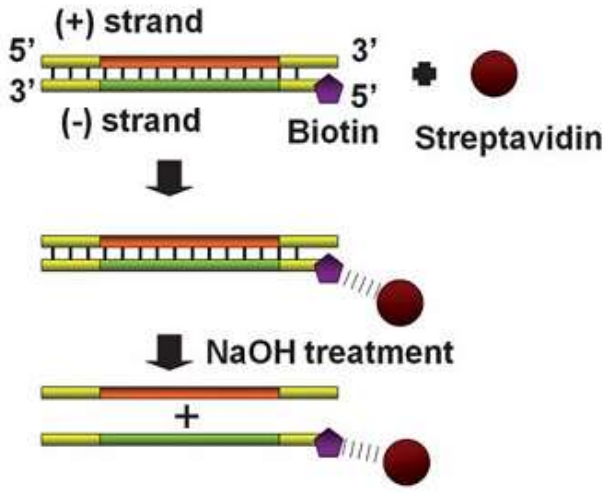

Figure 1.19 **Illustration of the ssDNA generation via biotin-streptavidin. Adapted from (Marimuthu *et al.*, 2012) with permission.**

Separation through lambda exonuclease digestion: This enzyme is derived from the lambda bacteriophage and it has been used for producing ssDNA from PCR products due to a special property. It is reported that this exonuclease has 20 times more affinity to degrade the strand of DNA that has a phosphorylated 5´ end than degrading strands that contain a non-phosphorylated 5´ end. Therefore, in this method one of the primers should be phosphorylated to be used as a substrate for this exonuclease (Fig. 1.20). Because this enzyme has very weak activity on the produced non-phosphorylated ssDNA, it can be useful for producing ssDNA libraries from PCR products (Marimuthu *et al.*, 2012).

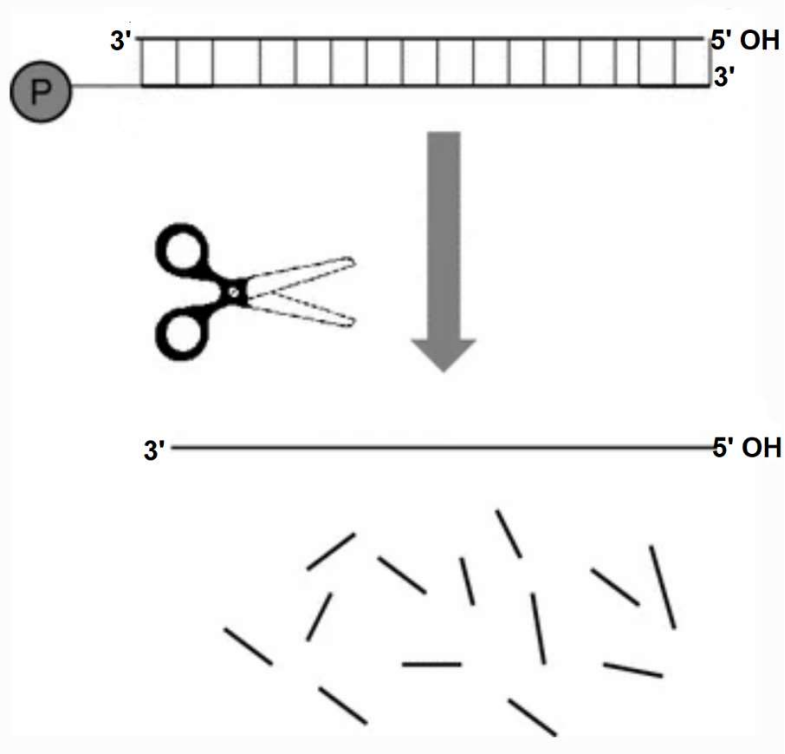

Figure 1.20 **Visual illustration of ssDNA preparation using Lambda exonuclease enzyme. ssDNA preparation from PCR products containing 5' phosphorylation at 5' terminal of one of the strands. Adapted from (Citartan *et al.*, 2011) with permission.**

1.4.1.4 Monitoring the selection progress

Each enrichment cycle can be monitored for an increased proportion of DNA aptamer by different methods, including qPCR. Therefore, after several rounds of selections when we reach to the point that we see no significant difference in the amount of selected DNA for two or three successive selected pools, we can determine the sequence of the selected aptamer by sequencing. Partial sequencing of the library by next generation sequencing (NGS) can provide several thousand sequences which should reveal the most abundant aptamers and thus permit selection of the best aptamer sequences for further assays.

1.4.2 Aptamer adaptation with RCA method

Ultrasensitive monitoring of protein biomarkers in plasma is challenging. Therefore, so far, many studies and research have been done for specific, low-level proteins in body fluids to improve detection sensitivity and avoid false negative results in clinical samples. One of the ways to solve the problem of sensitivity is using RCA as a signal amplification molecular tool to be coupled with protein-based detection platforms (Akter *et al.*, 2011). Therefore, so far a few attempts have been done in order to adapt aptamer selection through SELEX strategy with RCA technology (Lee *et al.*, 2009, Liu *et al.*, 2019, Yang *et al.*, 2007, Zhou *et al.*, 2007).

In one of the works, after the SELEX procedure for aptamer selection against PDGF-BB protein an oligonucleotide was added at the 3´ end of the aptamer via a (T)6 spacer which will be inserted between the aptamer and primer regions. This additional sequence not only uses a site for ligation reaction for PLP hybridization and circularization, but also it can serve as primer for RCA initiation and consequently signal magnification. Introduction of such a spacer is important to diminish steric hindrance of the aptamer for hybridization of PLP with the primer. Secondary structures of the aptamer-primer complex can also be predicted via Zucker's DNA folding program to avoid sequences that could interfere with aptamer affinity (Lee *et al.*, 2009, Zhou *et al.*, 2007). This oligonucleotide not only can work as a recognition module for specific ligand detection, but also can provide primer for initiation of the RCA reaction (Fig. 1.21). Using this strategy they developed several immune-RCA based biosensors for sensitive of targets using optical or electrochemical platforms.

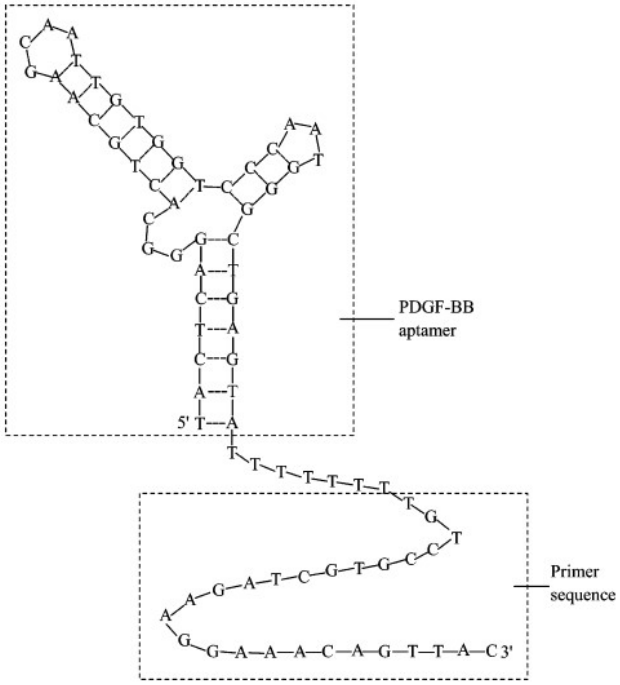

Figure 1.21 The sequence of aptamer-primer oligonucleotide. Adapted from (Zhou *et al.*, 2007).

In a recent work, for the fist time selection was done in the presence of circular aptamer against glutamate dehydrogenase (GDH) (Fig. 1.22) (Liu *et al.*, 2019). It is reported that circular aptamers have the advantages of higher stability in biological samples as well as higher affinity as compared with the linear counterparts. This is because circular aptamers are resistant against nuclease and exonuclease enzymes present in clinical sample and also they could be directly used as template for RCA reaction without requiring to use PLPs strategy. In addition, such selected circular aptamers can be used as a template for using RCA strategy that could lead to development of sensitive biosensors through signal magnification via RCA technique (Liu *et al.*, 2019).

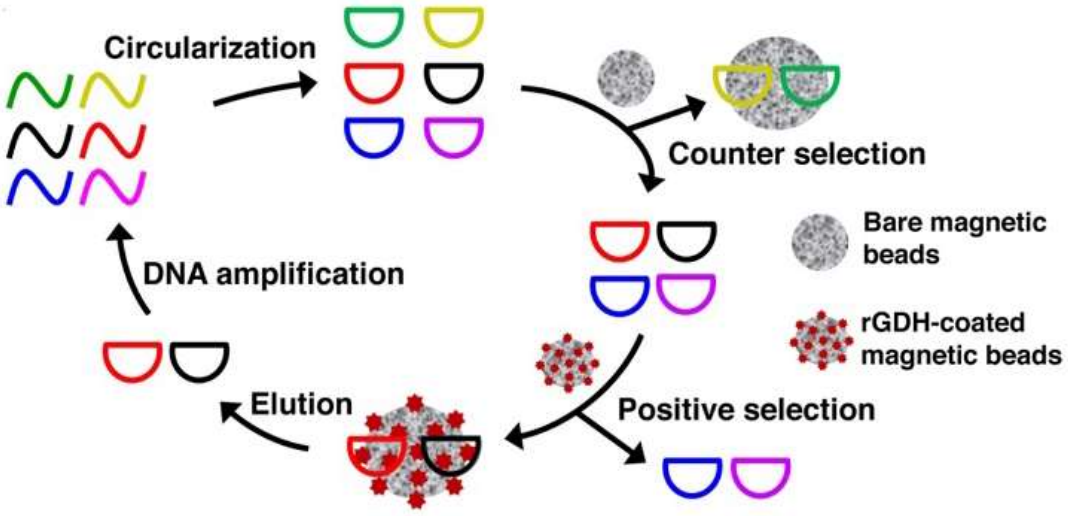

Figure 1.22 **Schematic representation of circular aptamer selection against GDH through SELEX procedure (Liu *et al.*, 2019) with permission.**

1.5 Pathogens used to develop our detection assays

1.5.1 H5N1 influenza virus

This virus was chosen for our work because it represents a major pathogen worldwide. The influenza virus belongs to the orthomyxoviridae and its propagation in the early 21st century caused 50 million birds death in European Union with a fear that it might spread to humans to cause a flu pandemic. Genome of the influenza virus is made of seven to eight pieces of segmented negative-sense RNA where each piece of RNA contains either one or two genes, coding for specific proteins. Influenza A virus is classified into types A, B and C and according to the genome structures. The type A is also classified based on the two surface antigens including hemagglutinin (HA) and neuraminidase (NA) (Fig. 1.23) (Fouchier *et al.*, 2005, Nguyen *et al.*, 2013, Payungporn *et al.*, 2006). H5N1 is one of the subtypes of the influenza A virus which is also known as bird flu or A (H5N1). It is worth saying that this virus is highly contagious in wild aquatic birds, domestic poultry, and other animal species (Gyarmati *et al.*, 2008). As previously mentioned, the gold standard method that is used for monitoring of infectious diseases (influenza A virus and coronavirus), including highly pathogenic avian H5N1 influenza virus, is qPCR. Based on other works reported in the literature, qPCR is more sensitive and specific than ELISA and cell culture based methods for detection of this infectious disease (Chen *et al.*, 2007). As well as these conventional methods, isothermal RCA based PLP technique has been also utilized for sensitive, simple and multiplex detection and subtyping of seasonal influenza A virus (Neumann *et al.*, 2018).

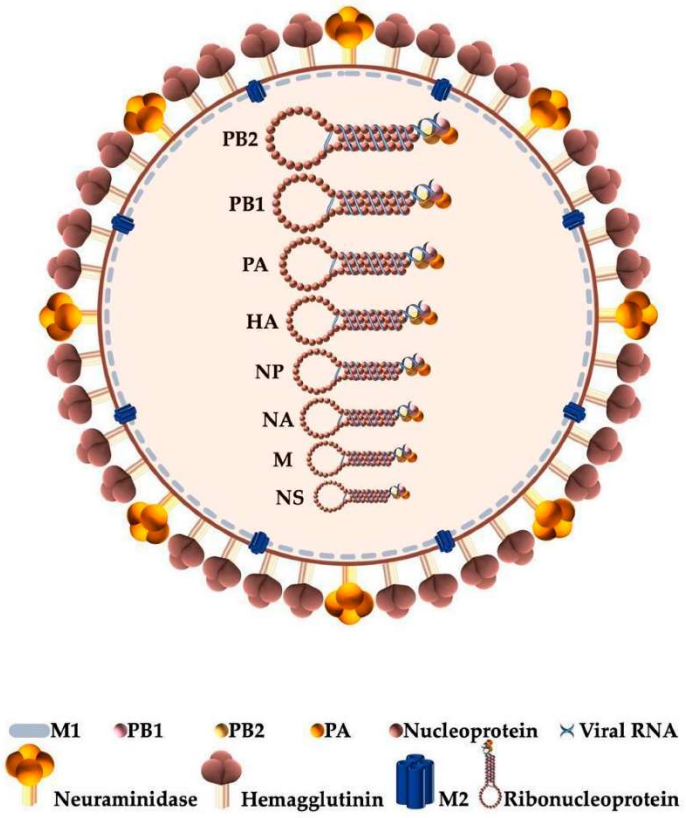

Figure 1.23 **Schematic structure of H5N1 influenzas virus. Adapted from (Rosário-Ferreira *et al.*, 2020) with permission.**

1.5.2 Middle East Respiratory Syndrome Corona Virus (MERS-CoV)

As with H5N1, MERS-CoV is a virus which has a big impact, making it a model target of great interest. Corona viruses are considered as one of the causes of the common cold since it usually leads to mild flu-like symptoms and as a result this virus family has been regarded as simple and nonfatal. However, a specific coronavirus outbreak during 2002 and 2003 encompassed many countries such as China, Thailand, Vietnam, Taiwan, Singapore and the United States of America, leading to Severe Acute Respiratory Syndrome (SARS) and high mortality rates in many patients. Thereafter, researchers started to understand the disease pathogenesis. In addition, a different outbreak in Saudi Arabia in 2012 caused many deaths, mainly in Middle East, and thus attracted much attention for this new coronavirus. Since this new respiratory syndrome originated from Middle East, it is called Middle East Respiratory Syndrome Corona Virus (MERS-CoV). It is reported that this virus can be transmitted through airborne zoonotic droplets and it causes cell damage and inflammation in the infected cells. It is also worth to note that corona viruses are spherical or pleomorphic with a single stranded RNA and their surface is covered with the Spike glycoprotein (Fig. 1.24) (Al-Osail *et al.*, 2017). It is worth noticing that as compared with SARS-

CoV-2 with fatality rates of 6.6% which is the most important present global health concern, the mortality rates for MERS-CoV is 34% highlighting the fact that MERS-CoV is still an important target to monitor (Toyoshima *et al.*, 2020). The Current detection methods for MERS-CoV are thermo-cycler based methods such as reverse transcriptase PCR (RT-PCR) and quantitative reverse transcription PCR (qRT-PCR), as well as isothermal DNA amplification methods including reverse transcription LAMP (RT-LAMP) and qRT-LAMP (Huang *et al.*, 2018). An alternative method that has been utilized for coronavirus detection is RCA based PLP that not only can offer detection in colorimetric mode but also has the advantage of different viruses' variants monitoring via specific SNP detection (Huang *et al.*, 2020). Accessibility to a fast, rapid and selective method for infectious diseases is essential in disease management for proper disease response especially in the light of the current pandemic where POC could have a huge impact on the monitoring of COVID-19 as well as monitoring of circulating subtypes for possible pandemic prediction.

All in all, the isothermal nature of the RCA reaction makes it possible to offer a portable and user-friendly detection system since RCA can even perform DNA amplification reaction at room temperature and as a result there is no need to use a sophisticated thermal cycler machine which is lab-based device. PLP based RCA also provides multiplex-based detection since it is easy to barcode spacer part of PLP and consequently detect several subtypes of influenza viruses and corona viruses at the same time. This is very important for such sorts of virus monitoring since influenza and corona viruses are very likely to mutate and change (during genetic shifts and genetic drifts) which may results in appearance of new subtypes of viruses that are more transmissible and have high rates of mortality (Gyarmati *et al.*, 2008, Neumann *et al.*, 2018).

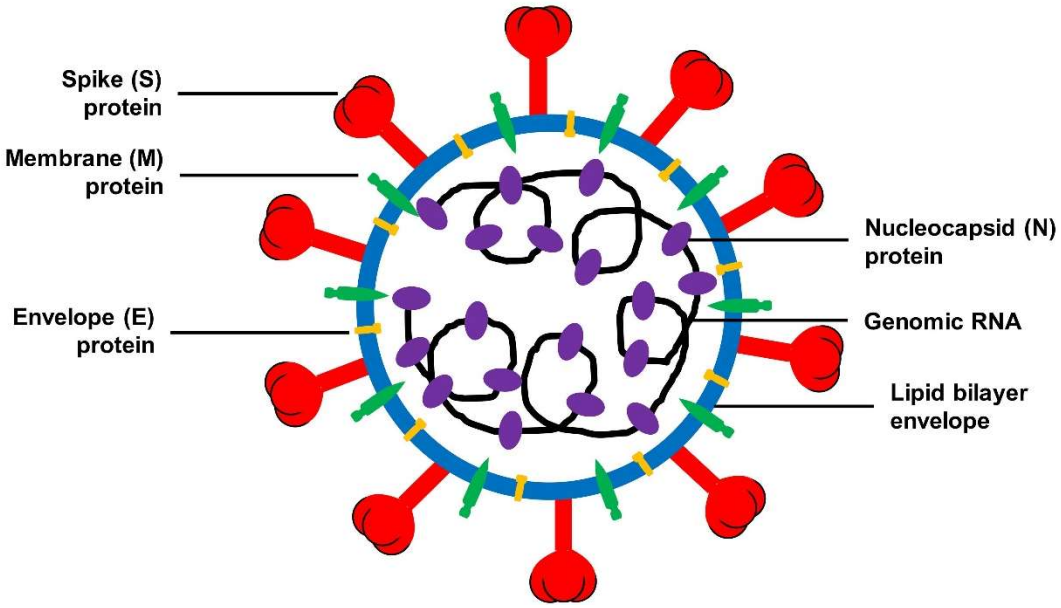

Figure 1.24 **Schematic structure of MERS CoV virus. Adapted from (Wang *et al.*, 2020) with permission.**

1.6 Problematic

Since the beginning of 21th century several pandemics relating to influenza A and coronavirus have happened that not only have taken many lives but also have caused trillions dollars loss for many industries, business and governments. Although the 2009 H1N1 pandemic showed how quickly a new emerged virus can spread all over the world, H1N1 pandemic was much milder than many scientists and experts expected. However, the global outbreak of bird flu or H5N1 virus in 2003 hit hard poultry industries which involved about 200 million birds and caused 50 million birds death in the European Union (Hamidi *et al.*, 2015b). In addition, the outbreaks of SARS-CoV (2002) and MERS-CoV (2012) with mortality rates of 9.6% and 34.3%, respectively, affected many lives and countries. However, fortunately these outbreaks had less continuity than expected (Toyoshima *et al.*, 2020). The current global health concern is coronavirus disease 2019 (COVID-19) pandemic that is caused by severe acute respiratory syndrome coronavirus 2 (SARS-CoV-2). This virus was first identified in Wuhan, China, in December 2019. As of 26 April 2021, the World Health Organization (WHO) confirmed more than 147.8 million worldwide infections and more than 3.1 million deaths causing by this virus.

In order to deal with infectious diseases, the first step is to develop a sensitive, rapid and selective method for monitoring of the pathogens since early recognition of pathogens is important in decision making and managing diseases. So far many effective and sensitive methods have been

developed for disease monitoring including virus or microorganism propagation and isolation from culture. However, these methods are costly, time consuming as well as being labor intensive. Although some alternative molecular methods such as PCR and qPCR are sensitive and less time consuming and more specific, they still need special expensive equipment and isolated genetic contents which make on-site monitoring very hard. In case of rapid test, although such sorts of diagnosis methods are usually cheap and instrument-free, their results are not quantitative and also are not sensitive enough for detecting very low concentrations of targets. Thus, developing a simple, rapid, sensitive, and selective diagnosis method for detection and identification of pathogens is still a big challenge for those scientists who are working on molecular diagnostics field. Different properties of biosensors that are commercialized based on isothermal DNA amplification techniques are summarized in the table 1.2 which clearly depicts advantages and disadvantages of each biosensors over the other (Craw *et al.*, 2012).

Table 1.2 Comparing of different aspect of commercially available diagnostic test that are developed based on isothermal DNA amplification techniques.

Product	Method	Samples No	Detection method	Diagnostic use	Test Duration	Cost (approx. US$)	ASSURED criteria							Size (cm)	Ref
							A	S	S	U	R	E	D		
Twista (TwistDX, UK)	RPA	8	2 channel Fluorescence	No (Assays in development)	10–15 min	$4552 Instrument	+	+ +	+ + + + +	-	+ +	-	+	19 × 18	[4]
Genie II (OptiGene, UK)	LAMP	16	1 channel Fluorescence	No (Assays in development)	Assay dependent	$13 000 Instrument	+	+ + + + +	+ + + + + +	-	+ + + +	-	+	20 × 21 × 30	[5]
Illumigene Meridian Bioscience	LAMP	10	Fluorescence	Yes (FDA[1] & CE[2])	60 min	POA[3]	-	+ + + + +	+ + + + + +	-	+ + + +	-	+	21 × 29 × 9	[6]
OligoC-TesT CorisBioConcept Belgium	NASBA	1	Lateral flow	Yes	~100 min	$26/test	+ + +	+ + +	+ +	-	+ + +	+ + + +	+ + + +	Single use dipstick	[7]
NucliSENSEasyQ Bio Merieux France	NASBA	8-48	Multichannel Fluorescence	Yes (CE)	120 min	$50 000 Instrumen	+	+ +	+ + + + +	+	+ + +	-	+	42 × 42 × 22	[8]
APTIMA/Tigris Gen-Probe USA	TMA	100	Chemiluminescent DNA probe	Yes (FDA & CE)	3.5 h	POA	-	+ +	+ + + + +	+	+ +	-	+	175 × 91 × 183	[9]
Colorimetric LAMP Assay Kit (NEB, USA)	LAMP	96	Colorimetrics	Yes (FDA)	30	1,088.00	+ + +	+ + + + +	+ +	-	+ + + + +	+ + +	+ + + +	Single use	[10]
Molecular Inversion Probes kit (Biolegio, Netherland)	RCA	10000	Fluorescence	No (Assays in development)	-	12,000	+ + + + + + +	+ + +	+ + +	+	+ + + +	-	+	Single use	[11]
ProbeTec Becton Dickinson & Co USA	SDA	46	Fluorescence	YES (FDA & CE)	60 min	POA	-	+ +	+ + + + +	+	+ +	-	+	55 × 72 × 72	[12]

[1]U.S. Food and Drug Administration
[2]conformité européenne
[3]Price On Application
[4]www.twistdx.co.uk.
[5]www.optigene.co.uk.
[6] www.meridianbioscience.com/illumigene
[7]www.corisbio.com.
[8] www.biomerieux-diagnostics.com
[9]https://www.hologic.com/package-inserts/diagnostic-products/aptima-combo-2-assay-ctng.
[10]www.neb.com
[11]biolegio.com
[12] https://www.bd.com/en-uk/products/diagnostics-systems/molecular-diagnostics.

As well as molecular tests, protein-based diagnosis are used for infectious diseases monitoring. The obvious example is conventional ELISA tests which is working based on immuno-sandwich formation upon specific formation of target. ELISA is composed of complicated workflows including numerous time-consuming washing steps. In addition, this conventional method is not useful for high-throughput monitoring and analysis of samples which makes this traditional protein-based detection method in some ways challenging. In a recent attempt, a simple method

was developed for specific detection of a protein biomarkers through circular aptamer selection in SELEX process (Liu *et al.*, 2019). Although circular aptamer selection has the advantages of specific target detection and signal amplification via RCA, the proposed aptamer selection process is gel based which makes the selection process (especially ssDNA preparation and purification) much harder and time consuming. Therefore, to simplify the time-consuming process of SELEX (which comprises about 15 cycles), developing simple non-gel-based ssDNA preparation and purification methods would be highly demanding. So far, several non-gel-based techniques for linear ssDNA preparation in SELEX procedure have been introduced. However, developing a simple and user-friendly method for circular ssDNA preparation (that can be done in just a tube) would be very promising due to rising applications of circular ssDNA in molecular biology and especially in circular aptamer selection.

1.7 HYPOTHESES AND OBJECTIVES

Hypotheses:

We hypothesize that:

- Combining a colorimetric strategy with RCA can be an efficient and simple way to design portable, instrumentation free and also quantitative biosensor.
- RCA is a robust signal amplification approach to be coupled with other sensitive detection platforms for ultra-sensitive detection of DNA and analytes.
- A novel strategy for circular DNA preparation from PCR would permit more efficient aptamer selection during SELEX.

Objectives:

Our main objective for this project is designing simple, sensitive, label free and portable biosensors using RCA technology. To achieve this goal, we have specific objectives including:

1. Developing a new RCA based colorimetric technology for simple detection of infectious diseases using phenol red as a pH sensitive dye.

2. Coupling RCA with other sensitive platforms including optical microcavity technology as a novel way for sensitive detection of biomarkers.

3. Developing a new technique for *in vitro* preparation of single stranded linear and circular DNA.

    3.1 Apply this novel technique for selection of linear and circular aptamer against MERS-CoV Spike protein.

2 SIMPLE ROLLING CIRCLE AMPLIFICATION COLORIMETRIC ASSAY BASED ON PH FOR TARGET DNA DETECTION

Simple dosage colorimétrique par amplification en cercle roulant basé sur le pH pour la détection d'ADN cible

Seyed Vahid Hamidi and Jonathan Perreault.

INRS, Centre INRS – Institut Armand-Frappier, 531 Boul. des Prairies, Laval, Québec, Canada.

This article is published in Talanta journal.

Received 10 January 2019, Revised 2 April 2019, Accepted 2 April 2019, Available online 5 April 2019.

https://doi.org/10.1016/j.talanta.2019.04.003

Author contributions:

Conceptualization, S.V.H.; Resources, J.P.; Methodology, S.V.H.; Validation, S.V.H. and J.P.; Data analysis, S.V.H. and J.P.; Experimental work: S.V.H.; Writing—Original Draft Preparation, S.V.H.; Writing—Review and Editing, S.V.H. and J.P.; Supervision: J.P.; Funding Acquisition, J.P.

A short description about this work:

This publication is related to the first objective of my PhD project which is about developing a new colorimetric strategy for detection of infectious diseases using RCA. Colorimetric methods are highly applicable in point of care testing (POC) where access to an equipped laboratory is often not convenient. Therefore. Such portable detection platforms are useful for monitoring and screening of patients, herds or poultry diseases or other sorts of contaminations without using sophisticated device and just via a naked eye. In this project, by employing phenol red as a pH sensitive dye and excluding Tris-HCl from reaction mixtures, a new colorimetric assay was developed for targeting H5N1 influenza virus using RCA. A great contrast was obtained between positive control (light orange color) and negative controls (pink). In addition, a good linear range from 0.61 to 78.1 nM and also a theoretical detection limit of 3.3 pM was achieved in this study. Because of its simplicity, portability and isothermal nature, this user-friendly technique has potential to be commercialized.

2.1 Abstract

Detection and identification of DNA by PCR has opened tremendous possibilities and allows detection of minute quantities of DNA highly specifically. However, PCR remains confined to laboratory settings because of the need of thermocyclers and other analytical equipment. This led to development of isothermal amplification techniques, among which Pad Lock Probe (PLP)-based Rolling Circle Amplification (RCA) has several advantages, but typically also requires a laboratory apparatus of some sort to measure DNA amplification. To circumvent this limitation, while still taking advantage of PLP-based RCA, we developed a colorimetric assay that relies on pH change. Using this assay, we can detect DNA in the low picomolar range and obtain results observable with the naked eye in only 20 minutes without any requirement for a thermocycler or other complex device, making it a particularly portable assay.

Keywords: Rolling circle amplification, Padlock probe, colorimetric assay, biosensor, Bst DNA polymerase, unbuffered ligation

2.2 Introduction

Because of portability, simplicity of diagnosis and efficiency in detection without requiring access to well-equipped laboratories, point of care (POC) testing is favored especially in areas with shortage of facilities [1-3]. The increasing interest in such type of diagnosis has led to develop fast and cheap devices which can analyze genetic profiles or various analytes easily and precisely. Eventually, we could relinquish the classical ways of medical diagnosis and use mostly miniaturized and label free systems [1, 4]. One of the integral tools in the field of life sciences is nucleic acid testing which is mainly based on PCR and is highly applicable either in research or clinical purposes. However, PCR needs sophisticated and expensive thermal cycler machines and centralized laboratories with professional personnel. Therefore, application of POC nucleic acid tests which use isothermal DNA amplification methods are on rise due to their simplicity and the fact that they do not require any special devices [5, 6]. These alternative techniques have been widely used for monitoring of diseases and mainly infectious diseases in developing countries [1, 5].

In the 1990's, an exclusive enzyme was introduced which can make tandem repeat single strand DNA (ssDNA) from circular DNA templates. This isothermal DNA amplification process which is called rolling circle amplification (RCA) is based on a circular DNA template and utilizes specific DNA polymerases (Bst, Vent exo- and Phi29 DNA polymerases) to elongate DNA strands either in linear (LRCA) mode or hyperbranched (HRCA) mode [7, 8]. Among these two models, HRCA

is more efficient and powerful in signal magnification and generates more products from each circular template [8, 9]. In view of the fact that RCA is based on the circular DNA template, in 1994 a long circularizable probe was proposed which is called padlock probe [10]. This circularizable probe forms circular DNA after specific recognition of target which then is utilized as a template for signal amplification via RCA [11, 12].

Like these two previous studies, in this work H5N1 influenza virus was targeted because this virus is still a major concern among scientists and public [13, 14]. However, due to high pathogenicity and virulence of H5N1 virus [15], in this study synthetic H5N1 target was employed for optimization of the colorimetric assay and the M13 bacteriophage genome was used as a model for evaluating the performance of the proposed method in real-sample condition.

Broad applications exist for pH sensitive dyes in different fields including determining pH of solutions, freshwater, pools, determination of CO2 and SO2 in air, developing pH-based sensors which usually work and respond based on alterations in the hydrogen ions or hydroxyl ions of the environment. [16-19]. On the other hand, other sensors are developed for different ion detection such as magnesium or cadmium [20, 21].

In 2015, Tanner et al. introduced a new method for visual monitoring of loop mediated isothermal amplification (LAMP) through inherent production of hydrogen ions by DNA polymerase during DNA amplification and pH indicator dyes (phenol red, cresol red, neutral red or m-cresol purple) [22]. Combination of pH sensitive dyes with LAMP, multiple displacement amplification (MDA), strand-displacement amplification (SDA) and PCR have been applied for developing colorimetric biosensors [6, 22-28], but in the current work this strategy is exploited for the first time with RCA based on Pad Lock Probes (PLPs) (Fig. 2.1). Also, in this project for the first-time DNA ligation has been done in a reaction mixture lacking Tris-HCl (or other typical buffering agent) to be able to develop a colorimetric assay using phenol red with PLP-based RCA. Furthermore, by using this strategy a new colorimetric method was introduced for specific monitoring of SNPs, highlighting the advantage of PLP colorimetric RCA assays over other isothermal amplification methods. Finally, we have shown the robustness of the proposed assay with different types of samples.

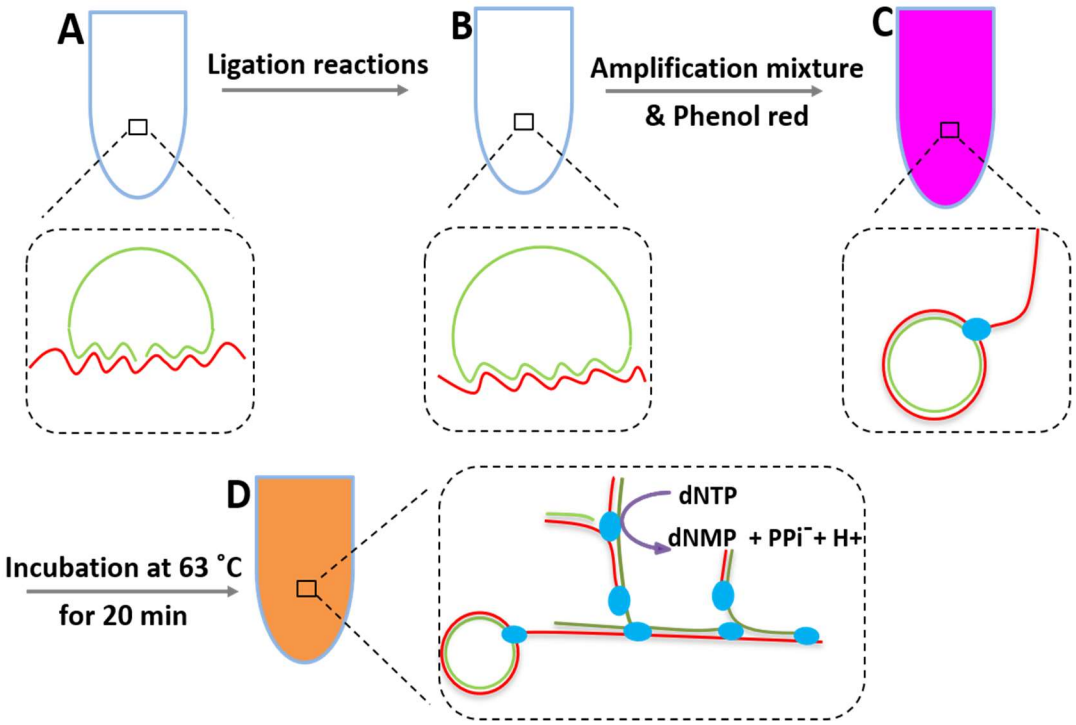

Figure 2.1 **Representation of colorimetric assay with phenol red. (A) In the first step the hybridization reaction is carried out. In this situation PLP (green line) and H5N1 target (red line) can be gradually and specifically hybridized. (B) After hybridization the mixture is treated to ligate the two ends of the PLP and generate a circular template for RCA reaction. (C and D) Afterward, amplification components including Phenol red are introduced to the ligation mixture. The Bst 2.0 enzyme (blue ellipse) initiates RCA by utilizing circular PLP as a template. During amplification, Bst 2.0 uses dNTPs to incorporate dNMPs into DNA chains and releases PPi- and H+ as by-products, thus decreasing pH.**

2.3 Material and methods

2.3.1 Probes and primers

The phosphorylated H5N1 PLP has specific arms complementary to the synthetic H5N1 target primers, which corresponds to a sequence in the hemagglutinin (HA) gene from H5N1 genome [13, 14, 29, 30]. Also, M13 PLP and synthetic M13 targets were selected from a conserved part of the M13 bacteriophage genome and this recognition sequence was also verified by PCR in the presence of real samples. All oligonucleotides including PLPs, forward and reverse primers and synthetic targets were provided from Sigma Aldrich Company and Integrated DNA Technologies (IDT) (Table 2.S1, Appendix 1).

2.3.2 M13 bacteriophage genome isolation

M13 bacteriophage solution was first treated with 50 µg/mL proteinase K per reaction (Bio Basic, Canada) at 37 ˚C for 60 min and then the genome was extracted using phenol: chloroform

extraction (phenol, Bio Basic, Canada; chloroform: Sigma-Aldrich, USA) [31] and then the extracted DNA was precipitated by utilizing conventional precipitation with ethanol [32]. Thereafter, the concentration of the extracted genome was determined using a Nanodrop device (Thermo Fisher Scientific, USA).

2.3.3 Ligation and amplification reactions

In previous studies pH shock was used instead of heat shock for simplification of the whole detection procedure [13, 14]. However, in the current work we employed heat shock for DNA denaturation since the signal is highly dependent on the pH change during the amplification reaction. For the ligation, 1 µL of target DNA, 2 µL of deionized water and 1 µL PLP (at final concentration of 0.075 µM) were added to the 5 µL of 2X “no-Tris” ligation solution (20 mM MgCl2 (Fisher Scientific, USA), 2 mM ATP, 20 mM DTT (Bio Basic, Canada), pH 8.50). Thereafter, reaction mixtures were incubated at 95 °C for 5 min then gradually cooled down to room temperature to allow hybridization between PLP and the target. This was followed by addition of 1 µL (5 units) of T4 DNA ligase (New England Biolabs, USA) and placing the reaction for 60 min at room temperature [33]. In this assay exonuclease reaction using Exonuclease I enzyme was not used due to two reasons: i) minimizing introduction of Tris-HCl to the reaction mixture which is already added to the enzyme stock by the company; and ii) the Bst DNA polymerase that is used in this assay can amplify circularized PLP even in a topologically constrained situation and thus there is no need for exonuclease enzymes prior to the amplification reaction [34]. This phenomenon was confirmed by using an extended synthetic M13 target to determine a M13 standard curve. Afterward, 30 µL of 2X amplification reaction solution (2.8 mM deoxynucleotide triphosphate (dNTP), 20 mM (NH4)2SO4, 16 mM MgSO4, 100 mM KCl, 0.2 % v/v Tween 20 (Fisher Scientific, USA), pH 8.2) as well as 1.6 µM forward and reverse primers, 0.1 µM phenol red and 8 units of Bst 2.0 WarmStart (WS) DNA polymerase enzyme (New England Biolabs, USA) were added to the ligation mixture in a final volume of 40 µL [6, 22]. The amplification reaction is carried out at 63 °C for 1 hour by utilizing a thermal cycler (C1000 Touch, Bio-Rad, USA) to adjust temperature and then reaction mixtures are poured into the 384 well plates (Greiner Bio-One, Germany) in order to determine the absorbance intensity between 500 and 600 nm using a plate reader device (Infinite M 1000 PRO, TECAN, Switzerland).

2.3.4 Visualization with gel electrophoresis

Evaluation of the performance of different ligation solutions was performed in the presence of 0.1 µM H5N1 PLP and target. The gel electrophoresis was done in 2% agarose gel with 1X TAE buffer (40 mM Tris-acetate, 1 mM EDTA, pH 8.0, Fisher Scientific, USA) for 45 min at 120 volts.

2.4 Results and Discussion

2.4.1 Optimization of ligation reaction

In contrast with LAMP reaction which is only composed of an amplification reaction, in the PLP-based RCA method it is necessary to perform a ligation reaction prior to the amplification reaction [35, 36]. Therefore, it is critical to adapt both reactions with this colorimetric technique to be able to witness color changes in phenol red resulting from the amplification reaction. For this, we optimized the ligation reaction and were able to ligate DNA in absence of Tris-HCl (normally used to buffer pH of T4 DNA ligase at 7.5) to prevent buffering of pH during amplification. In order to optimize PLP ligation-based RCA for our colorimetric assay with phenol red, the ligation reaction was carried out with the H5N1 target in three different situations (Fig. 2.2). Ligation reactions were performed with 2X no-Tris ligation solution (Lanes 1 and 2), with 2X NaCl/no-Tris (includes 100 mM NaCl) to improve ionic capacity of the ligation solution (Lanes 3 and 4) and with 10X T4 ligase buffer supplied by NEB (Lanes 5 and 6). Each reaction was also performed in the absence of H5N1 target as negative controls (Lanes 2, 4, 6) and all samples were treated with 0.5 unit of Exonuclease I enzyme [37] (New England Biolabs, USA) to degrade un-ligated PLPs.

To achieve PLP ligation after omitting Tris-HCl from T4 ligase reaction mixture, two strategies were utilized. Firstly, using a 2X ligation solution instead of 10X. This strategy improves control over possible pH change after addition of the rest of ligation mixtures. Because in this situation half of the reaction is encompassed of ligation solution, the reaction is less prone to sudden pH changes due to introduction of other elements. Secondly, adjusting pH of the ligation solution at the initial pH of 8.5 instead of 7.5. Using a pH of 8.5, rather than 8.0 or 8.1 (which would be just above the phenol red upper range) also could help the ligation solution have more room for possible alterations of pH since the reaction mixture is merely composed of $MgCl_2$, DTT and ATP. Absence of dedicated buffering agents makes this new ligation solution sensitive to pH variations and these approaches are important to aid T4 DNA ligase reactions and provide a ligation efficiency identical to the commercial buffer.

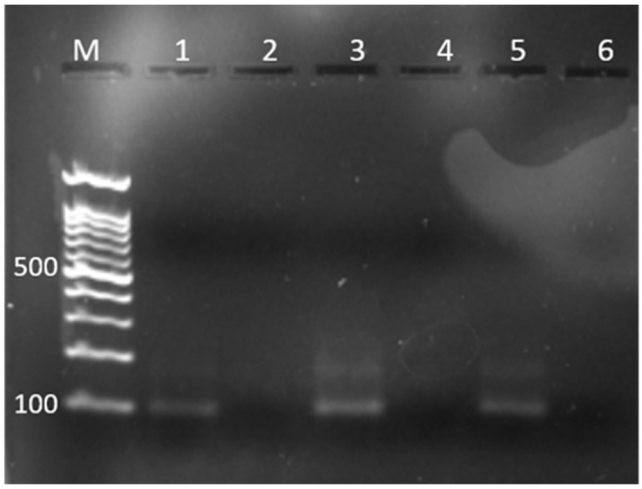

Figure 2.2 **Ligation reactions. Lane M: Marker, Lanes 1, 3 and 5: positive samples (with H5N1 target), Lanes 2, 4 and 6: Negative samples (without H5N1 target). Lanes 1 and 2: ligation reaction in 2X ligation solution with no-Tris (pH 8.5); lanes 3 and 4: ligation reaction with 2X ligation solution with NaCl/no-Tris (pH 8.5); and lanes 5 and 6: 10X buffer provided by the company. All ligation samples were done in 1X of the indicated buffer and treated with Exonuclease I enzyme before loading in gel. The electrophoresis has been done in 2% agarose gel for 45 min at a voltage of 120 V.**

2.4.2 Colorimetric tracking of RCA with phenol red

Phenol red is a well-known pH indicator with a pH shift range from 6.4 to 8.0. This pH sensitive dye is red (absorbance peak at λ1 = 560 nm) at the upper limit of the pH range and yellow (absorbance peak at λ2 = 440 nm) at the lower limit of its pH transition range [23]. In this project, λ1 has been selected as the optimum extinction coefficient to track amplification reaction because absorbance intensity for λ1 is much higher than that of λ2 [16] and also displays sharper differences to the pH change from 5 to 8 [17]. Therefore, this wavelength is a better indicator for colour change of phenol red during RCA reaction and it is more associated to the concentration of the target.

In order to use phenol red for colorimetric detection of RCA, the pH of the amplification reaction should be adjusted slightly above pH 8.0, which coincides with the optimum pH 8.2 found for our colorimetric assay (Fig. 2.3C). Furthermore, a pH 8.2 is compatible with the optimum pH condition for the activity of the Bst 2.0 Warm Start (WS) DNA polymerase enzyme which is 8.8 [13, 22] and at this pH the dye has pink colour due to the fact that it is above the phenol red pH transition range [23, 24]. Thus, at the beginning of the amplification reaction samples are pink, as illustrated in Fig. 2.1C and observable in negative controls from insets. However, during the amplification reaction and incorporation of deoxynucleotides to the strands of DNA, pyrophosphates and protons (hydrogen ions) are produced as by-products [6, 13, 23, 24], as a result the pH of positive

samples with specific targets decreases overtime due to generation of protons via exponential RCA reaction. Indeed, the production of hydrogen ions is high enough to change the pH from ~8.2 to ~ 6.5 and consequently the colour of solution from pink to light orange which is easy to discern by the naked eye (Fig. 2.1D and positive samples in insets) [22, 23]. This phenomenon causes a decrease of absorbance intensity at 560 nm [38] and leads to reduced signal intensity as the amplification reaction progresses, which was also confirmed by phenol red titration with pyrophosphoric acid concentration similar to that produced by DNA amplification (data not shown).

2.4.3 Optimization of colorimetric assay amplification

One of the important parameters in PLP-based RCA assays that has a pervasive effect in sensitivity is PLP concentration [13, 14]. Selectivity of RCA is grounded on specific and precise hybridization of PLP with its target which highlights the importance of this factor optimization [37]. We optimized concentration of PLP for a constant concentration of H5N1 target (0.25 μM) and different concentrations of PLP from 9 nM to 150 nM. Incrementation of the concentration of PLP is accompanied by a declining intensity at 560 nm (our detected signal) and it reaches a plateau at 37 nM (Fig. 2.3A). Because 37 nM is located at the lower limit of the plateau and may be more subject to disparities due to various small laboratory variations, the next point (75 nM) was deemed more robust as the optimized PLP concentration for the remaining optimization and calibration curves (Fig 2.3A, Inset 1). This trend is also observable via colour change of samples (Fig 2.3A, Inset 2).

As mentioned before, the signal in this colorimetric assay is in proportion with production of protons during isothermal DNA amplification reaction through incorporation of dNTPs into DNA strands [6, 24]. So, we evaluated the HRCA amplification time required to generate enough protons to witness colour change from pink to light orange. Absorbance intensity gradually decreases from 0 to 15 min, whereas at the time point of 20 min, the intensity suddenly drops (Fig. 2.3B, Inset 1) resulting in a colour change of samples which is clearly apparent by naked eyes (Fig. 2.3B, Inset 2). In this experiment the concentration of target was high enough to be discriminated after 20 min, whereas for lower range concentrations more time would be needed to see the colour change [22]. On the other hand, it is reported that incubating samples for more than 60 min at 63 ˚C could result in non-specific amplifications as the result of primers and conditions of reaction [6, 39]. This non-specific amplification could affect colour change in negative controls in a long period of incubation [6].

The last and main factor that was optimized in this project was initial pH of amplification mixture. Investigating this parameter is not only critical due to a pH-based detection but is also particularly challenging because of the two different reaction mixtures required, namely ligation and amplification. It is essential to have an initial pH value above the transition pH range of phenol red to have pink colour at the beginning of the reaction and light orange colour after HRCA reaction. It is also necessary for the optimized pH to be close to the pH range of Bst 2.0 WS DNA polymerase activity to make it possible for the polymerase enzyme to perform HRCA [22-24]. As a result, this parameter has dual impacts in the efficiency of phenol red-based RCA detection. The HRCA reaction does not affect absorbance intensity for initial pH values of 8.8 and 8.6 and it decreases a bit for pH of 8.4. Conversely, the intensity drops significantly for an initial pH value of 8.2 and remains at the same level for pH 8.0, where the intensity reaches a plateau. We have thus chosen 8.2 as an optimal initial pH for the amplification mixture (Fig. 2.3C, Inset 1). The primary pH of 8.8, 8.6 and 8.4 appeared too high to witness a colour change even after amplification reaction when exponential amounts of protons are produced. On the other hand, pH of 8.2 and 8.0 were low enough to permit a pH change in the transition range of phenol red and that is why they underwent colour change from pink to light orange after HRCA reaction (Fig. 2.3C, Inset 2).

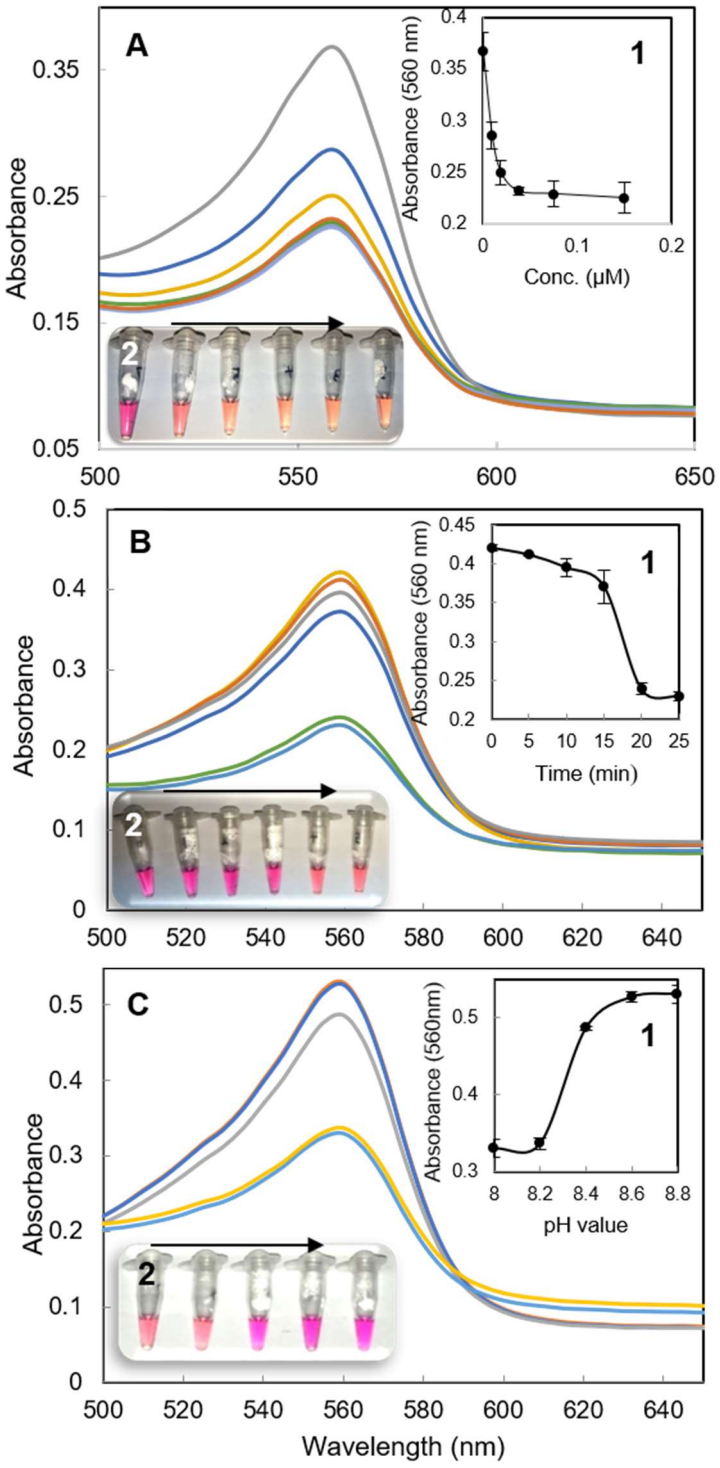

Figure 2.3 **Optimization of analytical parameters for colorimetric assay. (A) Optimization of PLP concentration was performed at a constant concentration of H_5N_1 target (0.25 μM) and different amounts of PLP (from top to bottom: 0, 0.009, 0.018, 0.037, 0.075, 0.150 μM). (B) HRCA amplification time optimization was carried out at the optimized concentration of 0.075 μM of PLP and 0.25 μM of target and different amplification times of 0, 5, 10, 15, 20, 25 min (from top to bottom). (C) pH of amplification buffer optimization was adjusted at a constant concentration of target (0.25 μM) and optimized concentration of PLP (75 nM), amplification**

time of 20 min and in the presence of different pH of amplification reaction 8.8, 8.6, 8.4, 8.2 to 8.0 (from top to bottom). Insets 1 and 2 in graphs A, B, C illustrate the absorbance of samples at 560 nm and a picture of the tubes, respectively (arrows indicate the direction of increasing PLP concentration, amplification time and pH of amplification buffer).

2.4.4 Calibration curve in phenol red-based RCA assay

After optimization of several parameters for the colorimetric assay, a standard curve was done with H5N1 as a target from 0.15 nM (and 0) to 625 nM to determine limit of detection (LOD), sensitivity and linear range of the proposed colorimetric assay (Fig. 2.4, Inset A). Phenol red absorbance intensity at 560 nm is concomitant with the target concentration and decreases by increasing the concentration of target. The logarithmic calibration curve highlights good linearity from 0.61 to 78.1 nM. (Fig. 2.4B). The LOD of the system was also calculated by using LOD = 3 s/m (where “s” is standard deviation and “m” is the slope of the linear range) [40]. Using this equation, we estimate a LOD of 3.3 pM at the signal to noise of three. However, for such concentrations to be properly determined, further optimization of the assay would be required because it is currently within three times standard deviation of background noise according to empirical measurements. The trend of post-HRCA colour gradually changes from pink to light orange by increasing the concentration of target. Importantly, the positive sample can be detected at 0.61 nM via an unaided eye where the absorbance intensity abruptly drops (Fig. 2.4, Inset C). Based on the Fig. 2.4 and the calculated error bar for the concentration of zero we cannot consider the two concentrations of 0.15 and 0.30 nM as signals since they are in the error bar area of the concentration zero. Therefore, the lowest concentration detected in this empirical experiment is 0.61 nM.

As it is shown in the standard curve plot (Fig. 2.4), this colorimetric biosensor is responding at nM ranges which is higher than representative concentration of target for clinical purposes. We tried to reach lower concentration by increasing the amplification time to more 1 hour and doing several optimizations to improve the assay sensitivity. However, we witnessed some non-specific amplification on negative controls by giving more amplification time (amplification time more than one hour) which causes color change in negative control samples from pink to orange. Therefore, more optimizations are needed to solve this problem to reach a better sensitivity and LOD. In addition, generally in case of infectious diseases such as influenza and corona virus, simple, fast and portable techniques for on site detection of viruses is important. Therefore, in this study we combined isothermal RCA assay with a colorimetric strategy to make the assay as simple as possible. However, the signal is also quantitated using absorbance spectroscopy to provide more advantages by presenting results either in quantitative or qualitative modes.

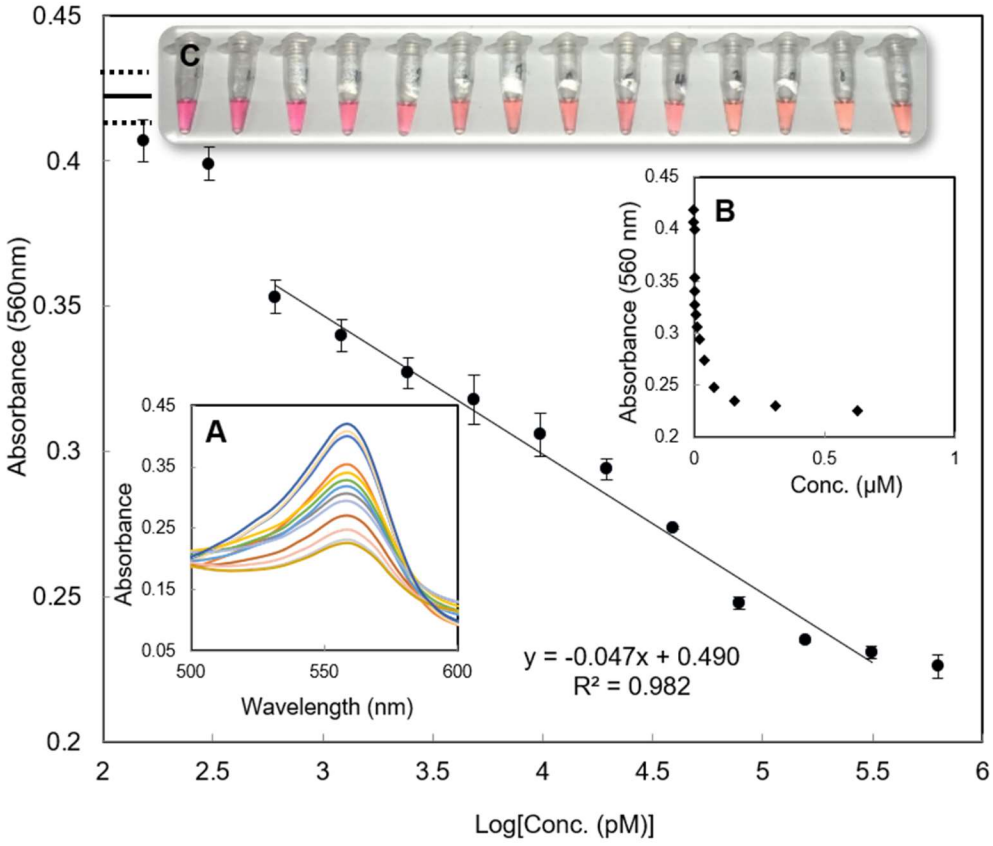

Figure 2.4 **Calibration curve of H5N1. (A) Determination of absorbance intensity for phenol red at different concentration of targets, from top to bottom, 0, 0.15, 0.30, 0.61, 1.22, 2.44, 4.88, 9.76, 19.53, 39.06, 78.12, 156.25, 312.5 and 625 nM. (B) Standard curve for determination of H_5N_1 target in colorimetric assay. (C) Changes in colors of samples by increasing the concentration of target (from left to right). The main graph represents the data in B on a logarithmic scale. The absorbance intensity for the concentration of zero is shown as a solid line and dash lines show error bars for zero concentration.**

2.4.5 Selectivity of the colorimetric biosensor

Selectivity is regarded as one of the significant characteristics of biosensors which means that the biosensors only respond in the presence of specific targets. Selectivity of this colorimetric assay was verified with various DNA sequences (unrelated viruses, as well as H5N1 target with a SNP at the ligation site). The absorbance intensity drops only for the sample containing the exact H5N1 target, while for the rest of the non-specific targets the intensity is the same as for the negative control (Fig. 2.5). This can also be seen by an unaided eye (Fig. 2.5, Inset), showing the use of this simple assay that requires no complex devices to evaluate the presence of a given target sequence. The fact that the colour change has not been observed in the sample that

contains a single point mutation further supports that the assay can even be used for SNP detection.

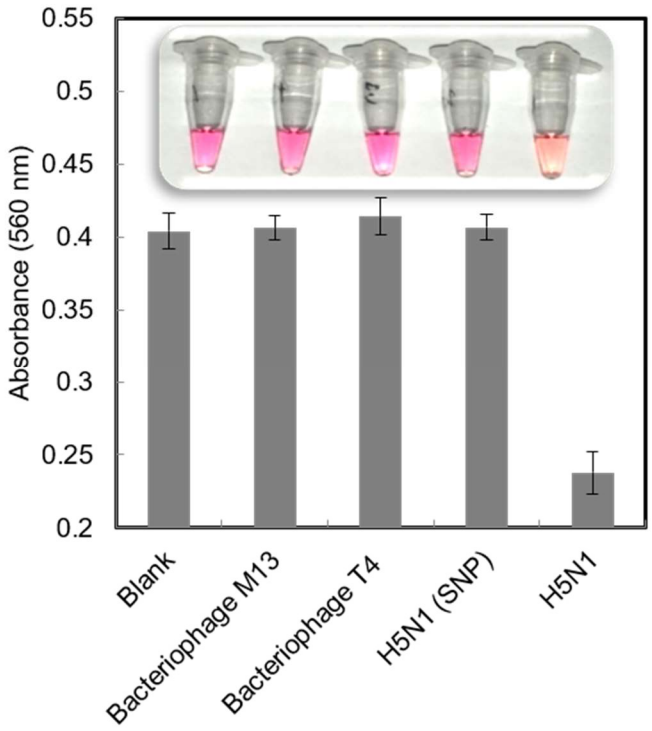

Figure 2.5 **Selectivity of the assay in the presence of different DNA samples. Selectivity of the system has been evaluated in the presence of different DNA molecules for the PLP targeting H5N1. These DNA molecules are the bacteriophage M13 and T4 genome, as well as a mutated H5N1 target with a SNP at the ligation site, blank control had no DNA except for PLP and HRCA oligonucleotides. Image shows changes in the color of the sample with specific target, however the color for the un-specific targets remains unchanged (tubes are in the same order as the histogram).**

2.4.6 Colorimetric assay with real sample

The performance of the proposed colorimetric assay in real samples was evaluated in two ways to see how it works in a matrix. First, we evaluated two different concentrations of H5N1 synthetic target (156 nM and 2.4 nM) in different dilutions of rat plasma. This evaluation was done due to the fact that the response of this assay is based on the change of pH and as a result including plasma, which is naturally buffered, could increase the buffering capacity of the reaction and consequently reduce intensity of the signal. As depicted in Fig. 2.6A, the signal intensity for the dilutions of 1/10, 1/100 and 1/1000 are almost the same as the signal intensity for the positive control signal that lacks plasma. However, the OD for the samples where undiluted plasma was added directly to the reaction is higher. This is likely due to the intrinsic coloration and

heterogenous composition of plasma, making it a bit cloudy which could have an impact on the absorbance of the samples. Nevertheless, the colour change for the undiluted plasma sample is still visible to the naked eye and it is comparable with the other samples that have lower dilutions of plasma (Fig. 2.6A, Inset). This result shows that this pH based colorimetric biosensor can work in complex situations which is the ultimate application for the proposed assay. We also tested our assay with another virus sequence for which full viruses were readily available, the M13 bacteriophage. Purified M13 phage genome was used as a model sample to simulate the performance of the assay in the presence of a real full length target. Therefore, another PLP was designed for M13 genome and response of the system was investigated in presence of different dilutions of samples of M13 phage in which the concentration was determined by a Nanodrop device. To compare results from the M13 genome, another standard curve was realized with oligonucleotides with the corresponding M13 sequence (Fig. 2.6B). Synthetic M13 target with extended ends were utilised in this assay to have DNA overhangs as would be the case with the M13 genome. Based on the calibration plot the concentration for four M13 real samples were 1.38 ± 0.09, 4.29 ± 0.3, 6.9 ± 1.3 and 9.3 ± 0.7 nM in which the concentrations were determined to be 2.50, 3.75, 5.00, 6.25 nM by a Nanodrop device. Therefore, a generally good consistency was obtained for assessing M13 genome concentration (+/- ~30% compared to short oligonucleotide, with good linearity as well over the range of three folds tested) which confirms the potential of this assay in different complex situations. Note that the excellent correspondence of the M13 and H5N1 standard curves suggests that the detection (whether quantitative or qualitative) is independent of the target and PLP sequences.

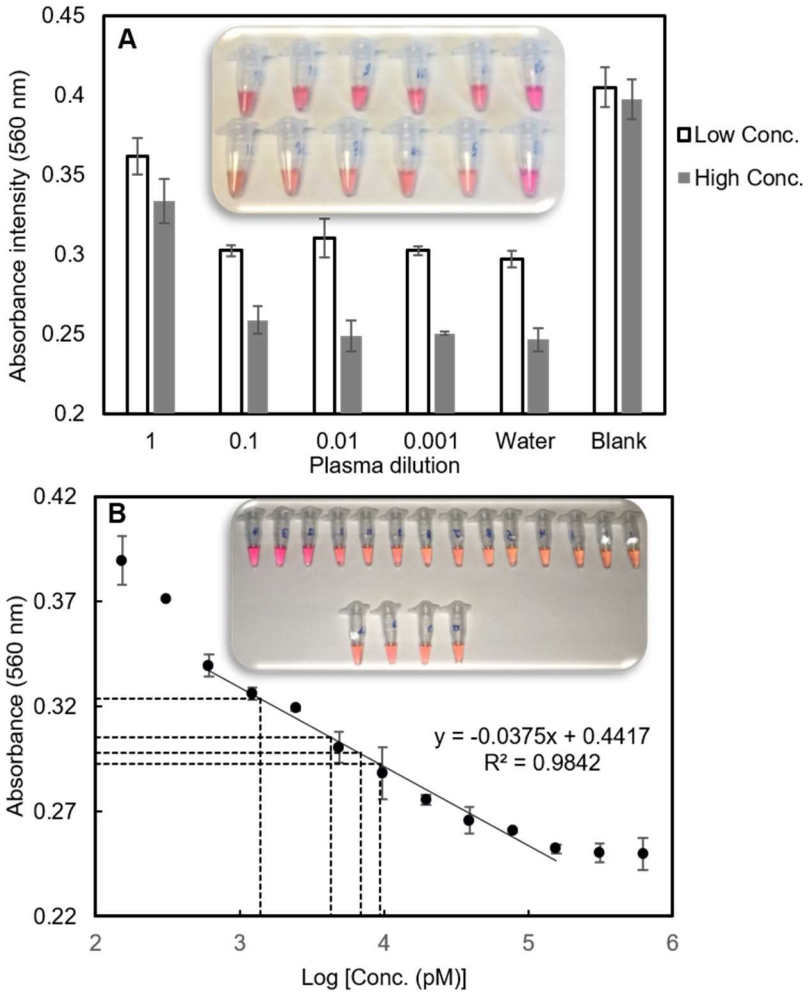

Figure 2.6 **Evaluating realistic samples. (A) The response was evaluated by adding 1 µL of different dilutions of plasma including direct plasma (1), 1/10, 1/100 and 1/1000 as well as a sample without plasma as a positive control and negative control without plasma nor H5N1 target. This experiment has been done at 156 nM (high concentration) and 2.4 nM (low concentration) of H5N1 target. Inset depicts the tubes with high concentration of target (upper samples) and low concentration of target (lower samples) in this experiment, in the same order as the bar graph. (B) Standard plot for M13 phage. Standard curve for M13 phage was realized by determining phenol red absorbance of samples at different concentrations of M13 synthetic targets, from left to right, 0, 0.15, 0.30, 0.61, 1.22, 2.44, 4.88, 9.76, 19.53, 39.06, 78.12 and 625 nM (black dots). Also, four samples which contain the full genome of M13 bacteriophage were used to determine the efficiency of the proposed biosensor in the presence of real M13 full circular genome target (dashed lines). Inset shows changing of colors of tubes from red to light orange by increasing the concentration of target (upper tubes correspond to synthetic target and lower ones to real M13 full genome).**

2.5 Conclusion

As compared with previous work shown in Table 2.1 [13, 41-47], we improve many analytical parameters, depending on the assay comparisons. In particular, the linear range, and enhanced contrast between positive and negative samples have improved. Reported uses of other dyes

namely hydroxy naphthol blue (HNB), malachite green and intercalating dyes [6] have not achieved this level of contrast. In addition, during this isothermal DNA amplification, signal is magnified enough to monitor trace amounts of the target whether in qualitive or in quantitative mode. As a result, this colorimetric assay offers a portable diagnostic technique that can be done in remote areas and with elementary instruments. In comparison with the large fragment of DNA polymerase (wild-type) and Bst 2.0, Bst 2.0 Warm Start DNA polymerase, the latest version of this enzyme, has been reported to be best because of a higher and faster amplification rate and the ability to preserve its amplification rate even after two hours of pre-incubation at room temperature [48]. That is why the colour of positive samples turns into light orange after only 20 min of incubation at 63 ˚C. Using a highly concentrated Bst 2.0 WS enzyme (120,000 U/ml) and T4 DNA ligase enzyme (400,000 U/ml) lessened additional introduction of Tris-HCl into reaction which has pervasive effect on the buffer capacity of solutions and consequently on the pH-based signal [22]. Moreover, in this work ligation reaction has been done efficiently in a reaction mixture without Tris-HCl or other buffering agents, enabling us to adopt RCA with the current colorimetric detection method using pH sensitive dyes. Although a previous report claimed that colorimetric detection using pH sensitives dyes applies to all isothermal amplification method including RCA [23], this previous work was just done on LAMP technique and does not explain how to adapt the ligation reaction with the amplification reaction, which is one of the most critical parts of the current work. So far, the PLP-based RCA method has been widely used for specific detection of SNPs in genomic DNA with high sensitivity [8, 49, 50]. In this work a new colorimetric method is established for the first time, with the possibility of monitoring SNPs, via a phenol red based RCA strategy that in turn further simplifies analysis of genetic material in a portable mode.

Table 2.1 Comparison of different parameters of the current work with those that have been reported in the literature.

Type of target	Amplification method	Detection method	Type of assay	Colour change / Portability	Linear range	LOD (pM)	Reference
DNA	HRCA	Colorimetric (HNB)[1]	Qualitative & quantitative	Violet to sky blue / +	0.16 -1.20 (pM)	0.008	[13]
DNA	SDA[2]	Colorimetric ($ATBS^{2-}$)[3]	Qualitative & quantitative	Colorless to green / +	1-100 (nM)	4	[41]
Protein	HRCA	Fluorescence (SYBR Green)	Quantitative	- / -	0.4-80 (nM)	400	[42]
Protein	LRCA	Electrochemical (Graphene)	Quantitative	- / -	10-200 (pM)	10	[43]
Protein	SDA	Colorimetric (AuNP)[4]	Qualitative & quantitative	Red to purple / +	2.0-80 (nM)	1100	[44]
DNA	HCR[5]	Colorimetric (AuNP)	Qualitative & quantitative	Red to purple / +	-	500	[45]
DNA	(Exo III)-aided Amplification[6]	Chemilumi-nescence (Luminol-H_2O_2)	Quantitative	- / -	0.01-1.0 (pM)	0.08	[46]
DNA	LAMP	Colorimetric (Calcein)	Qualitative	Dark yellow to green fluorescence / +	-	0.136[7]	[47]
DNA	HRCA	Colorimetric (Phenol red)	Qualitative & quantitative	Pink to light orange / +	0.61-78.12 (nM)	3.3	Current work

[1]Hydroxy naphthol blue
[2]Strand displacement amplification
[3]3-ethylbenzothiazoline-6-sulfonic acid
[4]Gold nanoparticle
[5]Hybridization chain reaction
[6]Exonuclease III-Assisted Cascade Signal Amplification
[7] Based in the information provided in the article, the average amplicon size used for LAMP reaction targeting *Fusarium graminearum* is 900 nucleotides. In addition, the lowest concentration of DNA target detected in this work was about 2 pg. By using this formula "*moles dsDNA (mol) = mass of dsDNA (g)/((length of dsDNA (bp) x 617.96 g/mol/bp) + 36.04 g/mol)*", we can determine moles of dsDNA in 2 pg of the dsDNA target which is calculated to be 342.4 amol. Also, since the LAMP reaction was performed in the final volume of 25 µL, we can determine the molarity of DNA target which is about 0.87 pM.

2.6 Acknowledgements

This work was supported by the Natural Sciences and Engineering Research Council of Canada (NSERC) and the Consortium de recherche et d'innovation en bioprocédés industriels au Québec (CRIBIQ). JP was a junior 1 research scholar and SVH received a fellowship from the Armand-Frappier foundation.

2.7 References

[1] M.R. Hartman, R.C. Ruiz, S. Hamada, C. Xu, K.G. Yancey, Y. Yu, W. Han, D. Luo, Point-of-care nucleic acid detection using nanotechnology, Nanoscale 5 (2013) 10141-10154.

[2] P. Yager, T. Edwards, E. Fu, K. Helton, K. Nelson, M.R. Tam, B.H. Weigl, Microfluidic diagnostic technologies for global public health, Nature 442 (2006) 412.

[3] M. Urdea, L.A. Penny, S.S. Olmsted, M.Y. Giovanni, P. Kaspar, A. Shepherd, P. Wilson, C.A. Dahl, S. Buchsbaum, G. Moeller, Requirements for high impact diagnostics in the developing world, Nature (2006) 73.

[4] V. Tsouti, C. Boutopoulos, I. Zergioti, S. Chatzandroulis, Capacitive microsystems for biological sensing, Biosens. Bioelectron. 27 (2011) 1-11.

[5] A. Niemz, T.M. Ferguson, D.S. Boyle, Point-of-care nucleic acid testing for infectious diseases, Trends Biotechnol. 29 (2011) 240-250.

[6] N.A. Tanner, Y. Zhang, T.C.E. Jr., Visual detection of isothermal nucleic acid amplification using pH-sensitive dyes, BioTechniques 58 (2015) 59-68.

[7] V.V. Demidov, Rolling-circle amplification in DNA diagnostics: the power of simplicity, Expert Mol. Diagn. 2 (2002) 542-548.

[8] P.M. Lizardi, X. Huang, Z. Zhu, P. Bray-Ward, D.C. Thomas, D.C. Ward, Mutation detection and single-molecule counting using isothermal rolling-circle amplification, Nature Genet. 19 (1998) 225.

[9] V.V. Demidov, Rolling circle amplification (RCA): toward new clinical diagnostics and therapeutics, first ed., Springer International Publishing, Switzerland, 2016.

[10] M. Nilsson, H. Malmgren, M. Samiotaki, M. Kwiatkowski, B.P. Chowdhary, U. Landegren, Padlock probes: circularizing oligonucleotides for localized DNA detection, Science 265 (1994) 2085-2088.

[11] D.C. Thomas, G.A. Nardone, S.K. Randall, Amplification of padlock probes for DNA diagnostics by cascade rolling circle amplification or the polymerase chain reaction, Arch. Pathol. Lab. Med. 123 (1999) 1170-1176.

[12] A. Mezger, M. Kühnemund, M. Nilsson, Rolling Circle Amplification with Padlock Probes for In Situ Detection of RNA Analytes, Rolling Circle Amplification (RCA), Springer (2016) 99-105.

[13] S.V. Hamidi, H. Ghourchian, Colorimetric monitoring of rolling circle amplification for detection of H 5 N 1 influenza virus using metal indicator, Biosens. Bioelectron. 72 (2015) 121-126.

[14] S.V. Hamidi, H. Ghourchian, G. Tavoosidana, Real-time detection of H 5 N 1 influenza virus through hyperbranched rolling circle amplification, Analyst 140 (2015) 1502-1509.

[15] E.D. Dawson, C.L. Moore, D.M. Dankbar, M. Mehlmann, M.B. Townsend, J.A. Smagala, C.B. Smith, N.J. Cox, R.D. Kuchta, K.L. Rowlen, Identification of A/H5N1 influenza viruses using a single gene diagnostic microarray, Anal. Chem. 79 (2007) 378-384.

[16] W. Yao, R.H. Byrne, Spectrophotometric determination of freshwater pH using bromocresol purple and phenol red, Environ. Sci. Technol. 35 (2001) 1197-1201.

[17] L. Rovati, P. Fabbri, L. Ferrari, F. Pilati, Plastic optical fiber pH sensor using a sol-gel sensing matrix, Fiber Optic Sensors, InTech (2012) pp. 415-438.

[18] M.I. Khan, K. Mukherjee, R. Shoukat, H. Dong, A review on pH sensitive materials for sensors and detection methods, Microsystem Technologies 23 (2017) 4391-4404.

[19] C. Chatterjee, A. Sen, Sensitive colorimetric sensors for visual detection of carbon dioxide and sulfur dioxide, J. Mater. Chem. A 3 (2015) 5642-5647.

[20] V.K. Gupta, S. Kumar, R. Singh, L. Singh, S. Shoora, B. Sethi, Cadmium (II) ion sensing through p-tert-butyl calix [6] arene based potentiometric sensor, J. Mol. Liq. 195 (2014) 65-68.

[21] V.K. Gupta, N. Mergu, L.K. Kumawat, A.K. Singh, Selective naked-eye detection of magnesium (II) ions using a coumarin-derived fluorescent probe, Sens. Actuator B-Chem. 207 (2015) 216-223.

[22] C.B. Poole, Z. Li, A. Alhassan, D. Guelig, S. Diesburg, N.A. Tanner, Y. Zhang, T.C. Evans Jr, P. LaBarre, S. Wanji, Colorimetric tests for diagnosis of filarial infection and vector surveillance using non-instrumented nucleic acid loop-mediated isothermal amplification (NINA-LAMP), PloS one 12 (2017) e0169011.

[23] D. Mitra, I.K. Dimov, J.R. Waldeisen, Colorimetric Detection of Nucleic Acid Amplification, U.S. Patent-US20170044599A1, 2017.

[24] N. Tanner, Y. Zhang, T.C. Evans, Detection of an amplification reaction product using pH-sensitive dyes, U.S. Patent-US20140057268A1, 2015.

[25] A. Alhassan, M.Y. Osei-Atweneboana, K.F. Kyeremeh, C.B. Poole, Z. Li, E. Tettevi, N.A. Tanner, C.K. Carlow, Comparison of a new visual isothermal nucleic acid amplification test with

PCR and skin snip analysis for diagnosis of onchocerciasis in humans, Mol. Biochem. Parasitol. 210 (2016) 10-12.

[26] A.E. Calvert, B.J. Biggerstaff, N.A. Tanner, M. Lauterbach, R.S. Lanciotti, Rapid colorimetric detection of Zika virus from serum and urine specimens by reverse transcription loop-mediated isothermal amplification (RT-LAMP), PloS one 12 (2017) e0185340.

[27] D. Yuan, J. Kong, X. Li, X. Fang, Q. Chen, Colorimetric LAMP microfluidic chip for detecting three allergens: peanut, sesame and soybean, Sci. Rep. 8 (2018) 8682.

[28] E. Tenaglia, Y. Imaizumi, Y. Miyahara, C. Guiducci, Isothermal multiple displacement amplification of DNA templates in minimally buffered conditions using phi29 polymerase, Chem. Commun. 54 (2018) 2158-2161.

[29] P. Gyarmati, T. Conze, S. Zohari, N. LeBlanc, M. Nilsson, U. Landegren, J. Banér, S. Belák, Simultaneous genotyping of all hemagglutinin and neuraminidase subtypes of avian influenza viruses by use of padlock probes, J. Clin. Microbiol. 46 (2008) 1747-1751.

[30] M.C. Steain, D.E. Dwyer, A.C. Hurt, C. Kol, N.K. Saksena, A.L. Cunningham, B. Wang, Detection of influenza A H1N1 and H3N2 mutations conferring resistance to oseltamivir using rolling circle amplification, Antivir. Res. 84 (2009) 242-248.

[31] M.R. Green, J. Sambrook, Isolation of high-molecular-weight DNA using organic solvents, Cold Spring Harb. Protoc. (2017) pdb. prot093450.

[32] M.R. Green, J. Sambrook, Precipitation of DNA with Ethanol, Cold Spring Harb. Protoc. (2016) pdb. prot093377.

[33] Y. Zhong, J. Han, Z. Zou, S. Liu, B. Tang, X. Ren, X. Li, Y. Zhao, Y. Liu, D. Zhou, Quantitation of HBV covalently closed circular DNA in micro formalin fixed paraffin-embedded liver tissue using rolling circle amplification in combination with real-time PCR, Clin. Chim. Acta. 412 (2011) 1905-1911.

[34] H. Kuhn, V.V. Demidov, M.D. Frank-Kamenetskii, Rolling-circle amplification under topological constraints, Nucleic Acids Res. 30 (2002) 574-580.

[35] T. Notomi, H. Okayama, H. Masubuchi, T. Yonekawa, K. Watanabe, N. Amino, T. Hase, Loop-mediated isothermal amplification of DNA, Nucleic Acids Res. 28 (2000) e63-e63.

[36] M. Nilsson, Lock and roll: single-molecule genotyping in situ using padlock probes and rolling-circle amplification, Histochem. Cell Biol. 126 (2006) 159-164.

[37] M. Szemes, P. Bonants, M. de Weerdt, J. Baner, U. Landegren, C.D. Schoen, Diagnostic application of padlock probes—multiplex detection of plant pathogens using universal microarrays, Nucleic Acids Res. 33 (2005) e70-e70.

[38] E. Wang, K.-F. Chow, V. Kwan, T. Chin, C. Wong, A. Bocarsly, Fast and long term optical sensors for pH based on sol–gels, Anal. Chim. Acta 495 (2003) 45-50.

[39] Y. Kimura, M.J.L. de Hoon, S. Aoki, Y. Ishizu, Y. Kawai, Y. Kogo, C.O. Daub, A. Lezhava, E. Arner, Y. Hayashizaki, Optimization of turn-back primers in isothermal amplification, Nucleic Acids Res. 39 (2011) e59-e59.

[40] D.C. Harris, Quantitative chemical analysis, Seventh Edition, W. H. Freeman and Company, New York, 2007, Chapter 5 (Quality assurance and calibration methods), 78-87.

[41] D. Wu, H. Xu, H. Shi, W. Li, M. Sun, Z. S. Wu, A label-free colorimetric isothermal cascade amplification for the detection of disease-related nucleic acids based on double-hairpin molecular beacon, Anal. Chim. Acta 957 (2017) 55-62.

[42] L. Yang, C.W. Fung, E.J. Cho, A.D. Ellington, Real-time rolling circle amplification for protein detection, Anal. Chem. 79 (2007) 3320-3329.

[43] M. Liu, J. Song, S. Shuang, C. Dong, J.D. Brennan, Y. Li, A graphene-based biosensing platform based on the release of DNA probes and rolling circle amplification, ACS nano 8 (2014) 5564-5573.

[44] H. Zhang, F. Li, H. Chen, Y. Ma, S. Qi, X. Chen, L. Zhou, AuNPs colorimetric sensor for detecting platelet-derived growth factor-BB based on isothermal target-triggering strand displacement amplification, Sens. Actuators B: Chem. 207 (2015) 748-755.

[45] C. Ma, W. Wang, A. Mulchandani, C. Shi, A simple colorimetric DNA detection by target-induced hybridization chain reaction for isothermal signal amplification, Anal. Biochem. 457 (2014) 19-23.

[46] Y. Gao, B. Li, Exonuclease III-Assisted Cascade Signal Amplification Strategy for Label-Free and Ultrasensitive Chemiluminescence Detection of DNA, Anal. Chem. 86 (2014) 8881-8887.

[47] L. Niessen, R.F. Vogel, Detection of Fusarium graminearum DNA using a loop-mediated isothermal amplification (LAMP) assay, Int. J. Food Microbiol. 140 (2010) 183-191.

[48] N.A. Tanner, Y. Zhang, T.C. Evans Jr, Simultaneous multiple target detection in real-time loop-mediated isothermal amplification, Biotechniques 53 (2012) 81-89.

[49] A.F. Faruqi, S. Hosono, M.D. Driscoll, F.B. Dean, O. Alsmadi, R. Bandaru, G. Kumar, B. Grimwade, Q. Zong, Z. Sun, High-throughput genotyping of single nucleotide polymorphisms with rolling circle amplification, BMC genomics 2 (2001) 4.

[50] C. Larsson, J. Koch, A. Nygren, G. Janssen, A.K. Raap, U. Landegren, M. Nilsson, In situ genotyping individual DNA molecules by target-primed rolling-circle amplification of padlock probes, Nat. Methods 1 (2004) 227.

3 REAL-TIME ISOTHERMAL DNA AMPLIFICATION MONITORING IN PICOLITER VOLUMES USING OPTICAL FIBER SENSOR

Suivi en temps réel de l'amplification isotherme d'ADN dans des volumes de picolitres à l'aide d'un capteur à fibre optique

Monika Janik[1,2,*,‡], Seyed Vahid Hamidi[3,‡], Marcin Koba[1,4], Jonathan Perreault[3], Ryan Walsh[3], Wojtek J. Bock[5], Mateusz Śmietana[1]

[1] Warsaw University of Technology, Institute of Microelectronics and Optoelectronics, Koszykowa 75, 00-662, Warszawa, Poland

[2] Gdansk University of Technology, Faculty of Electronics, Telecommunications and Informatics, Department of Metrology and Optoelectronics, Narutowicza 11/12, 80-233 Gdansk

[3] INRS Centre Armand-Frappier Santé Biotechnologie, 531 boulevards des Prairies Laval (QC) Canada

[4] National Institute of Telecommunications, Szachowa 1, 04-894, Warszawa, Poland

5 Photonic Research Centre, University of Quebec in Outaouais, 101 rue Saint-Jean-Bosco, Gatineau (QC), Canada

‡ Monika Janik and Seyed Vahid Hamidi contributed equally as first authors in this article.

This article is published in Lab on a Chip journal.

Received 23 October 2020, Accepted 25 November 2020, Available online 26 November 2020.

https://doi.org/10.1039/D0LC01069C

Author contributions:

Conceptualization, M.J., S.V.H., and J.P.; Software, M.K.; Resources, J.P., W.J.B.; Methodology, M.J., S.V.H., J.P.; Validation, M.J. and S.V.H.; Formal Analysis, M.J., S.V.H., J.P., R.W., M.K., and M.Ś.; Optical sensor preparation: M.J.; Biological materials preparation: S.V.H. and R.W.; Investigation: M.J.; Data Curation, M.J.; Writing—Original Draft Preparation, M.J., S.V.H ; Writing—Review and Editing, M.J., S.V.H., M.K., M.Ś., J.P. and R.W. ; Visualization: M.J.; Supervision: J.P., M.Ś. and W.J.B.; Funding Acquisition, J.P., M.Ś. and W.J.B.; Project administration: J.P., M.Ś. and W.J.B. All authors have read and agreed to the published version of the manuscript

A short description about this work:

In contrast to the previous chapter, which aimed at using RCA for a portable assay making it ideal for its convenient use at POC, this chapter tackles a different challenge. This publication is about the second objective of the PhD project, and it is about combining RCA with other powerful platforms for ultra-sensitive detection of infectious disease. While it requires specialized instrumentation, such ultra-sensitive detection system is suitable for targets present at very low levels. For instance, in a reported study HRCA-based PLP was employed for determining circulating serum microRNA levels for early breast cancer detection (Fan *et al.*, 2018). Prognosis of cancer patients at an early stage is crucial to improve survival rates in patients and prescribe a suitable treatment accordingly. Detection of very low concentration of viruses (especially those viruses that cause infectious diseases) is also important to screen individuals when the viral load is low and patients do not show symptoms. In this project, by coupling two robust techniques, including RCA and micro-cavity in-line Mach-Zehnder interferometer (μIMZI), an ultra-sensitive biosensor was developed for monitoring of H5N1 virus. A good linearity ranging from 283 to 2 830 000 circular DNA copies and very low LOD of 6 copies were achieved in this project. In addition to ultra-sensitivity, this biosensor provides signal from a circular DNA in 30 min even at very low concentration. Therefore, RCA based μIMZI method would be a good detection platform for fast and ultra-sensitive targeting of nucleic acid biomarkers. In addition, the proposed detection process should be done in equipped labs that have sophisticated and expensive laser devices and highly trained staffs to perform the experiments. However, very low concentrations of targets which is about few copy numbers were detected using this strategy which is not easily achievable by instrumentation-free and portable strategies.

3.1 Abstract

Rolling circle amplification (RCA) of DNA can be considered as a great alternative to the gold standard polymerase chain reaction (PCR), especially during this pandemic period, where rapid, sensitive, and reliable test results for hundreds of thousands of samples are required daily. This work presents the first research to date on direct, real-time and label-free isothermal DNA amplification monitoring using microcavity in-line Mach Zehnder interferometer (μIMZI) fabricated in an optical fiber. The solution based on μIMZI offers a great advantage over many other sensing concepts – makes possible optical analysis in just picoliter sample volumes. The selectivity of the biosensor is determined by DNA primers immobilized on the microcavity's surface that act as selective biorecognition elements and triggers initiating the DNA amplification process. In this study, we verified the sensing concept using circular DNA designed to target the H5N1 influenza virus. The developed biosensor exhibits an ultrahigh refractive index sensitivity reaching 14,000 nm per refractive index unit and a linear detection range between 9.4 aM and 94 pM of the target DNA sequence. Within a 30 min period, the amplification of as little as 9.4 aM DNA can be effectively detected, with a calculated limit of detection as low as 0.2 aM DNA, suggesting this methodology holds great promise in practical disease diagnosis applications in the future

3.2 Introduction

It has been more than thirty years since DNA amplification technologies were introduced and revolutionized molecular diagnostics.[1] Lately, interest in selective DNA amplification methods for diagnostics has become central to addressing the threat of the SARS-CoV-2 pandemic. Pandemic requires rapid, sensitive, and reliable test results for hundreds of thousands of samples daily. Invariably, the most frequently used techniques for detection rely on the polymerase chain reaction (PCR). PCR methods are based on the use of a thermostable enzyme (DNA polymerase) and thermocycler devices that can rapidly synthesize millions to billions of copies of a specific target DNA region. However, much of this gold standard method relies on precision thermal cycling, thus making it incompatible with on-chip analysis and difficult to adapt to many important diagnostic applications. Therefore, this limitation strongly justifies a quest for isothermal DNA amplification alternatives.[2,3] Rolling circle amplification (RCA) among all isothermal DNA amplification methods, such as loop-mediated isothermal amplification,[4] nucleic acid sequence-based amplification,[5] and signal mediated amplification of RNA technology,[6] is one of the simplest, most powerful, and versatile techniques. In contrast to PCR, which relies on linear, double-stranded DNA (dsDNA) templates, RCA utilizes a circular oligonucleotide as a template

for a strand displacing DNA polymerase, such as Phi29. The Phi29 polymerase produces a long repeating product strand that serves as amplified copies of the circle sequence.[7,8] The RCA offers several unique features that give it an advantage over conventional PCR-based processes. RCA does not need costly temperature cyclers or any other specialized instrumentation. Simplicity, short assay time, high sensitivity, and selectivity make this technique ideal for the low-cost and point-of-care diagnostics. Moreover, besides simplicity, RCA is compatible with all sorts of platforms, which makes it suitable for sensitive monitoring of a wide selection of infectious diseases.[9,10]

RCA-based assays are mainly analysed by quantification of the reaction products utilizing fluorescent measurements,[11–13] nanoparticle labeling,[13–16], or enzyme linkage.[16,17] This, in turn, enables monitoring of the reaction in real-time, but introduces additional materials and sample processing steps. Thus, it complicates the procedure, increases its time, as well as the cost of the assay, and limits the sensitivity of the method. However, thanks to the isothermal nature of RCA processes, there have been a few attempts to combine RCA with microfluidic platforms[18,19] or sensing schemes based on surface plasmon resonance (SPR),[14,20] electrochemistry,[21] and electrochemiluminescence.[22] Even though some of these sensing systems reached aM limits of detection for DNA, most of them require additional signal enhancement. To reach those detection limits, e.g., nanoparticles or additional enzymatic cleavage reactions have been utilized. To maximize the RCA potential in molecular diagnostics, we sought to reduce technical complications and simplify the sensing procedure. It was achieved by combining RCA with a reliable, highly sensitive, and compact sensor, embedded in an optical fiber. Despite the recent advance in fiber optic sensors along with their intrinsic benefits, such as immunity to electromagnetic interference, the possibility of multiplexing, the capacity for remote measurement, the high compatibility with telecom optoelectronic devices, the low power consumption, high resistance to harsh environmental conditions (including corrosive chemicals) and long-term reliability, to date, optical fiber sensors have not been utilized to monitor isothermal DNA amplification.

Designed for this experiment optical fiber sensor is 60 μm in diameter and about 62.5 μm deep microcavity. The microstructure is fabricated by a femtosecond laser ablation in a standard telecommunication fiber forming a microcavity in-line Mach Zehnder interferometer (μIMZI). Such a structure facilitates the analysis of liquid samples of picoliter volumes. The microstructure splits light guided in the fiber into two parts, where one continues to propagate inside the remaining part of the core (reference beam), while the other propagates through the cavity (sensing beam)

(Figure 3.1a). Two beams interfere at the distant sidewall of the microcavity resulting in an interference pattern. The sensitivity of this system to changes in optical properties in the cavity, i.e., refractive index (RI), exceeds 20,000 nm/RIU[23]. It makes the sensor one of the most sensitive fiber-optic platforms to date.

In contrast to other fiber optic sensors, e.g., those based on fiber gratings[24] or SPR-based fiber optic sensors,[24] μIMZI's sensitivity and character of the obtained response strongly depend on whether the RI changes taking place close to the μIMZI bottom or away from it, i.e., in the microcavity's volume. The spectral location of the transmission minimum – the mth-order interference dip, m is an integer (λm) – in the interference pattern can be described by Equation (3.1), where d is the diameter of the microcavity, Δneff = nco − ncl is the difference between the effective RI of the two interfering modes, namely nco, and ncl in the remaining part of the fiber core and micromachined circular cavity, respectively, and φ0 represents the initial phase.

$$\lambda_m = \frac{2\pi d \Delta n_{eff}}{(2m+1)\pi - \varphi_0} \qquad (3.1)$$

Assuming the spectral shift relies mainly on Δn_{eff}, the response of the μIMZI can be influenced by two different effects delivering opposite outcomes. First, an increase in RI of the liquid within the microcavity volume influences mainly n_{cl}, thus inducing a spectral shift towards shorter wavelengths (Figure 3.1b1 and 3.1c1). On the other hand, change in RI at the microcavity's bottom affects the propagation in the remaining part of the core (n_{co}) inducing a shift of the spectrum towards longer wavelengths (Figure 3.1c2). This increase may result from, e.g., chemical functionalization of the surface, deposition of small biological materials, such as a peptide or DNA aptamers, or thin-film deposition (Figure 3.1b2)[25].

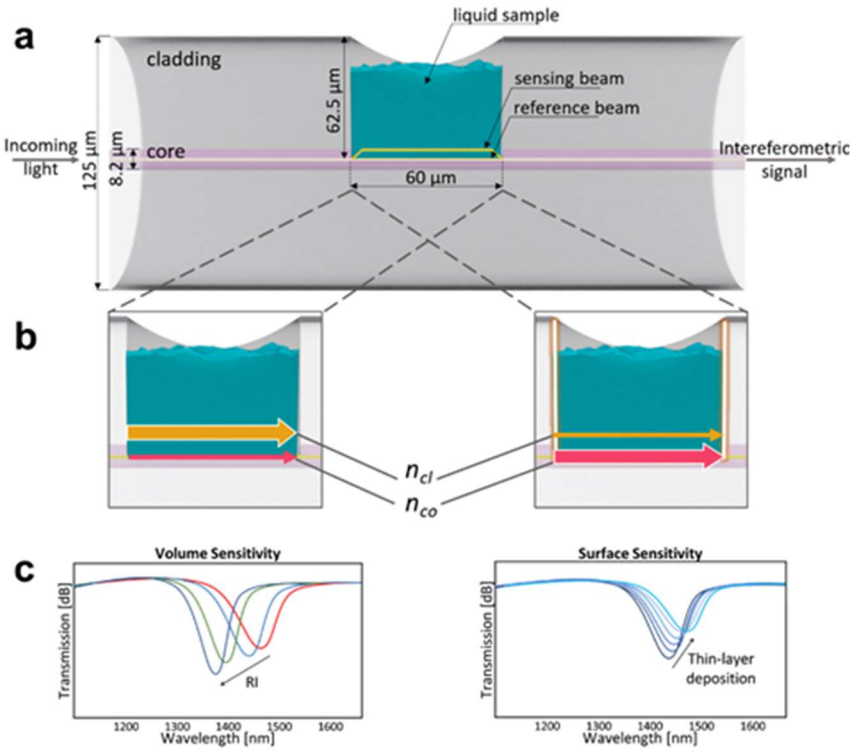

Figure 3.1 **a) A schematic illustration of the investigated µIMZI structure (cross-section view); b) Schematically shown two interfering modes – nco in the remaining part of the fiber core, and ncl in the micromachined cavity, influenced by the liquid inside the cavity and a thin layer, respectively. The drawings are not to scale; c) Exemplary transmission spectra of the µIMZI structure influences by RI changes and thin-layer thickness. Arrows indicate the shift of the minimum induced by each process.**

In this proof-of-concept research, a pre-circularized DNA (circDNA) designed in our previous work[26] targeting the H5N1 influenza virus was employed as a sample target to develop an optical-fiber-based RCA monitoring technique. Combination of µIMZI and RCA enables users to monitor the detection via the amplification process in (1) real-time without labels or additional signal enhancers, (2) a pL volume (as a volume of the biological samples are often highly limited and intended for more than one test), and (3) with the highest possible selectivity and sensitivity detecting as little as hundreds of target copies.

3.3 Results and discussion

3.3.1 The µIMZI characterization

Each µIMZI utilized in this work was precisely micromachined following the optimized parameters described in Section 3.5.1 Figure 3.2a presents SEM visualization of one of the µIMZI. The whole

surface of the structure is smooth, well-defined, the bottom is flat and precisely micromachined, and no additional damages are introduced to the cavity or the working area.

The microfabrication was followed by the RI sensitivity measurements of the μIMZIs. The measurements were performed on specially prepared hydrophobic test surfaces which allowed precise control of the amount of dosed liquid and filling of the microcavity. Figure 3.2b presents the transmission spectra of one of the chosen μIMZI samples where RI filling the cavity varied in the range from 1.3333 to 1.3496 RIU. Both the transmitted power and the wavelength of the minima change with RI. The minimum shifts towards shorter wavelengths with RI what illustrates the volume sensing effect (Figure 3.1c1). In Figure 3.2c, the corresponding values of the spectral minima are plotted vs RI. The points corresponding to each of the samples are linearly approximated with the least square method, and the sensitivity in the chosen RI region is obtained. The fabricated interferometric structures reveal high linearity (R^2=0,997) of the RI sensitivity.

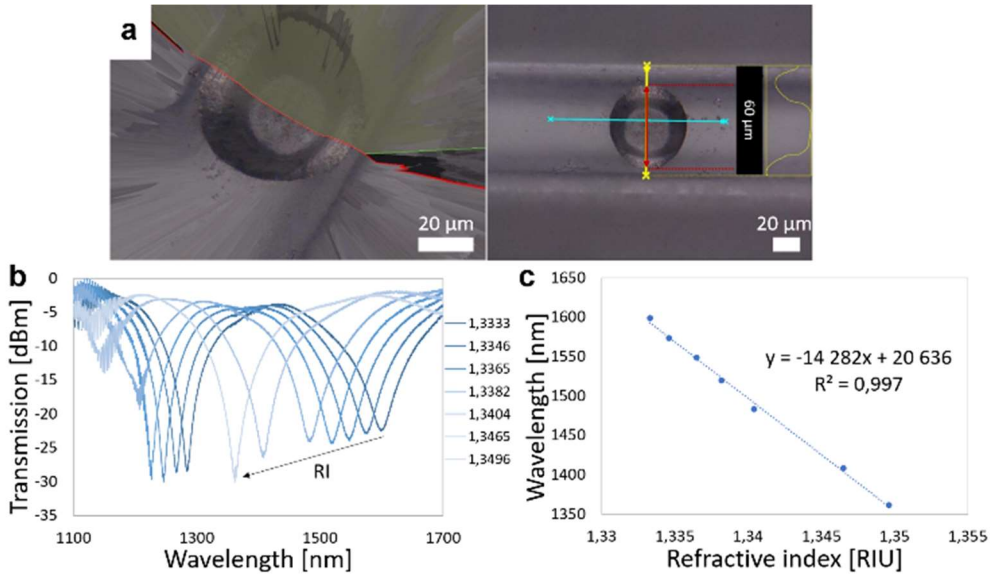

Figure 3.2 **(a) A SEM pictures (top view) where the red arrow indicates the diameter of the microcavity, and yellow and blue arrows indicate the area subjected to scanning. RI sensitivity of the μIMZI where (b) shows transmission spectra of μIMZI filled with RI ranging from 1.3333 to 1.3496 RIU and (c) shows corresponding minimum wavelengths (marked by the black arrow in Figure 2b) plotted vs RI.**

3.3.2 Chemical modification of the μIMZI's surface

To initiate the RCA reaction, the targeted DNA needs to hybridize with specific primers. This pair creates a binding site for DNA polymerase and enabling the DNA amplification. Therefore, to accommodate the RCA reaction inside the microcavity and be able to monitor the progress of the DNA amplification, both forward and reverse primers were immobilized on the μIMZI's surface. To ensure the covalent binding of the primers, the surface of the sensor was chemically modified

(Section 3.5.2). The chemical modification was based on the two silanes, namely Triethoxysilylpropyl Succinic Anhydride (TESPSA) and (Azidopropyl)triethoxysilane (AzPTES) attached to the fiber's hydroxyl-coated surface by ethoxy groups. TESPSA has been used as a non-reactive linker to passivate the surface, while AzPTES with its azido group clicks with a DCBO group on DNA primer and thus forms a covalent bond between the DNA and the μIMZI surface. This surface treatment strategy based on click chemistry highly increased the efficiency of the subsequent immobilization of biological material. Furthermore, in contrast to typical NHS-ester chemistry relying on a terminal amine group on the primer,[27] it allowed us to avoid additional blocking of the surface.

During the following experimental steps, the μIMZI transmission spectra were monitored in range λ = 1100–1700 nm at a constant temperature of 24.3 degrees Celsius. Figure 3.3a presents the transmission spectra after each stage of the surface functionalization. The solid blue curve represents a readout before silanization; the solid red curve – after silanization with AzPTES and TESPSA, and the solid green curve represents the spectra after immobilization of the primers via click chemistry. The 30 min-long silanization process resulting in a shift of the minimum towards longer wavelengths by about 1.6 nm with a simultaneous increase in the transmission. Next, the primers' incubation step resulted in a 1.0 nm shift of the minimum also towards longer wavelengths what indicated the formation of the DNA-overlay on the surface of the microcavity. Figure 3.3b depicts an evolution of the wavelength corresponding to the transmission minimum at subsequent steps of surface functionalization along with primers' immobilization. Each measurement takes approx. 20 sec. It is worth mentioning that a sudden wavelength shift at the beginning of primers' immobilization (marked by a red arrow) is a result of an increase of RI of the sample. The further gradual shift of the spectrum towards shorter wavelengths is caused by the formation of the primers layer on the sensor's surface. This, in turn, changes the effective RI inside the microcavity and thus, the propagation conditions. At the end of the incubation, after extensive washing of the surface with PBS, the wavelength changes (designated as "Primers" in Figure 3.3b) revealing the influence of the formed DNA layer.

Done in parallel ccontact angle measurements allowed us to monitor the impact of silanization on the surface wettability (Figure 3.3c). Cleaning of the glass surface decreased the contact angle to the immeasurable value. Next, 30 min of chemical modification process increased it to 74.7° making the surface hydrophobic and indicating successful silanization of the surface.

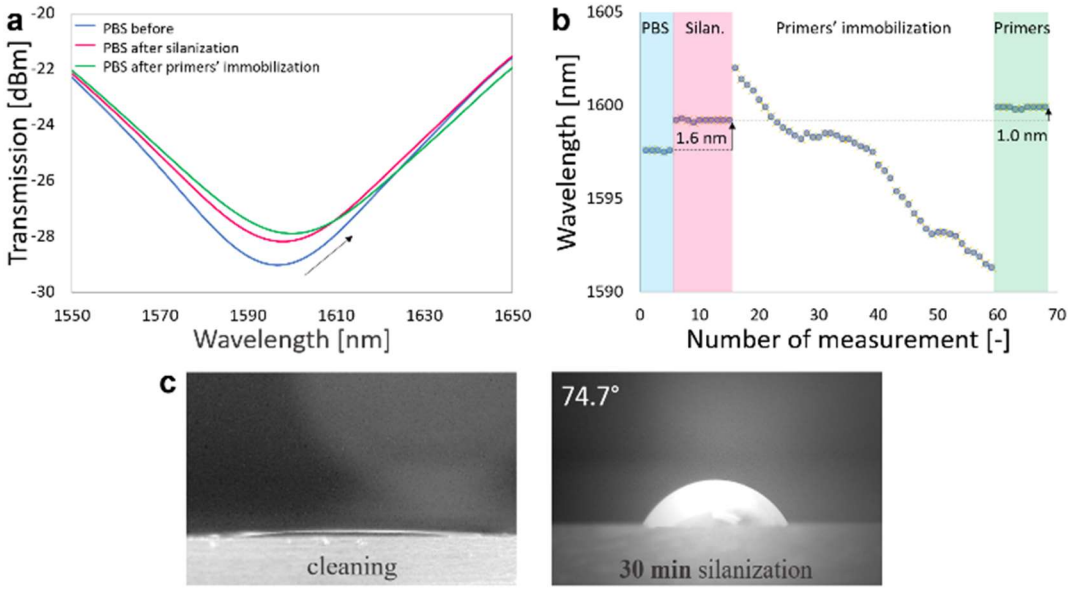

Figure 3.3 **(a) Transmission spectra of the μIMZI at each stage of the surface functionalization, namely: in PBS before silanization, silanization with AzPTES and TESPSA, and immobilization of DNA primers via click chemistry. (b) Wavelength corresponding to the transmission minimum at subsequent steps of surface functionalization. For further analysis, only measurements performed in PBS were considered ("PBS", "Silan", "Primers"). (c) Photographic images of water droplet deposited on the glass surface after cleaning and after 30 min silanization processes.**

3.3.3 RCA reaction mechanism

Functionalized μIMZI sensors were ready to proceed with the amplification reaction. The reaction started with the addition of an amplification mixture consisting of key elements. First, the circDNA – circular template/DNA target, the enzyme Phi29 DNA polymerase, and deoxynucleotide triphosphates (dNTPs) used to synthesize the new DNA strand. The components were diluted in Phi29 DNA polymerase buffer solution which provides an ideal chemical condition for optimum activity of the DNA polymerase.[26] Finally, bovine serum albumin is added as an adjuvant to stabilize the enzyme and preventing non-specific interactions.

The target circDNA described in our previous work[10,26] has an affinity to the forward primer immobilized on the μIMZI's surface. Thus, once specific hybridization between the target and forward primer on the microcavity's surface occurs (Figure 3.4a), Phi29 DNA polymerase starts DNA amplification from the 3´-hydroxyl group (OH) of the forward primer. When it reaches the starting point in the circular template it displaces the downstream strand and continues DNA polymerization (Figure 3.4b).[27,28] Therefore, the product of such amplification is a long tandemly repeated single-stranded DNA (ssDNA). Since the immobilized reverse primer is complementary to the long repeated single ssDNA (Figure 3.4c), it hybridizes with the produced ssDNA and brings

it into the μIMZI's surface. These leads Phi29 DNA polymerase to also use 3´ OH groups of the hybridized reverse primer and perform further DNA amplification (Figure 3.4d). Because this newly synthesized strand is of the same sequence as the initial circDNA, the forward primer can once again hybridize to it to produce a new strand, and so on, hence a rapid exponential amplification. The final product of such isothermal DNA polymerization is double-stranded DNA which makes the process similar to conventional hyperbranched RCA (HRCA).[8,26]

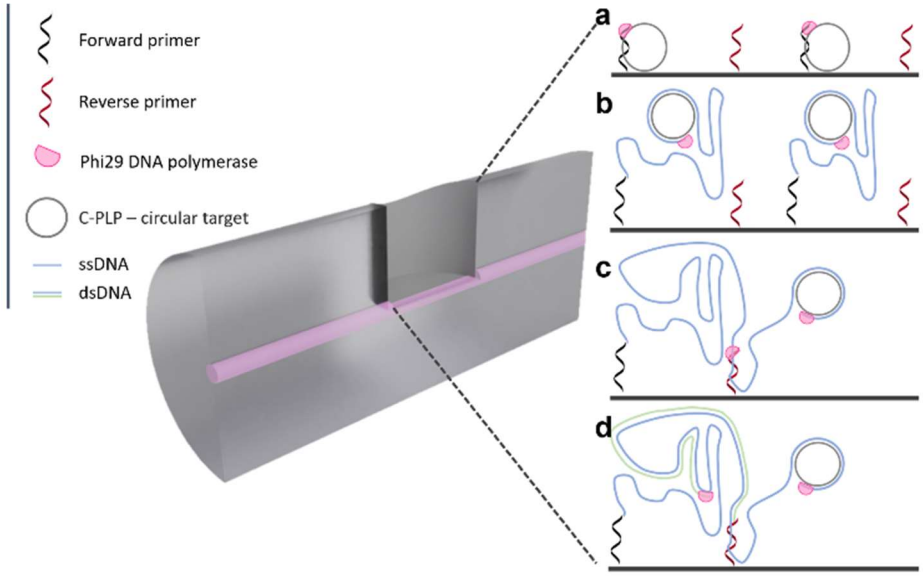

Figure 3.4 **The schematic illustration of the RCA process inside the microcavity, where (a) shows hybridization of the circDNA to the forward primers followed by Phi29 DNA polymerase attachment, (b) DNA amplification, (c) complementary ssDNA product binding to the reverse primer, and (d) further DNA amplification with the use of the 3'OH group of the reverse primers.**

3.3.4 The RCA real-time monitoring

The RCA process was monitored approx. every 20 sec. for 90 minutes. Each measurement corresponds to the 20 sec.-long intervals. Various circDNA concentrations starting from approximately 283 to 2 830 000 circDNA copies were applied. Within this experiment, we investigated the feasibility of performing a quantitative analysis of amplified DNA using the μIMZI sensor.

Figure 3.5a depicts the evolution of wavelength corresponding to the transmission minimum during the RCA monitoring and Figure 3.5b presents the exemplary spectral response (detection of 2 830 circDNA copies). As can be seen in Figure 3.5a, regardless of DNA concentration, the

transmission minimum shifts towards shorter wavelengths with the progress of the RCA reaction, which is caused by the formation of the DNA in the microcavity.

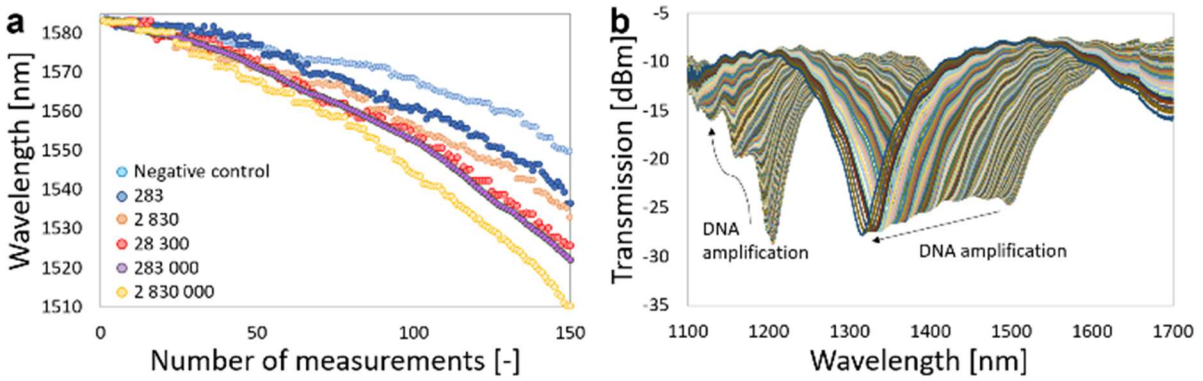

Figure 3.5 **The real-time μIMZI-based RCA monitoring diagram, where the concentration of the target varied from ca. 283 to 2 830 000 DNA copies. The negative curve (light blue line) resulted from a lack of phi29 polymerase. (b) Evolution of the transmission spectrum during the RCA process for the detection of 2 830 C-PLP copies. Arrows indicate the direction of the spectrum shift as it would be induced by increasing RI inside the microcavity.**

The change of mass of the DNA sample affects the obtained spectra by significantly changing the density and viscosity of the analyzed sample. Incorporation of dNTPs into the DNA backbone produces protons and pyrophosphate as by-products,[9,10,29] which may also affect the RI of the analyte. Consequently, the effective RI within the sensing region increases affecting propagation conditions of the cladding mode, as is shown with the RI measurements in Figure 3.1b2 and c2.

Following the schema shown in Figure 3.4, one could expect that at the beginning of the amplification the spectrum will be affected mostly by changes on the μIMZI's surface. It means that the $\mathbf{n_{co}}$ in the remaining portion of the fiber core should be influenced by shifting the spectra towards longer wavelengths (as shown in Figure 3.1c2). However, following utilized chemical modification of the surface, therefore distribution of the primers on the sensor's surface it can be stated that initial changes of the DNA amplification are indistinguishable. By initial changes, we mean hybridization of the circDNA to the forward primers followed by Phi29 DNA polymerase attachment and the first minutes of the DNA amplification. The analysis of the RI shows that the amplification mixture and synthesized DNA on the μIMZI's surface are very close to the RI of the buffer. This further confirms that any observable shift of the minimum can be recorded once the amplified DNA starts changing the RI within the whole pL volume of the microcavity, thus affecting the cladding mode.

Initially, the process was monitored for 90 minutes to determine an appropriate timeframe for the identification of the RCA reaction. Initially, it was assumed that the length of the generated DNA

strand would be proportional to the reaction time so the RI change should be proportional to the mass of products bounded to the sensor's surface. In spite of the fact that the shift does increase over time, very long amplification times do not appear to significantly improve the distinction between different starting concentrations of circDNA. Instead, it simply makes the experiment last longer, in contrast with a rapid assay which is more desirable for future development. The main reasons for that may be as follows. First, the same composition of the RCA reaction mixture (except for circDNA) limits the DNA concentration which can be synthesized during the reaction. Thus, as can be seen in Fig. 5a, after a defined time, the placement of the transmission minimum approaches similar values, therefore decreasing R^2. Second, the μIMZI tracks the effective RI which is changing during the RCA reaction. However, primers are immobilized on the sensor's surface. As we reported in our previous work[25], the layer deposited on the sensor's surface increases its surface sensitivity at the expense of changes occurring further away from surface. Therefore, it is possible that overpacking the surface with dense DNA coverage may make the sensor less volume sensitive as further RI changes caused by DNA amplification are displaced away from the sensor's surface. In contrast, short reaction times limit spectral shifts of the minima and make detection difficult at low concentrations of the target.

To find the optimal reaction time, correlation coefficients between the initial concentrations of DNA targets, and the spectral shift of the minimum at varying amplification times were analyzed. Table 3.1 presents the correlation coefficients of the obtained response curves.

Table 3.1 **Correlation coefficients of the experimental response curves obtained for the chosen time.**

Time of DNA amplification [min]	Correlation coefficient R^2
10	0,5219
20	0,9338
30	0,9917
40	0,9782
50	0,9610
60	0,9251

It was found that from the correlation coefficient point of view (maximum R^2) the time between 30-40 min is the most appropriate and therefore was used for further analysis of the sensitivity of the method.

3.3.5 Negative control

The RCA reaction was also confirmed with two negative controls. The first one was conducted using the amplification mixture without an enzyme responsible for DNA amplification, and the second one was without the primers immobilized on the sensor's surface. Both cases result in a lack of DNA amplification. As both curves revealed the same trend, just the control without the enzyme was included in Figure 3.5a (light blue dots). The changes of the minimum wavelength for this sample likely resulted from the binding of the circDNA to the immobilized primers and slight evaporation of the reaction buffer. In comparison to the spectral change of the positive probes, the change of the RI was much smaller in this case, and the shift of the minimum was steady throughout the whole experiment. Moreover, to visualize the presence of DNA resulting from RCA reactions we have performed another test (Figure 3.S1, Appendix 1) that confirmed the surface functionalization, amplification, and thus detection method.

3.3.6 Sensitivity of the method

Figure 3.6a depicts the evolution of wavelength corresponding to the transmission minimum during the RCA monitoring over 30 to 40 minutes. The graph displays the recorded raw data (dots) and the fitted curves (solid lines). We used a gaussian fit with four terms for best shape projection and minimalization of data fluctuation.

To evaluate the sensitivity of this method, we investigated the relationship between the concentration of the target in the reaction mixture and the transmission shift of the minimum at 30 minutes using fitted data. The change of the resonance shift versus the copy number of the target (Figure 3.6b) revealed linear behavior within the whole investigated range starting from 283 to 2 830 000 copies of the DNA target (representing a concentration range from 9.4 aM to 94 pM). Following the obtained data, the experimental limit of the detection (LOD) was set as 283 circDNA copies (9.4 aM), though the calculated LOD reached a remarkable value of 6 circDNA copies, which is equal to a circDNA concentration of 0.2 aM. To investigate the sensor resolution and repeatability especially for the lowest target concentrations, all the circDNA concentrations were run in triplicate under the same conditions, but with different microcavities. The calculated sensor-to-sensors relative standard deviation is equal to ~0.1% for all DNA concentrations suggesting both high resolution and reproducibility between the sensors.

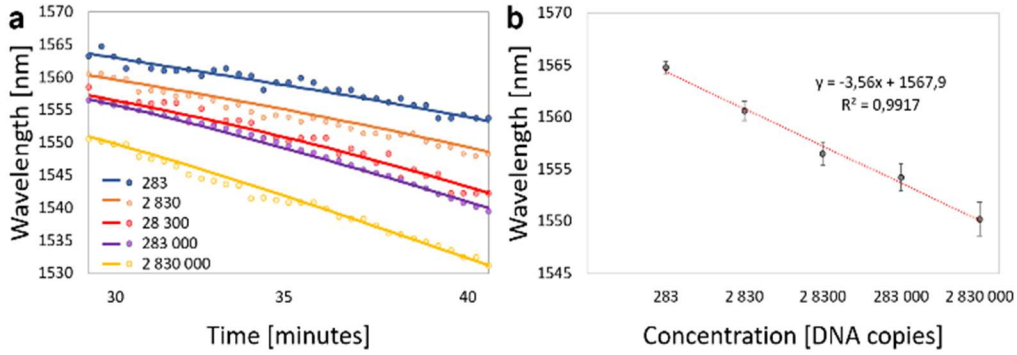

Figure 3.6 **(a) Real-time μIMZI-based RCA monitoring plot for the period between 30 and 40 minutes, where raw data are present as dots, and the fitted curves as solid lines; (b) corresponding minimum wavelengths are plotted vs circDNA copy number showing the sensitivity of the performed experiment at 30 minutes. Error bars represent standard deviation (n = 5) for single experiment.**

The other recent optical RCA sensors have been based on SPR.[14,15,20] Although the detection limit of one of the probes presented by Huang et al.,[15] reached 20 aM and the reported system showed some disadvantages. First, the sensor required the measured signal enhancement using Au nanoparticles. Second, besides the nanoparticles, also enzymatic cleavage was utilized for the signal enhancement. In the other sensor developed by Xiang et al.,[14] the authors reported a similar SPR-based system incorporating RCA and Au nanoparticle, where they were able to reach a LOD of 5 pM with a synthetic DNA target. Shi et al.[30] reached LOD of 0.5 pM using synthetic nucleotides, however, the circDNA was attached to the sensor's surface indirectly through a nanoparticle and biotin-avidin interaction. The introduction of additional materials and sample processing steps complicates the procedure, increases its time, as well as the cost of the assay. Furthermore, it can also influence the sensitivity of the method. Other reported RCA based sensors reached 0.28 fM using enzyme assisted electrochemical platforms[31] and 1.6 fM using an electrochemiluminescence sensor.[32] What is worth mentioning is real-time PCR, considered as a gold standard in detection methods. PCR offers a LOD around 384 DNA copies per mL (approximately 0.6 aM) with the H1N1 influenza virus.[33] This detection limit is comparable to the one reached in this work falling between the calculated LOD of 0.2 aM and the observed LOD of 9 aM in this study.

The biosensing system studied in this work offers distinct advantages over existing detection methods, such as PCR, ELISA, and cell culture, or a combination of those three. The use of RCA/HRCA combined with highly RI sensitive μIMZI makes the system ultra-sensitive. The DNA amplification additionally enhances the signal, making it possible to reach a low detection limit

without a culturing step. Moreover, the presented approach is universally applicable, making the sensor suitable for the detection of any DNA target based on proper primer design.

Considering the size of the presented sensor, and the pL volume analysis, the assay is highly compatible with the point-of-care field application and may be multiplexed in the future targeting more than one DNA sequence. As the RCA is an isothermal reaction there is no need for additional equipment, e.g., thermoblocks. Furthermore, because of the high specificity and selectivity provided by the incorporation of multiple primers and necessary circular template, the system should work well with without any interference from other DNAs/RNAs present in the sample. Also, these results demonstrate that the analysis can provide rapid quantitative detection of DNA amplification. Indeed, several isothermal assays have been designed for point-of-care applications and many of these provide a qualitative measure, while μIMZI-RCA provides quantitative measurements over an extended time without compromising its outstanding sensitivity.

3.4 Conclusions

In summary, for the first time optical-fiber-based sensor – the microcavity in-line Mach-Zehnder interferometer – has been investigated for the real-time and label-free monitoring of isothermal DNA amplification. The reported method takes advantage of an outstanding sensitivity of the sensing platform, its capability for analysis of as low as picoliter volumes, and highly efficient chemical functionalization of the sensor's surface based on click chemistry reaction. The sensor achieved a linear range of detection between 283 – 2 830 000 DNA target copies, which corresponded to between 9.4 aM and 94 pM circDNA. Within just 30 min amplification duration as low as 238 copies (9.4 aM) of DNA target could be detected, while the calculated limit of the detection was equal to 6 DNA copies – 0.2 aM circDNA, thus, outperforming other sensors reported to date. Considering all the above, the presented sensor may find the practical application in point-of-care testing including early disease diagnosis.

3.5 Methods

All the DNA sequences and DNA target-related information were described in detail in our previous work.[9,10,26]

3.5.1 µIMZI fabrication and analysis

Sensing structures in the form of cylindrical cavities with a diameter of 60 µm were fabricated in standard Corning SMF-28e fibers following the one-step method described in detail in.[23,34,35] During the entire experiment, the µIMZI transmission was monitored in the spectral range of 1100-1700 nm with an NKT Photonics SuperK COMPACT supercontinuum white light source and a Yokogawa AQ6370C optical spectrum analyzer (the resolution of the optical spectrum analyzer was equal to 0.1 nm). To perform the reference RI sensitivity measurements a set of water/glycerin solutions with RI varied in the range of 1.3330–1.3496 RIU was used. The RI of the solutions was measured using a digital refractometer VEE GEE PDX-95.

3.5.2 µIMZI's surface functionalization

First, to remove contaminations and enhance the density of hydroxyl groups (Si-OH) on the surface the cavity was washed with 70% ethanol (Sigma-Aldrich) and milliQ water. Then the microcavity was filled with 1 M NaOH (Sigma-Aldrich) for 5 min. This step was followed by extensively washing of the surface consecutively with 70% ethanol, phosphate-buffered saline (PBS) (Sigma-Aldrich), and finally with mili-Q water. Before surface silanization, 44.5 mg of 3-(Triethoxysilyl)propylsuccinic anhydride (TESPSA) (Oakwood Chemical, USA) and 6.08 mg of 3-(Azidopropyl)triethoxysilane (AzPTES) (Gelest, USA) were dissolved separately in 1 mL milliQ water. After mixing the two solutions (1:1, v/v), the microcavity was placed in the prepared mixture for 30 minutes. The effectiveness of the process was controlled by both the concentration of the precursor and exposure time. The sensor was then extensively washed consecutively in 70% ethanol, PBS, and milliQ water and dried at room temperature for 30 minutes. In the next step, the functionalization layer was cured at 105°C for 2 hours. Such a surface was ready for the click reaction. For the conjugation, the sensor was incubated in 10 µM DBCO-DNA primers (forward and reverse) solution for 1 hour. After this time, the surface of the microcavity was again extensively washed with 70% ethanol, PBS, and water to wash away non-attached primers. Finally, prepared microcavity was ready for monitoring of the RCA reactions. Figure 3.7 presents a schematic drawing of the surface functionalization.

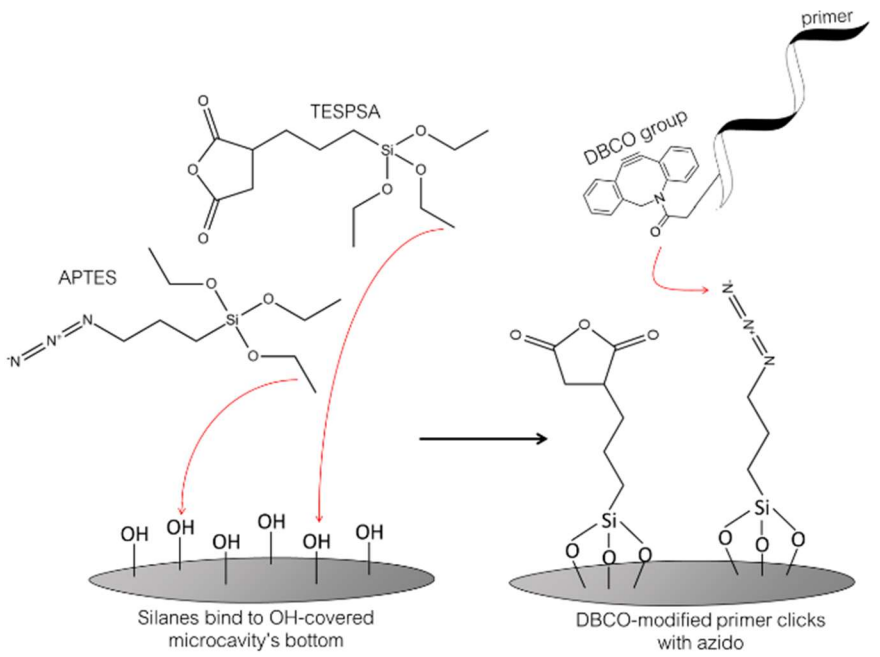

Figure 3.7 **Schematic drawing showing the surface functionalization of the µIMZI with copper-free click chemistry.First, TESPSA and AzPTES are attached to the -OH coated surface via ethoxy groups. TESPSA has been used as a non-reactive linker to passivate the surface, while AzPTES with its azido group clicks with a DCBO group on DNA primer and thus forms a covalent bond between the DNA and the µIMZI surface.**

3.5.3 RCA reaction

The purified circDNAs were dissolved in milliQ water and then diluted to produce a serial dilution of circDNA so the RCA assay could be examined at several circDNA copy numbers**.** The RCA reaction was performed in a total volume of 90 µL consisting of 5 µL circDNA, 416 µM deoxyribonucleotide triphosphate (dNTP) (Thermo Fisher Scientific, USA), 68.4 µL milliQ water, 1X Phi29 DNA polymerase buffer (NEB), 30 µg bovine serum albumin – BSA (NEB), and 24 units of Phi29 DNA polymerase (NEB). Then 50 µL of the amplification mixture was incubated with the functionalized µIMZI for 90 minutes at room temperature. The temperature was controlled during the experiment with an accuracy of 0.06°C (HP 34970A Data Acquisition Unit). The experiment was monitored in real-time during the whole process.

3.6 Acknowledgements

This work was supported by the National Science Center, Poland (NCN) (2018/29/B/ST7/02552), the Natural Sciences and Engineering Research Council of Canada [RGPIN-2019-06403], and the Canada Research Chairs Program; S.V. Hamidi received fellowships from Armand-Frappier

foundation and Fonds québécois de la recherche sur la nature et les technologies (FRQNT). J.P. is a junior 2 FRQS research scholar.

3.7 References

1 K. B. Mullis, Sci. Am., 1990, **262**, 56–65.

2 M. M. Ali, F. Li, Z. Zhang, K. Zhang, D. K. Kang, J. A. Ankrum, X. C. Le and W. Zhao, Chem. Soc. Rev., 2014, **43**, 3324–3341.

3 Y. Zhao, F. Chen, Q. Li, L. Wang and C. Fan, Chem. Rev., 2015, **115**, 12491–12545.

4 T. Notomi, Y. Mori, N. Tomita and H. Kanda, J. Microbiol., 2015, **53**, 1–5.

5 X. Lu, X. Shi, G. Wu, T. Wu, R. Qin and Y. Wang, Sci. Rep., 2017, **7**, 1–9.

6 P. J. Asiello and A. J. Baeumner, Lab Chip, 2011, **11**, 1420–1430.

7 V. V Demidov and H. Thorne, 2002, 542–548.

8 P. M. Lizardi, X. Huang, Z. Zhu, P. Bray-Ward, D. C. Thomas and D. C. Ward, Nat. Genet., 1998, **19**, 225–232.

9 S. V. Hamidi and J. Perreault, Talanta, 2019, **201**, 419–425.

10 S. V. Hamidi and H. Ghourchian, Biosens. Bioelectron., 2015, **72**, 121–126.

11 R. Ke, A. Zorzet, J. Göransson, G. Lindegren, B. Sharifi-Mood, S. Chinikar, M. Mardani, A. Mirazimi and M. Nilsson, J. Clin. Microbiol., 2011, **49**, 4279–4285.

12 R. R. G. Soares, F. Neumann, C. R. F. Caneira, N. Madaboosi, S. Ciftci, I. Hernández-Neuta, I. F. Pinto, D. R. Santos, V. Chu, A. Russom, J. P. Conde and M. Nilsson, Biosens. Bioelectron., 2019, **128**, 68–75.

13 K. W. Park, C. Y. Lee, B. S. Batule, K. S. Park and H. G. Park, RSC Adv., 2018, **8**, 1958–1962.

14 Y. Xiang, K. Deng, H. Xia, C. Yao, Q. Chen, L. Zhang, Z. Liu and W. Fu, Biosens. Bioelectron., 2013, **49**, 442–449.

15 Y. Xiang, X. Zhu, Q. Huang, J. Zheng and W. Fu, Biosens. Bioelectron., 2015, **66**, 512–519.

16 H. Su, R. Yuan, Y. Chai, L. Mao and Y. Zhuo, Biosens. Bioelectron., 2011, **26**, 4601–4604.

17 D. Zhu, Y. Yan, P. Lei, B. Shen, W. Cheng, H. Ju and S. Ding, Anal. Chim. Acta, 2014, **846**, 44–50.

18 Y. Jiang, S. Li, Z. Qiu, T. Le, S. Zou and X. Cao, J. Food Saf., 2019, **39**, 1–9.

19 T. Yasui, K. Ogawa, N. Kaji, M. Nilsson, T. Ajiri, M. Tokeshi, Y. Horiike and Y. Baba, Sci. Rep., 2016, **6**, 1–8.

20 Y. Y. Huang, H. Y. Hsu and C. J. C. Huang, Biosens. Bioelectron., 2007, **22**, 980–985.

21 L. Zhou, L. J. Ou, X. Chu, G. L. Shen and R. Q. Yu, Anal. Chem., 2007, **79**, 7492–7500.

22 Q. Su, D. Xing and X. Zhou, Biosens. Bioelectron., 2010, **25**, 1615–1621.

23 M. Janik, A. K. Mysliwiec, M. Koba, A. Celebanska, W. J. Bock and M. Smietana, IEEE Sens. J., DOI:10.1109/JSEN.2017.2695544.

24 R. Correia, S. James, S. W. Lee, S. P. Morgan and S. Korposh, J. Opt. (United Kingdom), DOI:10.1088/2040-8986/aac68d.

25 M. Śmietana, M. Janik, M. Koba and W. J. Bock, Opt. Express, 2017, 25, 26118–26123.

26 S. V. Hamidi, H. Ghourchian and G. Tavoosidana, Analyst, 2015, **140**, 1502–1509.

27 M. G. Mohsen and E. T. Kool, Acc. Chem. Res., 2016, **49**, 2540–2550.

28 R. Johne, H. Müller, A. Rector, M. van Ranst and H. Stevens, Trends Microbiol., 2009, **17**, 205–211.

29 N. A. Tanner, Y. Zhang and T. C. Evans, Biotechniques, 2015, **58**, 59–68.

30 D. Shi, J. Huang, Z. Chuai, D. Chen, X. Zhu, H. Wang, J. Peng, H. Wu, Q. Huang and W. Fu, Biosens. Bioelectron., 2014, **62**, 280–287.

31 S. Wang, Y. Ji, H. Fu and H. Ju, 2019, 691–697.

32 Y. Lin, X. Huang, Y. Zhang, D. Chen, J. Wang and F. Luo, 2019, 827–833.

33 M. Panning, M. Eickmann, O. Landt, M. Monazahian, S. Ölschläger, S. Baumgarte, U. Reischl, J. J. Wenzel and H. H. Niller, 2009, 1–6.

34 M. Janik, S. Member, T. Eftimov, M. Koba, M. Smietana, W. J. Bock and L. Member, J. Light. Technol., 2019, **37**, 4501–4506.

35 M. Janik, M. Koba, A. Celebańska, W. J. Bock and M. Śmietana, Opt. Laser Technol., 2018, **103**, 260–266.

4 SIMPLE IN-VITRO SINGLE STRANDED LINEAR AND CIRCULAR DNA PREPARATION AND VALIDATION VIA SELEX USING PHOSPHOR-DERIVED MODIFICATIONS

Préparation et validation simples d'ADN simple brin linéaire et circulaire *in vitro* via SELEX à l'aide de modifications dérivées du phosphore

Seyed Vahid Hamidi and Jonathan Perreault

INRS Centre Armand-Frappier Santé Biotechnologie, 531 boulevards des Prairies Laval (QC) Canada.

This article will be re-submitted soon.

Author contributions:

Conceptualization, S.V.H.; Resources, J.P.; Methodology, S.V.H.; Validation, S.V.H. and J.P.; Data analysis, S.V.H. and J.P.; Experimental work: S.V.H.; Writing—Original Draft Preparation, S.V.H.; Writing—Review and Editing, S.V.H. and J.P.; Supervision: J.P.; Funding Acquisition, J.P.

A short description about this work:

The two previous chapters demonstrated different applications of RCA for biosensing, here we revisit different ways of making circular DNA and single stranded DNA, with implied applications. This manuscript is about the third objective of my thesis and in this work a novel method was proposed for *in vitro* preparation of linear and especially circular ssDNA from PCR products using phosphor-derived modifications such as phosphorylation and phosphorothioate bond modifications. ssDNA preparation has lots of applications in molecular biology such as SELEX, library preparation in sequencing, PCR based PLP generation, DNA origami, etc. In this work a simple and fast method for generation of ssDNA in both linear and circular conformation was proposed. This technique can be a bridging method to connect PCR with RCA. Utilizing phosphorylated-phosphorothioated primers not only protects the strand from digestion by Lamda exonuclease enzyme but also the protected phosphor group can be directly used for the circularization step via a ligase enzyme and complementary strands. Therefore, this gel-free and fast ssDNA generation could be useful for many commercial kits and services implying sequencing or SELEX. Moreover, the proposed method has been also validated by selecting linear and circular aptamers against MERS-CoV spike protein. In contrast with the two precedent chapters, which aim at detecting RNA or DNA, an aptamer made of a circular DNA would

potentially allow detection of other types of analytes, like proteins, with the possibility of using RCA for signal amplification.

4.1 Abstract

Interest in preparation of single stranded circular DNA library has been increasing recently, therefore developing a simple and efficient method for circular DNA generation will be very useful for all procedures and techniques that are dependent on single stranded circular DNA preparation. In this study a new simple method for in vitro preparation of circular single stranded DNA is proposed. We hypothesized that using a phosphorylated-phosphorothioated primer would not affect the efficiency of PCR reactions, but, more importantly, would suppress the activity of Lambda Exonuclease enzyme even if it is phosphorylated. The produced phosphorylated single stranded DNA is ready to be circularized via a ligation reaction using a bridging oligonucleotide. Several optimizations and enhancements have been conducted in the ligation reaction, notably by embedding an extra thymine nucleotide at the ligation site to compensate for the additional adenosine nucleotide added by Taq during the PCR reaction. In addition, the performance of the proposed method has been validated by selecting linear and circular aptamers against MERS-CoV spike protein during 15 successive cycles of SELEX. Because this new method is simple and user-friendly, it has a potential to be automated for high-throughput purposes and may further stir growing interests in preparation of single stranded circular DNA and its applications.

Keywords: single strand circular DNA, phosphorothioate modification, single stranded PCR product, Lambda exonuclease, ligation.

4.2 Introduction

Due to the broad applications of in-vitro single stranded DNA (ssDNA) preparation in molecular biology numerous techniques have been developed for this purpose. So far, ssDNA preparation methods have been utilized for systematic evolution of ligands by exponential enrichment (SELEX) (1), oligonucleotide microarray preparation (2), PCR based padlock probe (PLP) generation (3), circular aptamer selection (4-6), single stranded labeled probe production (7), coupled PCR-rolling circle amplification (RCA) for gene production (8). In addition, it has been recently used for linear and circular ssDNA library generation for DNA sequencing (9), production of origami nanostructure (10) as well as long ssDNA donor for genome editing using clustered regularly interspaced short palindromic repeats (CRISPR) (11-14). A good example of the use of ssDNA is aptamers. Aptamers are small ssDNA or RNA molecules that fold into a well-defined three-dimensional structure with a high affinity and specificity for their target molecules. Also, they have better thermal stability, lower cost and are easier to modify compared to antibodies. They are selected by SELEX procedure which starts with a random oligonucleotide library (e.g. 1015

sequences) followed by four key steps: (i) specific binding of oligonucleotides (aptamer) with the target, (ii) extracting the bound oligonucleotides, (iii) amplifying of the extracted sequences with PCR (iv) producing an enriched pool of single stranded aptamer sequences that will be used again in step i, and so on. After completion of the SELEX procedure, the candidate aptamers are sequenced for characterization (15). However, developing a simple, fast, efficient and user-friendly technique to produce pure ssDNA is still challenging (16). The majority of ssDNA producing procedures such as denaturing polyacrylamide gel electrophoresis (PAGE) and biotin-streptavidin based techniques are dependent on double strand DNA (dsDNA) denaturation and detachment of the sequence of interest from the complementary strand. Denaturing PAGE has been frequently utilized for pure ssDNA preparation, however it is not convenient for high-throughput approaches because it is complex and time consuming (16-18). In addition, asymmetric PCR and biotin-streptavidin based methods are also criticized because of dsDNA impurity by-products that are generated during the process (7,16,19-21). On the other hand, enzymatic degradation of undesired strand via Lambda exonuclease enzyme is a simple and robust way to produce pure ssDNA. It is reported that this enzyme has 20 folds more activity on 5′-phosphorylated strands of dsDNA than on hydroxylated strands, causing the hydroxylated strands to get single stranded following digestion (19,21,22), but in principle this also precludes its use for any application that require the presence of a 5′-phosphate, such as preparation of PLPs and circular DNA.

The effect of chemically modified nucleotides resistant to nucleases including phosphorothioate bond modifications for ssDNA generation has already been investigated (23,24). In this study, phosphor-derived modifications have been used for in-vitro production of ssDNA, linear or circular depending on the application. For this purpose, PCR was performed using phosphorylated-phosphorothioated forward primer and phosphorylated reverse primer using a 100 bases template (Fig. 4.1, A and B). In the current work we show that although Lambda exonuclease enzyme has robust digestion activity on phosphorylated strand of dsDNA, its degradation activity is completely suppressed on phosphorothioate modified strand even if it enjoys 5´ phosphorylation modifications (Fig. 4.1C). In addition, the produced phosphorylated ssDNA can be circularized using complementary strands without prior phosphorylation steps (Fig. 4.1, D and E). Therefore, the whole procedure of circular ssDNA preparation has become much faster and simpler. In addition, an increased DNA ligation efficiency using T4 DNA ligase has obtained by embedding an additional thymidine nucleotide exactly at the ligation site to account for the adenine added by Taq during PCR. Therefore, this simple, fast and robust method will be useful for specific ssDNA applications and is a good candidate for automation purposes due the broad application of ssDNA

preparation in molecular biology. In addition, this technique has been successfully applied on SELEX for linear and circular aptamer selection against MERS-CoV spike protein. This coronavirus is a serious health concern, with close to 30% of affected patients dying from it (25).

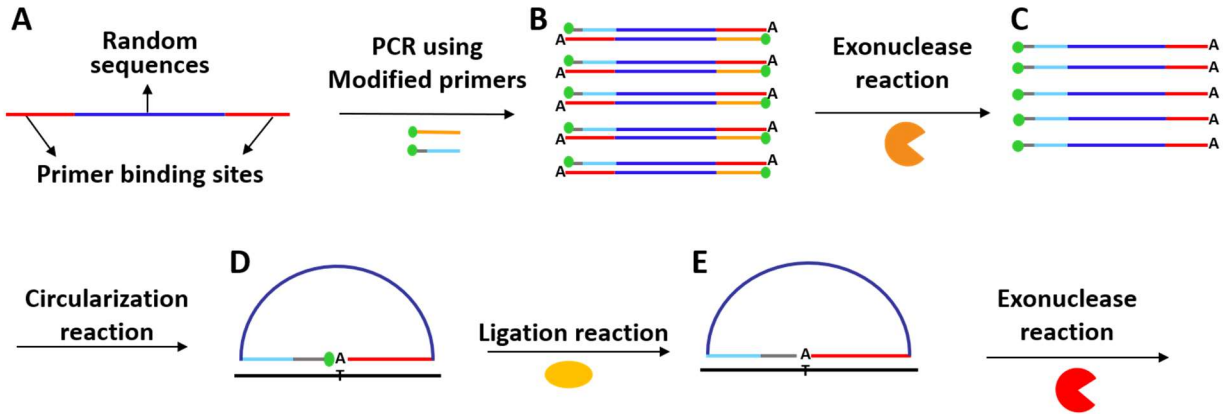

Figure 4.1 **PCR products circularization strategy. (A) Schematic representation of the target used with specific sequences as PCR primers binding sites (red line) at the extremities and random sequences (dark blue line) in the middle. (B) PCR reaction using reverse primer (orange line) with 5´ phosphorylation modification (green dot) and forward primer (light blue line) with 5´ phosphorylation modification (green dot) and five phosphorothioate bonds (gray line) at the far 5´end of the primer. The "A" illustrates the adenine added by the Taq DNA polymerase at the 3´ end of its product. (C) Exonuclease reaction by utilising the Lambda exonuclease enzyme (orange semi-circle) for degradation of non-phosphorothioated reverse strand. (D) ssPCRP circularization via complementary strand (black line). (E) Sealing head to tail of ssPCRP through ligation reaction using a ligase enzyme (yellow ellipse). Finally, non ligated ssPCRP are degraded by the action of Exonuclease I enzyme (red semi-circle)**

4.3 Results

4.3.1 PCR optimization using modified primers

A gradient PCR was performed with normal primers (suggested Tm of 61 ˚C) using a range of temperatures from 58 to 68 ˚C to find the best annealing temperature for a sharp PCR band. The sharpness of PCR product bands improved by increasing the annealing temperature and it is at 68 ˚C that we obtained the best band (data are not shown). Thereafter, PCR using modified primers were performed at 68 ˚C including with: a phosphorylated reverse primer, as well as phosphorothioated, phosphorylated-phosphorothioated, normal and normal-phosphorylated forward primers (Fig. 4.2). As it can be seen from Fig. 4.2, applying phosphorylation and phosphorothioate bond modifications did not have any effects on the quality of PCR bands, including for the PCR reaction using phosphorylated reverse primer and protected-phosphorylated forward primer, the focus of this study. Furthermore, the performance of PCR

reactions using modified primers were evaluated by qPCR (Fig. 4.S1, Appendix 1). Although signal intensity was decreased by ~25% using modified phosphorylated and phosphorylated/phosphorothioated forward primers, the PCR product quantity is still high enough for all required applications.

The quality of PCR products with one distinct length dsDNA is important to get high yield and pure linear ssDNA preparation through exonuclease treatment and subsequently for circular DNA formation (21). Thus, optimization of PCR conditions such as primers and template concentrations, number of cycles and also prudent design of primers to avoid primer dimer formation as well as ensuring specific binding of primers to template is important to avoid pervasive effects on obtaining a defined dsPCR band (21,22).

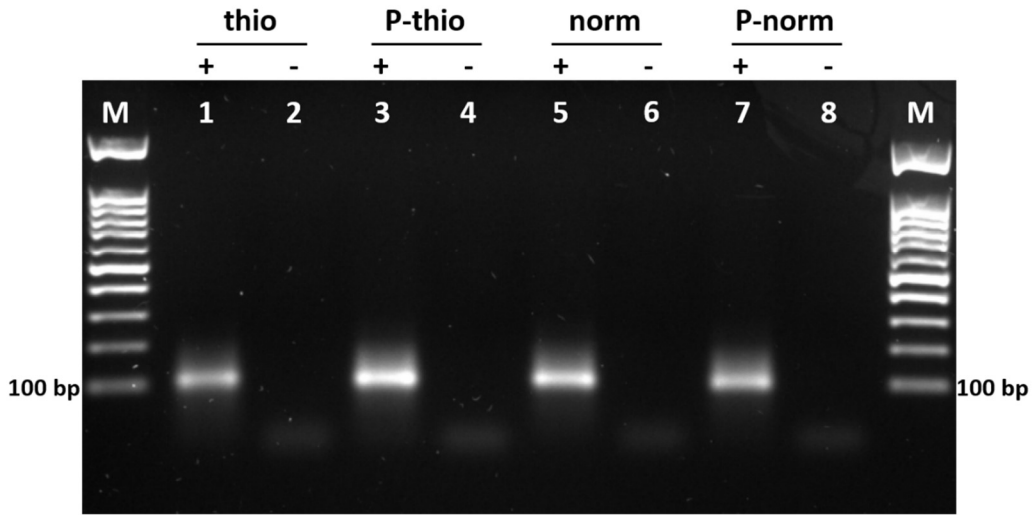

Figure 4.2 **PCR reaction using modified primers. Lanes M: Markers; lanes 1, 3, 5 and 7: positive reactions (with template); lanes 2, 4, 6 and 8: negative reactions (without template). All PCR reactions have been done by utilising a phosphorylated reverse primer (1 µM). Lanes 1 and 2: PCR reaction with phosphorothioated forward primer. Lanes 3 and 4: PCR with phosphorothioated-phosphorylated forward primer. Lanes 5 and 6: PCR products using normal forward primer (no modifications). Lane 7 and 8: PCR with phosphorylated forward primer. All PCRs have been done in the presence of 1 µM of forward primers and 0.02 µM of template.**

4.3.2 Phosphorothioate protects 5´-phosphorylated DNA from degradation

DNA amplification through PCR generates dsDNA products (26). As previously mentioned, the Lambda exonuclease enzyme has an exodeoxyribonuclease activity on dsDNA substrates from 5´ to 3´ and is about 20 times more active on a 5´ phosphorylated terminus compared to a non phosphorylated one. Thus, by phosphorylating one of the primers of the PCR reaction it is possible

to use the Lambda exonuclease to easily get a single stranded PCR product (ssPCRP) from a PCR product (22,27,28). Therefore, in this work Lambda exonuclease digestion reactions have been evaluated by employing a phosphorylated reverse primer (to serve as substrate for digestion reactions) and several forward primers with different chemical modifications. All PCR products (size of 100 base pairs) are aligned with the 100 base pair mark of the DNA ladders (Fig. 4.3A: lanes 2, 5, 8 and 11, as well as lanes M). Whereas ssPCRPs (Fig. 4.3A: lanes 3, 6 and 9) ran lower in the gel and at the same level as the single stranded 100 bases template (Fig. 4.3A: lanes 1 and 14) confirming that ssPCRPs became single stranded after Lambda exonuclease treatment. Moreover, we confirmed that the Lambda exonuclease-treated PCR products have been converted to ssDNA, we degraded the DNA with Exonuclease I, a phosphodiesterase enzyme that degrades linear ssDNA in the 3´ to 5´ polarity (29-31). Since all ssPCRPs were digested by Exonuclease I (Fig. 4.3A: lanes 4, 7 and 10) it confirmed the single stranded nature of ssPCRPs. In addition, because of its 3´ to 5´ exodeoxyribonuclease activity, Exonuclease I it was not blocked by phosphorothioate bonds since these modifications are located at the 5´ extremities of the sense strands (23,24). In principle, using a phosphorylated reverse primer would allow the production of ssPCRP after Lambda exonuclease digestion, however using a phosphorylated forward primer leads to both strand being degraded (Fig. 4.3A lane 12). To obtain ssPCRP, most laboratories ensure that the forward strand is protected by using a 5´ hydroxyl-forward primer (Fig. 4.3A: lane 9). Unfortunately, this is not compatible with applications that require a phosphorylated 5´end. Although PCR sense strands without any modifications and with phosphorothioate bonds modification were protected from degradation (Fig. 4.3A: lanes 6 and 9), it is noticeable that the phosphorylated sense strand with five phosphorothioate-modified bonds was protected from digestion by Lambda enzyme (Fig. 4.3A: lane 6 and Fig. 4.1C). Lambda exonuclease action inhibition by phosphorylated-phosphorothioated modifications enables us to circularize the ssPCRP using a complementary strand without requiring to phosphorylate ssPCRP after exonuclease reaction. Thus, in addition to excluding the phosphorylation step after exonuclease action, with this approach the protected phosphorous group can be used for ssPCRP circularization by ligase enzymes (32,33). Therefore, the whole circularization procedure has become much simpler and more efficient.

In order to verify the inhibition of Lambda exonuclease action at the very 5´phosphorylated end of PCR strands modified by phosphorothioated bonds, highly sensitive [γ-32P] radio-labeling was used. Phosphor imaging of Lambda exonuclease degradation pattern of [γ-32P] radio-labeled PCR products was evaluated using a phosphorylated reverse primer and [γ-32P] radio-labeled forward primers without and with phosphorothioate modifications (Fig. 4.3B: lanes 3 and 6,

respectively) and employing denaturing 6% PAGE (Fig. 4.3B). The two different undigested PCR products showed similar band patterns, with the main PCR bands migrating to the same level as the 100 bases template (Fig. 4.3B: lanes 3, 6 and 1). Importantly, the sense normal PCR strand was completely digested by Lambda Exonuclease (Fig. 4.3B: lane 4), whereas the sense phosphorothioated PCR strand remained intact during degradation reaction (Fig. 4.3B: lane 7). As opposed to agarose gels (Fig. 4.3A), double stranded PCR products and ssPCRP run similarly on denaturing PAGE because hydrogen bonds between bases are weakened in the latter (34,35). Afterward, radio-labeled-phosphorothioated ssPCRP was again digested by Exonuclease I enzyme to confirm the single stranded property of phosphorothioated ssPCRP (Fig. 4.3B: lane 8). Finally, the [γ-32P] nucleotide residues resulting from digestion accumulated at the bottom of the gel, further verifying the digestion activity of exonuclease enzymes.

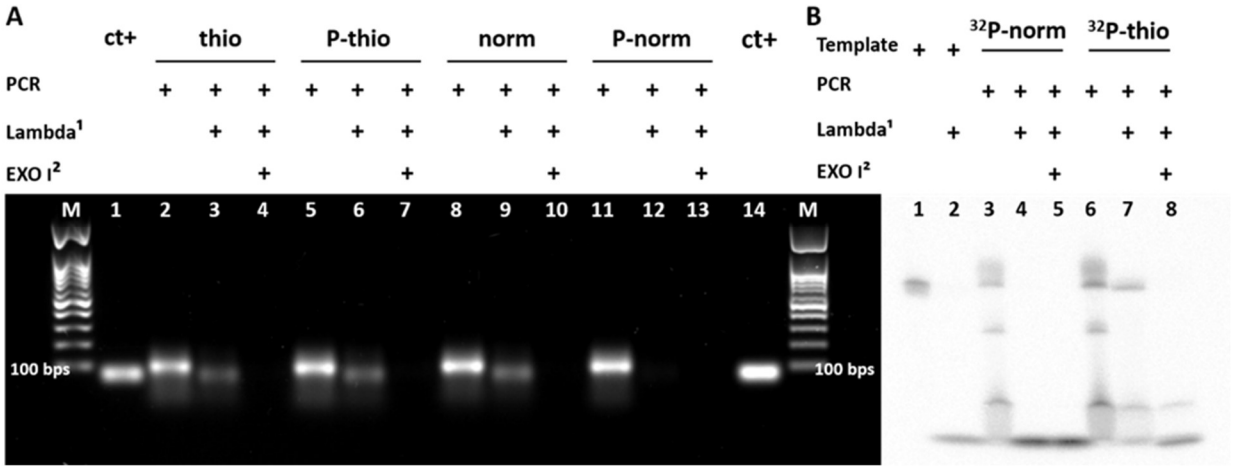

Figure 4.3 **Preparation of ssPCRP. (A) Visualization via a 2% agarose gel. Lanes M: Markers. Lanes 1 and 14: single stranded target with final length of 100 bp (80 µM). Lanes 2, 5, 8 and 11: PCR products. Lanes 3, 6, 9 and 12: ssPCRP preparation with Lambda Exonuclease enzyme from PCR products. Lanes 4, 7, 10 and 13: ssPCRP treatment using Exonuclease I enzyme. All PCR reactions were performed using phosphorylated reverse primers (1 µM). Lanes 2, 3 and 4; 5, 6 and 7; 8, 9 and 10; and 11, 12 and 13 have been done using phosphorothioated, phosphorothioated-phosphorylated, normal and phosphorylated forward primers, as indicated in the figure, in final concentration of 1 µM, respectively. (B) ssPCRP analysis using 6% denaturing PAGE. Lanes 1 and 2: ^{32}P-labeled 100 bases oligonucleotide (0.1 pmol), intact or treated with Lambda exonuclease, respectively. Lanes 3 and 6: PCR reaction with phosphorylated reverse primers (1 µM). Lanes 4 and 7: ssPCRP preparation by Lambda Exonuclease. Lanes 5 and 8: ssPCRP incubation with Exonuclease I enzyme. Lanes 3, 4 and 5; and lanes 6, 7 and 8: PCR reactions were done by employing normal-^{32}P-labeled and phosphorothioated -^{32}P-labeled forward primers, respectively, in final amount of 4 pmoles.**

4.3.3 ssPCRP circularization

Circular DNA has some advantages over linear DNA, including higher stability against misfolding and exonucleases as well as compatibility to be utilized as template for exponential signal generation (5,36,37). In order to convert linear ssPCRP to circular ssPCRP, six different

complementary strands in different sizes including 50, 42 and 35 bases were employed as bridging oligonucleotides for ligation (Fig. 4.4A). Taq DNA polymerase enzymes add an additional adenosine nucleotide at the 3´ ends of PCR strands during amplification reaction (38-40). Thus, one additional thymine (T) nucleotide was embedded in the complementary strands exactly at the ligation spot to compare the ligation efficacy with thymine-less counterparts. Furthermore, in an attempt to improve the efficiency of ligation, two different DNA ligase enzymes were used: the T4 DNA ligase and the thermostable Taq DNA ligase enzymes (Fig. 4.4, B and C). The ligation efficiency was affected by the presence of an additional T, the length of complementary strand and the type of ligase enzyme. Since covalently closed circular ssPCRPs have lower migration rates as compared with linear ssPCRPs in agarose or PAGE gels (3,41), we used gel electrophoresis to monitor ligation efficacy. As previously mentioned the overall size of ssPCRP is 100 bases thus if a bridging oligonucleotide of 50 complementary bases is utilized for ssPCRP circularization, it hybridizes with half the length of ssPCRP which likely hinders the full hybridization due to the lack of flexibility of the allowed by a ssDNA region the same length of the dsDNA region (Fig. 4.4A, 1). However, by decreasing the complementary strand sizes, less bases in ssPCRP are occupied in base-pairing which favors more efficient hybridization reactions (Fig. 4.4A, 1 and 2). When T4 DNA ligase and complementary strands with an additional T are used for ligation reactions, elevated ligation efficiency was seen for 42 and 35 bases complementary strands compared to 50 bases for ssPCRP circularization (Fig. 4.4B lanes 1, 2, 4 and 6). However, when complementary strands without additional T were used, we witnessed lower ligation efficacy even in the presence of 42 and 35 bases strands (Fig. 4.4B lanes 3 and 5), reducing by ~30% the amount of circularized DNA; and, perhaps more importantly, increasing by as much as ~7 fold the amount of linear DNA left over (from 5% to 37% for 35 bp bridging oligonucleotide). This can be explained by the adenosine nucleotide added by Taq DNA polymerase enzyme which leads to a one base mismatch pairing at the ligation site. Therefore, in absence of the added T to the bridging oligonucleotide, T4 DNA ligase is not able to properly seal head to tail of the ssPCRP efficiently because of the base mismatch at this strategic spot (33,42,43). On the other hand, when ligation is done via the Taq DNA ligase enzyme, satisfying ligation bands were detected just by employing 35 bases complementary strands even without an additional T (Fig. 4.4C lanes 5 and 6). Better ligation efficiency was expected via Taq DNA ligase because of its thermostability and ability to apply several denaturing-annealing cycles for ligation reaction (44). Although we observed lower selectivity for Taq ligase than T4 ligase enzyme at the ligation spot, for the purpose of circularization of a library this does not represent a significant problem. Indeed, by using four T nucleotides at the ligation junction, we likely increased the ability of the DNA strand to be ligated

even when using only four instead of the ideal five T nucleotides complementary to the extra A nucleotide added during PCR at the ligation junction (Table 4.S1, Appendix 1). Therefore, we tried ligation efficiency in presence of different bases at the ligation site (Fig. 4.4, E and F). Better ligation efficiencies were obtained for both T4 and Taq DNA ligase enzymes when bridging strands with an additional T are used. In addition, better signal intensity was observed by hyperbranched RCA (HRCA) reaction on circularized ssPCRP using + T bridging strand which shows higher ssPCRP circularization rates compared to the strand without the additional T (Fig. 4.S2, Appendix 1). All in all, T4 DNA ligase would be a better candidate for ssPCRPs circularization in this study due to its efficiency (90%-95% of DNA ligated with bridging oligonucleotide of 42 and 35 bp), due to the fact that it works at moderate temperature and also due to its lower price that can eventually improve the throughput of approaches that use the proposed method; overall providing a more user-friendly technique (45).

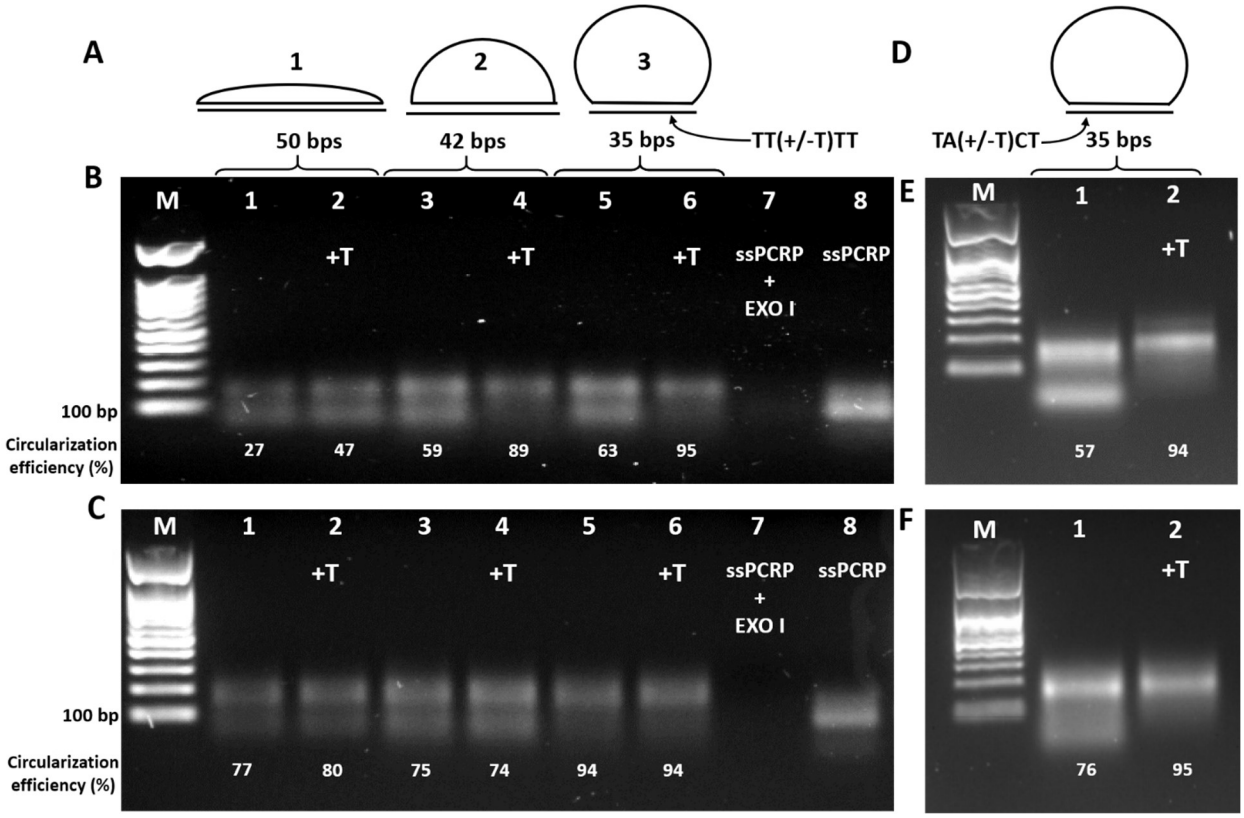

Figure 4.4 **ssPCRP circularization using complementary strands. (A) Schematic representation of ssPCRP circularization with 50, 42 and 35 complementary bases bridging oligonucleotide containing TT(+/-T)TT at ligation site. (B) ssPCRP circularization with T4 DNA ligase. Lane M: Marker. Lanes 1, 3 and 5: circularization reaction in presence of 50, 42 and 35 bp complementary strands (TTTT sequences at ligation sites) and lanes 2, 4 and 6 in combination with 50, 42 and 35 bp complementary strands with an additional T nucleotide at the ligation site (TTTTT) at a final concentration of 1 μM, respectively. Lane 7: ssPCRP treatment with Exonuclease I. Lane 8: ssPCRP. (C) ssPCRP head to tail sealing using Taq DNA ligase enzyme. Order of the lanes are the same as part A. (D) Schematic illustration of ssPCRP circularization using 35 bases complementary strand containing specific sequences at ligation site. (E and F) ssPCRP circularization via T4 and Taq DNA ligase enzymes respectively. Lane M: Marker; Lanes 1: Circularization reaction using bridging oligonucleotides containing TACT sequence at ligation position; Lanes 2: Circularization reaction via additional T in ligation position.**

4.3.4 HRCA reaction using circularized ssPCRPs

To confirm that ssPCRP is covalently closed though a ligation reaction, circular ssPCRP has been used as a circular DNA template in presence of PCR primers (forward and reverse) and highly processive Phi29 DNA polymerase for exponential HRCA amplification. Signal amplification caused by HRCA reaction leads to production of a large amount of dsDNA which in turn can be monitored in real-time by an intercalating fluorescent molecule (SYBR green) (46). Fluorescence intensity increases overtime during exponential HRCA and it almost reaches a plateau after 120 minutes where the amplification reaction gets saturated (Fig. 4.5A). Moreover, the intensity of

fluorescence signal is proportional to the initial concentration of circular ssPCRP because lower amplification signal slopes are observed by two folds diluting of circular ssPCRP (Fig. 4.5A, from top to bottom). The product of real-time HRCA reaction was migrated on agarose gel to confirm production of high molecular weight and hyperbranched nature of the generated DNA, which leads to long smeared DNA bands (Fig. 4.5B: lanes 1 to 8: from high to low concentrations).

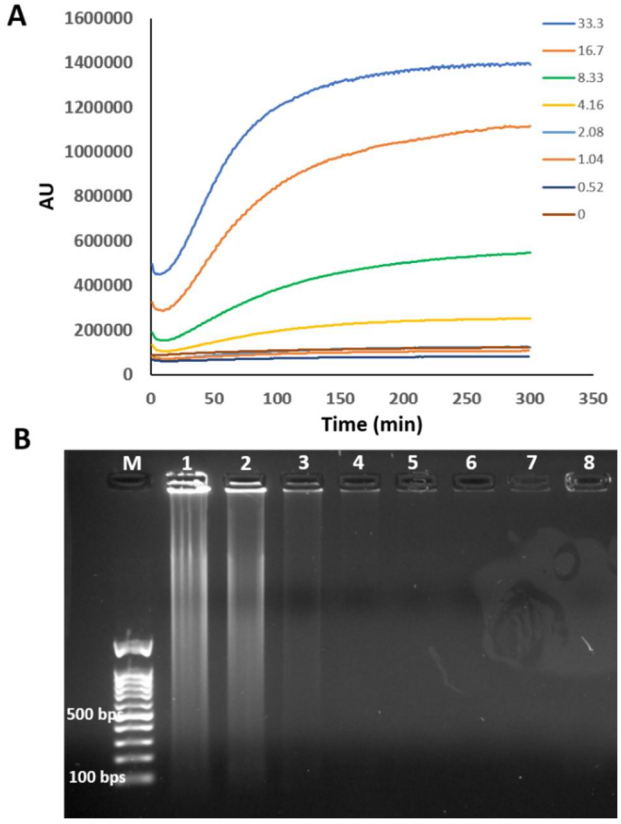

Figure 4.5 **HRCA reaction using circular ssPCRP. (A) Real-time monitoring of HRCA reaction via real-time PCR machine in different concentration of circular ssPCRP (from top to bottom: 33.3, 16.7, 8.33, 4.16, 2.08, 1.04, 0.52 and 0 nM). (B) Visualization of HRCA product by agarose gel electrophoresis. Lane M: Marker. Lanes 1 to 7: HRCA product from the highest concentration of circular ssPCRP (33.3 nM) to the lowest one (0.52 nM). Lane 8: Negative control (no ssPCRP).**

4.3.5 SELEX based on phosphorylated-phosphorothioate primers

In order to verify the performance of the proposed method in a relevant application, this technique has been used to select circular and linear aptamers through 15 successive rounds of SELEX against the whole MERS-CoV spike protein as well as a fragment from spike protein. In addition, four negative selections were performed using agarose magnetic beads and lysozyme protein immobilized on agarose magnetic beads to exclude nonspecific aptamers from the library (Fig. 4.S3, Appendix 1). By increasing SELEX cycles, the amount of ligand and ligand/library incubation

time were gradually decreased and washing times and number of washing were gradually increased. Therefore, based on the utilized conditions, selected aptamers through generation 15 are supposed to have lowest K_D compared to other cycles. In Table 4.1, selected aptamers were categorized based on their cluster sizes obtained from generation 15 and frequency of mutations that appeared during SELEX cycles. These results confirm the applicability of the proposed technique to generate diverse libraries for the SELEX procedure. After 15 successive cycles of SELEX, the first rank selected aptamers from all four libraries including circular and linear aptamers against full size spike protein and RBD fragment were characterized for K_D determination. To do this, aptamers labeled with Cy5 were used in order to be able to check K_D using powerful NanoTemper Monolith machine. In addition, since the circular aptamers are covalently closed circular DNA and thus have no ends for 5' Cy5 modifications, a short labeled complementary strand which is specific to the 5' end region of aptamers were used (Fig. 4.6A-upper). The same approach was employed for linear aptamers K_D determination to be able to compare affinities with circular aptamers (Fig. 4.6A-below). As it can be seen from Fig. 4.6B, an average K_D of ~ 50 μM was obtained using Labeled complementary strand and Monolith strategy. In addition, the selectivity of selected aptamers was also determined in the presence of bovine serum albumin (BSA) as a non-specific ligand and no specific bindings were detected (data are not shown). In addition, since labeled short oligo strategy was used in this experiment, the selectivity of procedure was determined in the presence of full spike and RBD and labeled complementary stands (without adding aptamers) and no affinity was observed (data are not shown). This shows that the complementary strand has not affinity to the specific targets.

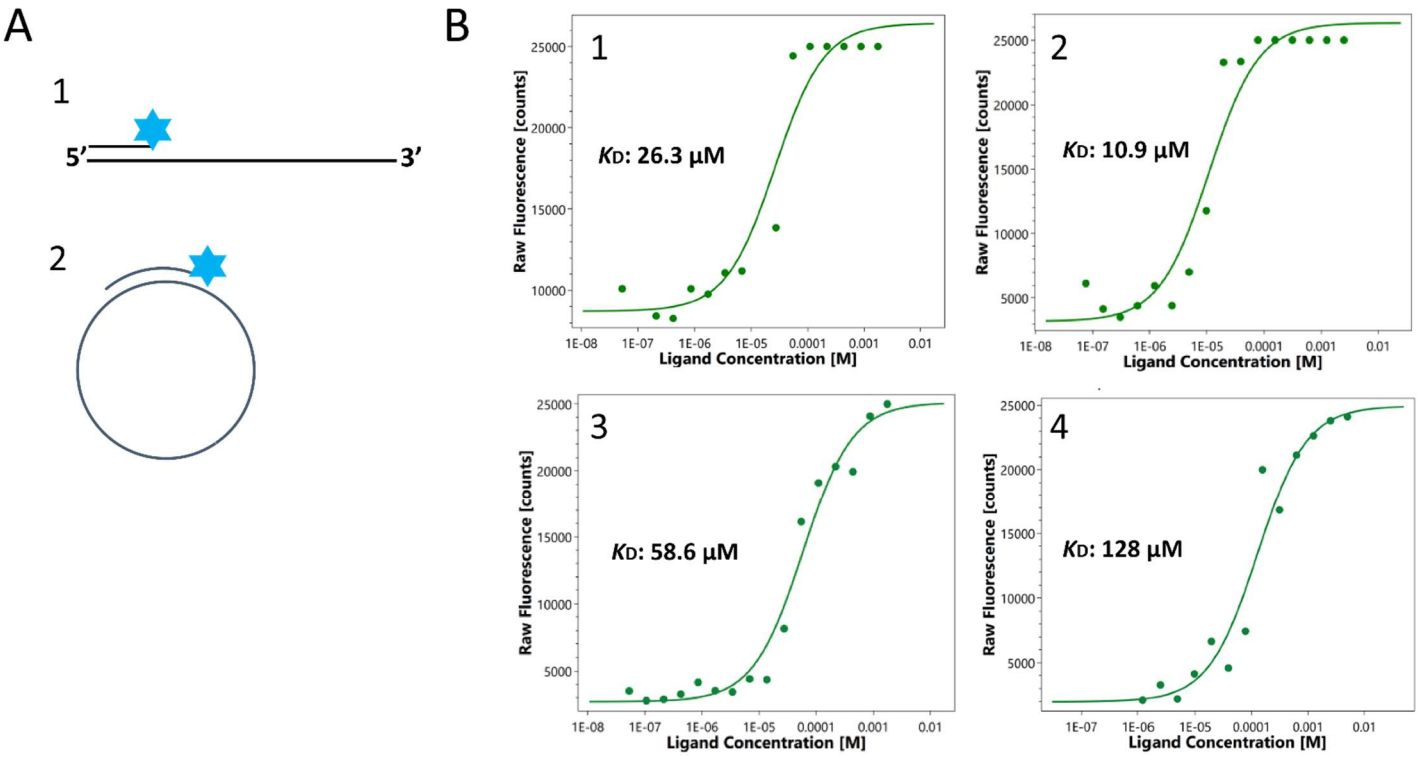

Figure 4.6 **K_D determination. (A) Schematic illustration of selected linear and circular hybridization using labeled Cy5 complementary strand. (B) Binding affinity of selected aptamers (Linear/full spike (1), Linear/RBD (2), circular/full spike (3) and circular/RBD (4)) in the presence of 5 nM of labeled aptamers and 1mM to ~ 10^{-8} M of ligands (full spike and RBD).**

Table 4.1 Selected circular and linear aptamers.

Target	Library	reads/ cluster (%)	Mutations (Positions and frequencies)	K_D (μm)	Aptamer sequence (random region)
Spike	Linear	7.4	G2(1.1%)	-	CATGGTGGAGACATAAAGCTTGAGAGGGTTCCAT
		2.4	G1(6.2%)	-	A**CCGGCGTCACCAC**A**CGGGGAGGTTAGATGTGCCCAGGGTCCTGT**
		11.5	A1(6%), C7(1%)	-	G**CCGGCGTCACCAC**G**CGGGGAGGTTAGATGTGCCCAGGGTCCCGT**
		6.9	A1(4.5%)	-	G**CCGGCGTCACCAC**G**CGGGGAGGTTAGATGTGCCCAGGGTCCTGT**
		5.1		-	**CCTAG**C**T**TGTGAAA--------GATCCACAGACCGCTGCTTGTTAGGGCTGGGTTCCC--
		23.9	T9(8%), C10(2%)	26.3	**CCTAGAT**GCTAC----------GGTTCAAAGCAGTGCT**TG**C**GCT**AAGGCTGGTGTACCTT
		19.4	C11(1.15%)	-	**CCTAGAT**GCATTCAACCCGTTTGGTCTCAACTGTTGAA**TG**G**GCT**GGGTCC----------
	Circular	50	G6(1%)	58.6	---**G**G**T**GAAC-TTGTTAG**TGT**A**GG**CTG**G**TGTACCTACACTA**TG**GCCCTA**G**ACAT
		34.5	C1(4.5%)	-	TGC**G**A**T**TAGG-GTTTGGC**TGT**G**GG**CCT**G**GCAGAGATCGCAA**TG**GGGACG**G**---
		5.4		-	GCC**G**G**T**GGTATTCACAGC**TGT**T**GG**TTT**G**GTTGGTCTGGTCT**TG**TGAGTT**G**----
RBD	Linear	0.9		-	CCGGGGGGGTGGGTGGGTAATGGCTGCGAATGCCTT**G**CCTTGTGAC----CCGA------
		59.5	G42(1.5%)	10.9	**GCGCGCGAAAGTGACAATTG**---------**GGCCTCGGCTGTGATTG**T**TCGAGGGGAGAC**-
		2.3		-	**GCGCGCGAAAGTGACAATTG**---------**GGCCTCGGCTGTGATTG**C**TCGAGGGGAGAC**-
		12.5	T1(3.3%), C2(1%), C13(2.8%), C29(1%)	-	--CTGGGACTGCGATCTGTA**CACCTATC**TTTCCCAA**GATTAGAGACT**ACGGC--------
		6.6		-	----------GCTGCAGTT**CACCTATC**CGTTTATG**GATTAGAGACT**TCTCGGGGACTAC
	Circular	45.5	C1(4.5%)	128	TGC----**G**ATTAGGGTTTGG**C**T**GT**G**GG**CC**TGG**CA**G**AGA**T**CGCAATGG**GG**ACGGG
		28.3	C44(9%), A46(13.5%)	-	--**GCCG-GTGGTATTCACAGCTGTTGGTTTGGTTGGTCTGGTCTTGTGTGT**TG-
		1.2	C48(1%), T49(2.3%)	-	--**GCCG-GTGGTATTCACAGCTGTTGGTTTGGTTGGTCTGGTCTTGTGTGT**CG-
		1.3		-	T-GCCGT**G**TCATGTCATCAC**CA**GT**TGGA**T**TGG**GG**GGTCTGG**CATTCT**G**GTG---

Different properties of selected circular and linear aptamers analyzed by Aptasuite program. Samples from generation 15 were sent for sequencing (MiSeq), total reads obtained for each library is shown, as well as the number of reads corresponding to each selected sequence (reads/cluster). For the aptamer sequences ranking 1 and 2, mutations found in >1% of sequences are also shown. Other sequences with more than 1,000 reads are also shown. The total number of reads for spike (linear and circular) and RBD (linear and circular) are 114,552, 129,423, 115,739 and 133,535, respectively. The bolded sequences in the aptamer sequence part are aligned using Clustal Omega software. The conserved sequences are highlighted in yellow.

4.4 Discussion

As compared with other reported in vitro ssDNA generating techniques in the literature, the proposed method is more user-friendly and has improvements as well as other advantages (Table 4.2) (3,8,16,22,47-49). This method is much simpler and faster than conventional gel-based ssDNA preparation because the whole reaction happens in just a tube which bypasses the time consuming steps of gel preparation and running, as well as DNA elution and precipitation that are followed in gel-based procedures (18). In addition, ssDNA generation through biotin-streptavidin and NaOH treatment causes possible disruption of hydrogen bonds and hydrophobic forces between streptavidin and biotin which leads to detachment of biotinylated strand and rehybridization with complementary strands in the solution, and thus presence of unwanted dsDNA in the ssDNA preparation (19,20). The same dsDNA impurity also happens in asymmetric PCR reaction where some level of DNA complementary to the strand of interest remains (7,16). Lambda exonuclease digestion of a phosphorylated reverse strand bypasses the problems

mentioned above (22), but is not compatible with applications that require a phosphate group at the 5´end of the DNA strand. However, embedding chemical phosphorothioate modifications at the 5´end inhibits the Lambda exonuclease enzyme activity leaving the strand intact after the degradation of the reverse strand (19,27). Therefore, in this study we devised a 5´ phosphorylated strand that is not affected by the digestion reaction by also including phosphorothioate modifications. Our approach allows the omission of the normally required phosphorylation step before ssPCRP circularization, thus making the whole procedure simpler (4). Furthermore, in comparison with circle-to-circle amplification (C2CA) which is another enzymatical way for single stranded linear or circular DNA production (50-52), the proposed method is faster and less complicated and no dsDNA impurity is produced during the process. Indeed, in C2CA in order to reach the sequence with desire polarity it is necessary to do at least two rounds of C2CA reaction and repeat even more rounds to get more products (51). C2CA also as more dsDNA impurities because it includes steps of polymerisation and endonuclease reactions where the produced ssDNA is partially double stranded (50).

By employing a template with random sequences and non-proof-reading Taq DNA polymerase enzyme as well as DNA circularization optimization using a complementary strands and DNA ligase enzymes, we confirmed the applicability of this method for either linear or circular aptamer selection through the SELEX procedure. Furthermore, because the method does not rely on gels and the whole reactions are done in a tube, it is possible to automate ssDNA preparation using this procedure. This technique is a good alternative for coupling of PCR with HRCA for exponential gene generation and for PCR-based PadLock Probes, as well as single stranded library production in general (2,3,7-9). Sequencing technologies such as Nanopore and PacBio use circularized DNA templates to increase quality of sequencing (53-55), the method explained herein could provide an alternative to the current protocols which could, in addition, also allow ligation of a few DNA fragments before circularization, thus providing a longer fragment for sequencing of even longer reads compared to the current methodology. Moreover, it was recently found that long ssDNA provides a very efficient way of making CRISPR-mediated knock-ins (11), in this case also, the inclusion of a phosphate at the 5´ end of PCR products allows ligation of different ssPCRP to make ssDNA beyond the typical range of PCR products, allowing insertions of larger DNA fragments in the genome, in addition to simplifying the procedure for ssDNA preparation (or reducing the cost if Megamers are used). Overall, the proposed method is likely to help many technical advancements in a number of areas in molecular biology and genetics.

Table 4.2 Comparison of different aspects of reported methods in the literature with the proposed technique.

Method	Application	Type of modifications	Amplification Method(s)	Gel based technique	dsDNA impurity	circDNA[1] preparation	Reference
Lambda Exo[2]	ssDNA preparation	Phosphorothioate & phosphorylation	PCR	-	-	+	Present work
	ssDNA preparation	Phosphorylation	PCR	-	-	-	(22)
Biotin-streptavidin	SNP[3] detection	Biotinylation	PCR	-	+	+	(3)
	Genomic DNA production	Biotinylation & phosphorylation	PCR & RCA	-	+	+	(8)
	ssDNA preparation	Biotinylation	PCR	+	+	-	(47)
C2CA[4]	Gene detection	-	RCA	-	+	+	(51)
Denaturing PAGE	Aptamer selection	HEGL[5] & fluorescein	PCR	+	-	-	(49)
Asymmetric PCR	ssDNA preparation	Phosphorylation	PCR	-	+	-[6]	(16)

[1]Circular DNA
[2]Lambda exonuclease enzyme
[3]Single nucleotide polymorphism
[4]Circle to circle amplification
[5]Hexaethyleneglycol
[6]This study has not performed circularization with the ssDNA, but it would theoretically be possible

4.5 Experimental procedures

4.5.1 Targets, primers and aptamers

The 100 bases template with two primer binding sites (25 bases for each) and 50 random bases in the middle is provided form Integrated DNA Technologies (IDT). All primers (forward and reverse) either with modifications (phosphorothioate bonds and phosphorylation) or without modifications and aptemrs were purchased from Sigma Aldrich Company. Also, complementary strand targets were obtained from IDT and Alpha ADN company (Quebec, Canada) (Table 4.S1, Appendix 1).

4.5.2 PCR and ssPCRP ligation reactions

PCR amplification was performed in PCR reaction mixture including target (0.02 µM), phosphorylated reverse primer (1 µM), phosphorothioated-phosphorylated forward primer (1 µM), 0.20 µM deoxynucleoside triphosphate (dNTP) (DGel Electrosystem, Canada), milli-Q water, 10X HotStarTaq buffer (QIAGEN) and 0.5 units HotStarTaq DNA Polymerase (QIAGEN) in final volume of 50 µL. PCR was achieved in 12 cycles and at optimized melting temperature (tm) of 68.2 ˚C thorough C1000 touch thermal cycler (Bio-rad). For single stranded PCR product (ssPCRP) preparation, each 10 µL of double stranded PCR products were treated with 5 units Lambda exonuclease enzyme (New England Biolabs, NEB) at 37 ˚C for 45 min which is followed by 10 min at 75 ˚C for enzyme inactivation.

To circularize ssPCRP, ligation reactions with T4 DNA ligase were prepared: 1 µM of ssPCRP was added to 1 µM complementary strands in 1X T4 ligation buffer (NEB) in a final volume of 10 µL. For the circularization reaction, DNA was denatured by increasing temperature to 95 ˚C for 5 min and then gradually cooled down to room temperature for DNA hybridization and circular ssPCRP formation. Afterward, the ligation reaction was performed by introducing 10 units T4 DNA ligase enzyme (NEB, USA) and incubating at 20 ˚C for 1 hour to seal the 5´ and 3´ ends of the ssPCRP. Alternatively, it is possible to use the Taq DNA ligase (NEB) with ~20 cycles of denaturation at 95 ˚C for 1 min followed by annealing and ligation steps using proper Tm for 1 min (Tm of 68, 64 and 60 ˚C for 50, 42 or 35 complementary bases between strands, respectively). After ligation, either by using T4 or Taq DNA ligase enzymes, 10 units Exonuclease I enzyme (NEB) is added to ligation mixture for non-circular ssPCRP degradation.

4.5.3 HRCA reaction

HRCA reaction was performed using different dilutions of circular ssPCRP (33.33, 16.66, 8.33, 4.16, 2.08, 1.04, 0.52 and 0 nM) in a final volume of 30 µL of amplification mixture including: 1X Phi29 DNA polymerase buffer (NEB), 0.3 µM non-modified PCR forward and reverse primers, 0.40 µM dNTP, milli-Q water, SYBR green 1X (Invitrogen), 10 µg bovine serum albumin (BSA) and 8 units Phi29 DNA polymerase enzyme (NEB). Amplification reactions were monitored for 5 hours at 30 ˚C in MicroAmp fast reaction tubes with cap (Applied Biosystems) and using real-time PCR machine (Applied Biosystems).

4.5.4 Agarose gel electrophoresis

DNA illustration by agarose gel electrophoresis has been conducted by exploiting 2% agarose gel and 1X TAE buffer (1 mM EDTA and 40 mM Tris-acetate, Fisher Scientific) and by applying constant voltage of 120 V for 40 to 60 min. Thereafter, gels were illuminated under UV radiation via gel doc (Bio-Rad) and 1X pre-added Gel Stain (TransGen Biotech). Power supply and DNA ladder were purchased from Bio-Rad and Bio-Helix, respectively.

4.5.5 [γ-^{32}P] radio-labeling

[γ-32P] labelling of 100 bases target and forward primers (phosphorothioated and non-phosphorothioated) were manipulated in a final volume of 20 µL labeling mixture containing 1X T4 polynucleotide kinase (PNK) enzyme buffer (NEB), milli-Q water, 20 pmoles of DNA substrate, 5 µCi [γ-32P] ATP (PerkinElmer) and 10 units T4 PNK enzyme (NEB) at 37 ˚C for 30 min.

4.5.6 Visualization via polyacrylamide gel electrophoresis (PAGE)

Phosphor imaging of [γ-32P] radio-labelled DNA sequences was accomplished through 6% denaturing PAGE constituted of 1X TBE (89 mM Tris base, 2 mM EDTA and 89 mM boric acid, Fisher Scientific) (57), 8 M urea (BioShop, Canada), 6% Acrylamide/Bis-acrylamide (BioShop, Canada), 16 µL N,N,N',N'-tetramethylethane-1,2-diamine (TEMED) (Fisher Scientific), 300 µL ammonium persulfate (APS) 10% (BioShop, Canada) in a total volume of 40 mL. Denaturing PAGE ran for 1 hour under constant power of 15 watt (W), subsequently the gel was exposed to a phosphorimager cassette (GE Healthcare) for 10 min and finally the cassette scanned by a Typhoon FLA 9500 biomolecular imager (GE Healthcare).

4.5.7 Recombinant MERS-CoV spike protein

Recombinant MERS-CoV spike protein and MERS-CoV spike protein fragment were produced from the MERS-CoV genome sequences (human betacoronavirus 2c EMC/2012) which encodes spike protein and receptor binding domain (RBD), respectively. For construction of MERS-CoV Spike/RBD Protein fragment (RBD, aa 367-606), the DNA sequence that encodes MERS-CoV RBD protein (#AFS88936.1, Glu367-Tyr606) was fused to the C-terminus of the Fc region of rabbit IgG. RBD obtains 464 aa and has molecular mass of 51.5 kDa with purity of > 80 % that is determined by SDS-PAGE. For construction of MERS-CoV Spike Protein (S1+S2 ECD, aa 1-1297, His Tag), the DNA sequence that is encoding the MERS-CoV spike protein extracellular domain (AFS88936.1, Met1-Trp1297) was fused with a polyhistidine tag at the

C-terminus. The recombinant spike protein MERS-CoV extracellular domain obtains 1291 aa and has molecular mass of 142.52 kDa with purity of > 85 % as determined by SDS-PAGE. For expression of recombinant MERS-CoV spike proteins Baculovirus insect cells were used. The recombinant RBD and full spike proteins were directly purchased from Sino Biological, China.

4.5.8 Spike proteins immobilization

Recombinant spike proteins immobilization on agarose magnetic beads (CNBr-activated SepFastTM MAG 4HF, BioToolomics, UK) was performed based on the protocol provided by BioToolomics. In this work, 10 mg of each recombinant protein was immobilized on 300 mg/ml agarose magnetic beads. After doing several steps for spike protein functionalization on agarose magnetic beads, the immobilized beads washed several times using SELEX buffer and magnet to remove un-bound spike proteins from stock solution. Thereafter immobilized spike protein was diluted in 500 µl of SELEX buffer which was used as stock spike protein solution to perform 15 cycles of SELEX. This solution should be vortexed well before addition to each cycle to make sure that homogeneous concentration of immobilized protein is added to SELEX cycles.

4.5.9 SELEX procedure

Circular library preparation was performed in final T4 ligation mixture of 100 µl including 1X T4 DNA ligase buffer (NEB, USA), 1 µM phosphorylated library, 1 µM 35 bp complementary strand, 20 U T4 DNA ligase enzyme (NEB, USA) and milliQ water for 1 hour at 16 ˚C which was followed by enzyme inactivation for 20 mins at 80 ˚C. Thereafter, the ligation reaction was treated by 10 U of Exonuclease I enzymes (NEB, USA) for 1 hour at 37 ˚C for degradation of non-circularized library. Then, the exonuclease was inactivated at 80 ˚C for 20 mins.

The first round of SELEX was started separately in the presence of 100 pmol of linear and circular libraries using immobilized spike proteins and spike proteins fragments. During the first round the linear and circular libraries were incubated for 2 hours with immobilized spike proteins on agarose magnetic beads at room temperature in 1 ml of 1× SELEX buffer (20 mM Tris-HCl (pH:7.4), 2 mM CaCl2, 5 mM KCl, 100 mM NaCl, 1 mM MgCl2). Thereafter, the bound libraries were collected by applying a magnet (Invitrogen, USA) which is followed by supernatant removal and washing agarose beads with 500 µL 1× SELEX buffer. Afterward the beads were diluted in 20 µL of SELEX buffer and 5 µL of the diluted library was directly used for enrichment step using PCR protocol described in the main text of paper and in the final volume of 50 µL. In this step a phosphorothioated forward primer and phosphorylated reverse primer were used for the linear

library and a phosphorothioated/phosphorylated forward primer and phosphorylated reverse primer utilized for the circular library. After verification of PCR bands using agarose gel, ssPCRPs were produced from PCR products using the previously described procedure and at this point the linear library has been regenerated for another round of SELEX. For the circular library the produced phosphorylated libraries were circulated using the process explained earlier with a T4 DNA ligase enzyme for sealing the library head to tail. The positive selection process has been done for 15 rounds of SELEX using circular and linear libraries and using the spike protein and the spike protein fragment as targets. Moreover, four SELEX rounds were performed as negative selection cycles using non-specific targets including agarose magnetic beads and lysozyme protein immobilized on agarose magnetic beads (Table 4.S2, Appendix 1). From SELEX rounds 1 to 15 concentration of ligands and incubation time have gradually decreased, while number of washes as well as washing time have gradually increased. The detailed information about SELEX conditions used for each SELEX round is shown in Table 4.S2, Appendix 1.

4.5.10 K_D determination using Monolith device

5’ phosphorylated circular aptamers against full spike/RBD were circularized using procedure mentioned in section 4.5.2, however in this ligation reaction 35 bp complementary strand without was used since the aptamers were directly purchased and were not the product of PCR (ssPCRP). Thereafter, selected linear/circular aptamers were equally diluted with 5’ Cy5 labeled complementary strand to reach the optimum concentrations of 5 nM where satisfying fluorescence intensity was obtained for K_D determination using Monolith device (NanoTemper, Germany). Affinity of the selected aptamers was evaluated in 16 test tubes where spike/RBD proteins were diluted by double from the initial concentration 1 mM and then 5 nM of aptamer/Cy5 labeled complementary strand complex were added to each protein dilution in final volume of 20 µl. The labeled aptamer/protein mixture is incubated for 30 min at room temperature before loading them in Monolith NT.115 Capillary (NanoTemper, Germany) and determining binding affinity using Monolith machine.

4.5.11 qPCR reaction

Real-time monitoring of qPCR reaction using modified primers including normal, phosphorylated, phosphorothioated and phosphorylated/phosphorothioated forward primers as well as a phosphorylated reverse primer were done in qPCR reaction mixtures including 1X reaction mixture of GoTaq 2-Step RT-qPCR kit (Promega, USA), 400 nM forward and reverse primers and

in final volume of 20 µL. PCR was performed a total of 20 cycles and at an annealing temperature of 68 ˚C and via an Applied Biosystems qPCR machine.

4.6 Funding and additional information

SV Hamidi received fellowships from Armand-Frappier foundation and Fonds québécois de la recherche sur la nature et les technologies (FRQNT). JP is a junior 2 FRQS research scholar. Other funding, including for open access charge: NSERC [RGPIN-2019-06403].

4.7 References

1. Tuerk, C. and Gold, L. (1990) Systematic evolution of ligands by exponential enrichment: RNA ligands to bacteriophage T4 DNA polymerase. Science, 249, 505-510.

2. Gao, H., Tao, S., Wang, D., Zhang, C., Ma, X., Cheng, J. and Zhou, Y. (2003) Comparison of different methods for preparing single stranded DNA for oligonucleotide microarray. Anal. Lett. ,36, 2849-2863.

3. Antson, D.-O., Isaksson, A., Landegren, U. and Nilsson, M. (2000) PCR-generated padlock probes detect single nucleotide variation in genomic DNA. Nucleic Acids Res., 28, e58-e58.

4. Liu, M., Yin, Q., Chang, Y., Zhang, Q., Brennan, J.D. and Li, Y. (2019) In vitro selection of circular DNA aptamers for biosensing applications. Angewandte Chemie International Edition, 58, 8013-8017.

5. Brennan, J.D., Bialy, R.M., Ali, M.M. and Li, Y. (2020) Protein-Mediated Suppression of Rolling Circle Amplification for Biosensing with an Aptamer-containing DNA Primer. Chem. Eur. J., 26, 5085-5092.

6. Li, J., Mohammed-Elsabagh, M., Paczkowski, F. and Li, Y. (2020) Circular Nucleic Acids: Discovery, Functions and Applications. ChemBioChem, 21, 1547-1566.

7. Tang, X., Morris, S.L., Langone, J.J. and Bockstahler, L.E. (2006) Simple and effective method for generating single-stranded DNA targets and probes. BioTechniques, 40, 759-763.

8. Van Emmerik, C.L., Gachulincova, I., Lobbia, V.R., Daniëls, M.A., Heus, H.A., Soufi, A., Nelissen, F.H. and van Ingen, H. (2020) Ramified rolling circle amplification for synthesis of nucleosomal DNA sequences. Anal. Biochem., 588, 113469.

9. Gansauge, M.-T. and Meyer, M. (2013) Single-stranded DNA library preparation for the sequencing of ancient or damaged DNA. Nat. Protoc., 8, 737.

10. Hu, Q., Wang, S., Wang, L., Gu, H., and Fan, C. (2018) DNA Nanostructure-Based Systems for Intelligent Delivery of Therapeutic Oligonucleotides. Adv. Healthc. Mater. 7, 1701153.

11. Bai, H., Liu, L., An, K., Lu, X., Harrison, M., Zhao, Y., Yan, R., Lu, Z., Li, S., and Lin, S. (2020) CRISPR/Cas9-mediated precise genome modification by a long ssDNA template in zebrafish. BMC genomics. 21, 1-12.

12. Badenhorst, D., Dannebaum, R., Hayes, A., Herrera, M., Margeridon, S. and Ranik, M. (2020). U. S. Patent- US20200199663A1

13. George, M., Johnson, J.A., Nguyen, D. and Schlecht, U. (2020). U.S Patent- US20200208208A1.

14. Nehdi, A., Samman, N., Aguilar-Sánchez, V., Farah, A., Yurdusev, E., Boudjelal, M. and Perreault, J. (2020) Novel strategies to optimize the amplification of single-stranded DNA. Front. Bioeng. Biotechnol. , 8, 401.

15. Darmostuk, M., Rimpelova, S., Gbelcova, H., and Ruml, T. (2015) Current approaches in SELEX: An update to aptamer selection technology. Biotechnology advances 33, 1141-1161

16. Tolnai, Z., Harkai, Á., Szeitner, Z., Scholz, É.N., Percze, K., Gyurkovics, A. and Mészáros, T. (2019) A simple modification increases specificity and efficiency of asymmetric PCR. Anal. Chim. Acta., 1047, 225-230.

17. Williams, K.P. and Bartel, D.P. (1995) PCR product with strands of unequal length. Nucleic Acids Res., 23, 4220-4221.

18. Lopez-Gomollon, S. and Nicolas, F.E. (2013) In Lorsch, J. (ed.), Methods Enzymol. Academic Press, 529, pp. 65-83.

19. Marimuthu, C., Tang, T.-H., Tominaga, J., Tan, S.-C. and Gopinath, S.C. (2012) Single-stranded DNA (ssDNA) production in DNA aptamer generation. Analyst, 137, 1307-1315.

20. Holmberg, A., Blomstergren, A., Nord, O., Lukacs, M., Lundeberg, J. and Uhlén, M. (2005) The biotin-streptavidin interaction can be reversibly broken using water at elevated temperatures. Electrophoresis, 26, 501-510.

21. Avci-Adali, M., Paul, A., Wilhelm, N., Ziemer, G. and Wendel, H.P. (2010) Upgrading SELEX technology by using lambda exonuclease digestion for single-stranded DNA generation. Molecules, 15, 1-11.

22. Citartan, M., Tang, T.-H., Tan, S.-C. and Gopinath, S.C. (2011) Conditions optimized for the preparation of single-stranded DNA (ssDNA) employing lambda exonuclease digestion in generating DNA aptamer. World J. Microbiol. Biotechnol., 27, 1167-1173.

23. Nikiforov, T.T., Rendle, R.B., Kotewicz, M.L. and Rogers, Y.-H. (1994) The use of phosphorothioate primers and exonuclease hydrolysis for the preparation of single-stranded PCR products and their detection by solid-phase hybridization. Genome Res., 3, 285-291.

24. Nikiforov, T. T., and Knapp, M. R. (1996) Method for generating single-stranded DNA molecules. U.S. Patent US5518900A.

25. Toyoshima, Y., Nemoto, K., Matsumoto, S., Nakamura, Y., and Kiyotani, K. (2020) SARS-CoV-2 genomic variations associated with mortality rate of COVID-19. Journal of Human Genetics 65, 1075-1082

26. Mullis, K.B. (1990) The unusual origin of the polymerase chain reaction. Sci. Am., 262, 56-65

27. Kujau, M.J. and Wölfl, S. (1997) Efficient preparation of single-stranded DNA for in vitro selection. Mol. Biotechnol., 7, 333-335.

28. Little, J.W. (1967) An exonuclease induced by bacteriophage λ II. Nature of the enzymatic reaction. J. Biol. Chem., 242, 679-686.

29. Kushner, S.R., Nagaishi, H. and Clark, A.J. (1972) Indirect suppression of recB and recC mutations by exonuclease I deficiency. Proc. Natl. Acad. Sci. U. S. A., 69, 1366-1370.

30. Lehman, I. and Nussbaum, A. (1964) The deoxyribonucleases of Escherichia coli V. On the specificity of exonuclease I (phosphodiesterase). J. Biol. Chem., 239, 2628-2636.

31. Hamidi, S.V. and Perreault, J. (2019) Simple rolling circle amplification colorimetric assay based on pH for target DNA detection. Talanta, 201, 419-425.

32. Lehnman, I. R. (1974) DNA ligase: structure, mechanism, and function. Science 186, 790-797.

33. Hamidi, S. V., and Perreault, J. (2019) Simple rolling circle amplification colorimetric assay based on pH for target DNA detection. Talanta 201, 419-425

34. Priyakumar, U.D., Hyeon, C., Thirumalai, D. and MacKerell Jr, A.D. (2009) Urea destabilizes RNA by forming stacking interactions and multiple hydrogen bonds with nucleic acid bases. J. Am. Chem. Soc., 131, 17759-17761.

35. Singer, A., Kuhn, H., Frank-Kamenetskii, M. and Meller, A. (2010) Detection of urea-induced internal denaturation of dsDNA using solid-state nanopores. J. Condens. Matter Phys., 22, 454111.

36. Di Giusto, D. A., Knox, S. M., Lai, Y., Tyrelle, G. D., Aung, M. T., and King, G. C. (2006) Multitasking by multivalent circular DNA aptamers. ChemBioChem 7, 535-544

37. Di Giusto, D.A., Knox, S.M., Lai, Y., Tyrelle, G.D., Aung, M.T. and King, G.C. (2006) Multitasking by multivalent circular DNA aptamers. ChemBioChem, 7, 535-544.

38. Brownstein, M.J., Carpten, J.D. and Smith, J.R. (1996) Modulation of non-templated nucleotide addition by Taq DNA polymerase: primer modifications that facilitate genotyping. Biotechniques, 20, 1004-1010.

39. Marchuk, D., Drumm, M., Saulino, A. and Collins, F.S. (1991) Construction of T-vectors, a rapid and general system for direct cloning of unmodified PCR products. Nucleic Acids Res., 19, 1154.

40. Smith, J.R., Carpten, J.D., Brownstein, M.J., Ghosh, S., Magnuson, V.L., Gilbert, D.A., Trent, J.M. and Collins, F.S. (1995) Approach to genotyping errors caused by nontemplated nucleotide addition by Taq DNA polymerase. Genome Res. , 5, 312-317.

41. Nilsson, M., Malmgren, H., Samiotaki, M., Kwiatkowski, M., Chowdhary, B. and Landegren, U. (1994) Padlock probes: circularizing oligonucleotides for localized DNA detection. Science, 265, 2085-2088.

42. Krzywkowski, T., and Nilsson, M. (2018) Padlock probes to detect single nucleotide polymorphisms. in RNA detection, Springer. pp 209-229

43. Larsson, C., Koch, J., Nygren, A., Janssen, G., Raap, A.K., Landegren, U. and Nilsson, M. (2004) In situ genotyping individual DNA molecules by target-primed rolling-circle amplification of padlock probes. Nat. Methods, 1, 227.

44. Barany, F. (1991) Genetic disease detection and DNA amplification using cloned thermostable ligase. Proc. Natl. Acad. Sci. U. S. A., 88, 189-193.

45. Gansauge, M.-T., Gerber, T., Glocke, I., Korlević, P., Lippik, L., Nagel, S., Riehl, L.M., Schmidt, A. and Meyer, M. (2017) Single-stranded DNA library preparation from highly degraded DNA using T4 DNA ligase. Nucleic Acids Res., 45, e79-e79.

46. Hamidi, S.V., Ghourchian, H. and Tavoosidana, G. (2015) Real-time detection of H 5 N 1 influenza virus through hyperbranched rolling circle amplification. Analyst, 140, 1502-1509.

47. Pagratis, N.C. (1996) Rapid preparation of single stranded DNA from PCR products by streptavidin induced electrophoretic mobility shift. Nucleic Acids Res., 24, 3645-3646.

48. Alhassan, A., Osei-Atweneboana, M.Y., Kyeremeh, K.F., Poole, C.B., Li, Z., Tettevi, E., Tanner, N.A. and Carlow, C.K. (2016) Comparison of a new visual isothermal nucleic acid

amplification test with PCR and skin snip analysis for diagnosis of onchocerciasis in humans. Mol. Biochem. Parasitol., 210, 10-12.

49. Kim, Y.S., Hyun, C.J., Kim, I.A. and Gu, M.B. (2010) Isolation and characterization of enantioselective DNA aptamers for ibuprofen. Bioorg. Med. Chem., 18, 3467-3473.

50. Song, S., Wang, X., Xu, K., Li, Q., Ning, L. and Yang, X. (2019) Selection of highly specific aptamers to Vibrio parahaemolyticus using cell-SELEX powered by functionalized graphene oxide and rolling circle amplification. Anal. Chim. Acta, 1052, 153-162.

51. Dahl, F., Banér, J., Gullberg, M., Mendel-Hartvig, M., Landegren, U. and Nilsson, M. (2004) Circle-to-circle amplification for precise and sensitive DNA analysis. Proc. Natl. Acad. Sci. U. S. A., 101, 4548-4553.

52. Ke, R., Zorzet, A., Göransson, J., Lindegren, G., Sharifi-Mood, B., Chinikar, S., Mardani, M., Mirazimi, A. and Nilsson, M. (2011) Colorimetric nucleic acid testing assay for RNA virus detection based on circle-to-circle amplification of padlock probes. J. Clin. Microbiol., 49, 4279-4285.

53. Wenger, A. M., Peluso, P., Rowell, W. J., Chang, P.-C., Hall, R. J., Concepcion, G. T., Ebler, J., Fungtammasan, A., Kolesnikov, A., and Olson, N. D. (2019) Accurate circular consensus long-read sequencing improves variant detection and assembly of a human genome. Nat. Biotechnol. 37, 1155-1162

54. Travers, K. J., Chin, C.-S., Rank, D. R., Eid, J. S., and Turner, S. W. (2010) A flexible and efficient template format for circular consensus sequencing and SNP detection. Nucleic Acids Res. 38, e159-e159

55. Calus, S. T., Ijaz, U. Z., and Pinto, A. J. (2018) NanoAmpli-Seq: a workflow for amplicon sequencing for mixed microbial communities on the nanopore sequencing platform. Gigascience. 7, 140.

5 DISCUSSION

Recent advances in biology and medicine have let to better realization of diseases bases and developing new strategies for curing and treating of diseases. However, the global health is still threatened by many diseases and especially infectious ones which cause several pandemics during 19th and 20th centuries. The current COVID-19 pandemic cases by SARS-CoV-2 has led to the deaths of millions of people and the whole world lockdown as well as million jobs lost. Therefore, such pandemic not only highly endangers the public health but also has pervasive effects on society, including the world economy. As a result, broad scientific research on infectious disease is quite essential to control and manage of epidemics and pandemics. Disease management during pandemics relies on fast and sensitive monitoring of the cases at airports, developing countries and remote areas where accesses to equipped labs for conventional molecular tests are limited. Thus, there are many detection methods, especially isothermal amplification techniques, that have been developed for fast, cheap, portable, and specific detection of infectious diseases.

This PhD project provides an overview on PLP based RCA as a molecular tool for sensitive and simple monitoring of infectious diseases. In this thesis RCA as a signal amplification tool was coupled with different platforms, namely: colorimetric and optics, depending on purposes and applications. Although RCA is not being used as much as the conventional PCR-based techniques, so far several RCA based kits have been developed, such as kits for analysis of virus genome, SNP detection and protein-protein interaction monitoring and kits only for research purposes (Rector *et al.*, 2004, Sable *et al.*, 2018).

Fast, specific, and reliable monitoring of viruses is very important for public health and restricting the spread of viruses. It is also crucial to monitor mutated and circulating subtypes of viruses to be able to predict potential pandemics. As previously mentioned, nucleic acid amplification tests (NAATs) have replaced the arduous task of viral cell culturing and insufficient immune-assay tests for virus detection. Although, real time PCR is a conventional and leading technique compared to other NAATs, this method relies on sophisticated and expensive real time thermal cycler device which is not user-friendly for viruses monitoring in remote areas (Neumann, 2020). In the first paper published in *Talanta Journal* a novel colorimetric PLP/RCA biosensor was developed for detection of H5N1 virus using phenol red as a pH sensitive dye. This PLP/RCA based method is not only able to detect a specific virus but also it can be used to surveillance mutated virus and subtyping of viruses for multiplexing purposes. In this work several analytical parameters such as

linear range, and improved contrast between positive and negative control samples were enhanced compared to previous reported dyes such as hydroxy naphthol blue, calcein with $MnCl_2$ and Quant-iT PicoGreen that were used for colorimetric monitoring of isothermal DNA amplification reaction and which have not accomplished such level of contrast (Hamidi *et al.*, 2015a, Hamidi *et al.*, 2019, Wastling *et al.*, 2010) (Fig. 5.1). Moreover, in this isothermal DNA amplification, signal is amplified enough to monitor the target in either a qualitive or quantitative way. It is worth to note that the LAMP based phenol red colorimetric detection has been commercialized by New England Biolabs (NEB) company which is now being used as a simple method for COVID-19 detection[2]. However, our RCA/PLP based phenol red based detection method has the advantage of detecting SNPs that would be useful for monitoring of variants (Hamidi *et al.*, 2019). Although the color change for phenol red is quite visible (pink to yellow) compared to other reported colorimetric strategies (Fig. 5.1), in this colorimetric detection method DNA amplification should be performed in reaction mixture without Tris-HCl (which is very sensitive to the pH change) and thus all the reaction mixture should be well optimized and we should avoid adding DNA samples with very high and low pH values. This unfortunately limits the shelf-life, robustness and reproducibility of the assay for the moment Thus, until further development improves these aspects, it is not ideal for a more widespread use.

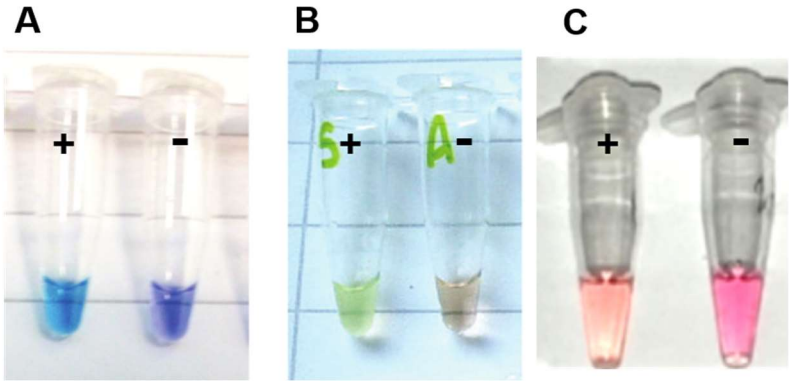

Figure 5.1 **Reported dye were used for colorimetric detection of isothermal DNA reaction. (A) hydroxy naphthol blue. (B) calcein with $MnCl_2$. (C) phenol red. Adapted from (Hamidi *et al.*, 2019, Wastling *et al.*, 2010) with permission.**

Early detection of diseases especially for cancer and infectious diseases is of great importance in medical diagnosis field because, in several types of diseases such as cancer early detection leads to increased survival rates in patients and in case of infectious diseases early detection

[2]https://international.neb.com/products/e2019-sars-cov-2-rapid-colorimetric-lamp-assay-kit#Product%20Information

limits the spread of virus. One of the main challenges that scientists have been dealing with, since the emergence of medical diagnosis, is detection of very low amount of target. Techniques that can detect single molecule should have several properties including: 1) they should be highly specific to the target in order to minimize the background. 2) they must be ultra sensitive to be able to detect a single molecule of interest. 3) they should be able to amplify signal because such sensitivity cannot be achieved without possessing a signal amplification property. In addition, the resolution of these detection methods should be high enough to recognize a single (or a few) molecule (Weibrecht *et al.*, 2010).

To reach this goal, in the second article published in *Lab on a Chip Journal,* an ultra-sensitive detection platform was established by combining two robust techniques including optical microcavities and RCA. The detection system presented in this project has exceptional advantages over other conventional detection methods such as PCR, ELISA and even LAMP. First, coupling high RI sensitive μIMZI with signal amplification by the RCA method makes it possible to reach a very low limit of detection. This novel optical biosensor can be used for high throughput purposes due to its pL volume size. Due to the pL volume size of μIMZI channel, very tiny amount of sample is needed to do the test compared to ELISA and PCR where at least 50 μL of reaction mixture is needed for a test. On the other hand, a very small volume reduces the LOD when high sensitivity is required. For instance, when 1000 virus copies exist in a 1 mL sample, lower than 1 virus copy presents in 100 nL. In addition, as compared with PCR where a thermal cycle machine is used, in μIMZI based RCA method, DNA amplification is performed at room temperature thanks to phi29 DNA polymerase enzyme and isothermal nature of RCA. Although, LAMP offers isothermal DNA amplification strategy, in LAMP method amplification happens at 65 ˚C which makes it hard to be integrated with optical fiber-based detection systems. Furthermore, although the selectivity of the biosensor was not been evaluated in this study, the selectivity of the same PLP toward H5N1 was evaluated in our previous study where phenol red was used for colorimetric H5N1 virus monitoring (Hamidi *et al.*, 2019). Moreover, this biosensor offers rapid quantitative (30 min) responses for highly sensitive (LOD of 6 copies) DNA/RNA target detection which is much faster than qPCR that needs at least 2 hours amplification to reach such sensitivity.

Although in this thesis RCA has been used as a central molecular tool for infectious diseases detection, PCR and qPCR are still conventional methods that are frequently used in labs. RCA and other isothermal DNA amplification techniques such as LAMP are only useful for detection purposes due to their isothermal nature and an increasing application of such NAATs in areas

with limited resources. However, since the products of RCA and LAMP are branched and huge tandemly repeated DNA which make them not useful to be applied with techniques like cloning and sequencing. In addition, the Taq DNA polymerase enzyme that is used in PCR is much cheaper and more available than Bst and Phi29 DNA polymerases that are utilized in LAMP and RCA methods. Furthermore, designing primers for PCR is very easy compared to sophisticated 3 pairs primers using in LAMP which still makes PCR popular after about 50 years of introduction. Besides, in contrast with RCA/PLP which a long probe with a length of about 80 to 115 bases is employed, the length of primers in PCRs are about 18-25 bases which makes the price of PCR test much lower that RCA based PLP technique. So far, several diagnostics kits that are based on isothermal amplification technique such as Affymetrix SNP array (Thermo Scientific), WarmStart Colorimetric LAMP 2X Master Mix (NEB) for specific DNA target detection and, Duolink in situ - proximity ligation assay (Sigma Alderich) for investigation of protein-protein-have been developed. However, these kits are only used for research and have not been utilized for clinical purposes yet. One may conclude that such diagnostics approaches are very new and need time to be well established in clinics or hospitals. Also, all the clinical labs are developed based on the conventional methods such as qPCR/PCR and ELISA and applying new technologies that are based on isothermal DNA amplification methods need lots of efforts and budget to train staffs and update labs accordingly. The other reason would be the fact that such conventional methods have been developed about 50 years ago and since then many detection methods and procedures are developed based on this gold standards technique which in turn would empower resistant toward these recent technologies.

In all biosensors developed in this thesis, PLP have been utilized as a molecular tool for specific detection of targets. PLP can specifically detect the target through specific hybridization of PLP arms with the target which leads to formation of circular DNA (C-PLP). Thereafter, a covalently closed circular PLP is formed by sealing the head to tail of PLP using a ligase enzyme (Fig. 1.9 B). This circular DNA is then used as a template for HRCA reaction. As previously described, even a single mutation at the ligation site can avoid proper PLP and target hybridization and thus suppresses PLP head to tail ligation. This further highlights the selectivity of PLPs toward their specific targets (Fig. 1.10) (Larsson *et al.*, 2004a). In fact in LAMP and NASBA selectivity is determined by overall hybridization of primers with their target, while this selectivity can be tuned by using either the 3’ or 5’ end of the PLP in PLP-based HRCA.

Methods for *in vitro* ssDNA preparation are regarded as fundamental tools in molecular biology due to their broad applications in gene editing, DNA origami, DNA storage, SELEX and other

applications (Hao *et al.*, 2020). Due to the increasing application requirements, various approaches have been established to generate ssDNA. Some of methods have been developed to allow to generate defined ssDNA sequences in different lengths, yield, and purity. In addition, so far several methods have been developed for preparation of circular ssDNA because of growing interests in selection of circular aptamer and library (Liu *et al.*, 2019). Most of ssDNA generation methods rely on gels which is a time-consuming procedure and is not user-friendly method for high-throughput purposes.

In this thesis, by using simple chemical modifications including a phosphorylated-phosphorothioated forward primer and a phosphorylated reverse primer, a simple Lambda Exonuclease enzyme-based method was developed for circular ssDNA preparation. Due to the high potential of applications of ssDNA preparation methods in molecular biology and rising interests in circular aptamer and library preparation, this simple user-friendly and non gel-based technique would be a good alternative to be used for facile linear and circular ssDNA preparation for high-throughput purposes. Because in the proposed method all steps including PCR, ssDNA preparation and circular DNA preparation steps are done in just one tube, there is no need to use complicated and time-consuming processes and gel-based methods for ssDNA preparation and purification. This can indeed improve the throughput of linear and circular DNA library preparation due to its simplicity and efficiency, notably by making it easier to automate. The performance of this method has been evaluated by doing 15 cycle of SELEX for selecting linear and circular aptamer against the spike protein of MERS-CoV which confirms the possibility of employing the proposed method for real applications. It is worth saying that by using this novel method for circular and linear aptamer selection not only the whole SELEX procedure was simplified but also this method improves circular and linear aptamer selection process (Table 3.1). The selected circular aptamers can not only be used for specific MERS-CoV spike protein detection but also, they can be used as circular template for exponential signal amplification though HRCA. Thus, the detection procedure will be simplified compared to other RCA based protein detection method already reported in the literature (Lee *et al.*, 2009, Zhou *et al.*, 2007). In addition, unlike the other gel-based ssDNA methods, this method is very fast allowing us to complete two and three rounds of SELEX from circular and linear aptamers in just a day, respectively. As well as the application of this method in SELEX, the proposed process could be useful to prepare libraries for technologies like nanopore sequencing technique, where linear ssDNA is used, however the use of circular DNA would allow generation of multimers that in turn strengthen the confidence in the validity of the reads obtained.

Due to the high sensitivity, simplicity and versatility of rolling circle amplification (RCA), this technique is more applicable and efficient as compared to other isothermal DNA amplification methods such as LAMP and NASBA. Unlike other isothermal DNA amplification techniques, RCA has the advantage of performing DNA replication at room temperature (Table 1.1). Therefore, RCA has been coupled with other platforms: SPR (Huang *et al.*, 2007), electrochemistry (Zhou *et al.*, 2007), microfluidic systems (Jiang *et al.*, 2019), electrochemiluminescence (Lin *et al.*, 2019), and recently with optical microcavity (Janik *et al.*, 2021). In addition, RCA/PLP based methods can be used for multiplexing due to the fact that the spacer portion of PLP (Fig. 1.9 B) can be barcoded with different fluorescent molecule tags so that several targets can be monitored at the same time (Fig. 5.2). Furthermore, the tandemly repeated DNA-sequence in RCPs is an excellent template and programmable building block to make nano- or micro-scale structure. It is also possible to manipulate the properties of RCPs by changing the length and sequence of template circular DNA. Therefore, the technique has been frequently used for different purposes in nanotechnology and biomaterial (Ali *et al.*, 2014, Zhao *et al.*, 2008). Strömberg and colleagues utilized RCPs as periodic template for one-dimensional aggregation of magnetic nanobeads which are coated with complementary probes for sensitive molecular diagnostics. In this study they were able to detect DNA target down to pM levels (Strömberg et al., 2008). In another approach, RCA based surface Plasmon resonance was used via two-dimensional aggregation of gold nanoparticles (AuNPs). In this method genomes of pathogenic microorganisms were detected with LOD of 0.5 pM), (Shi *et al.*, 2014). In addition, a similar strategy was utilized for detection of multiple point mutations with gold nanoparticles improved surface-anchored RCA (Xiang *et al.*, 2013). The colorimetric detection of SNP in β-thalassemia gene was achieved at femto level by hybridizing AuNP-conjugated probes onto the RCPs. In this study, PLPs are circularized if the mutation exists in genomic DNA. By proceeding with the RCA reaction, the RCPs are digested to short similar sequences which serve as linkers to close the AuNPs to each other. This process led to a change in color solution by which the SNP could be detected by either UV-vis or even naked eyes (Li *et al.*, 2010) (Fig. 5.3).

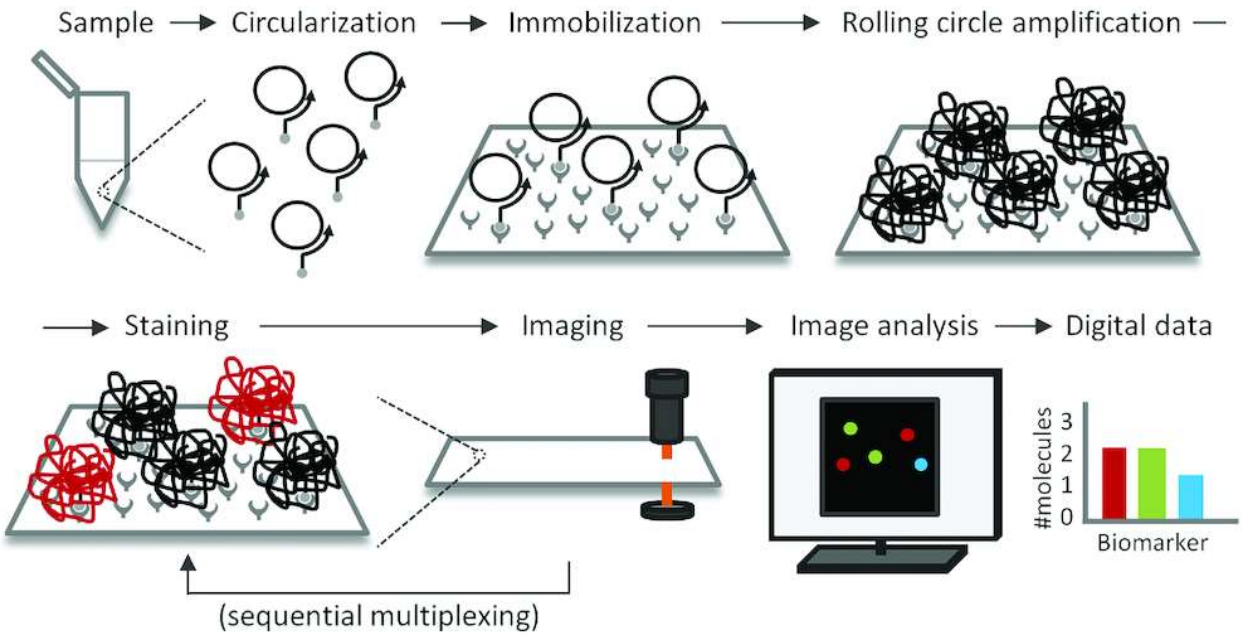

Figure 5.2 **Multiplex digital monitoring of RCPs. First, circular PLPs are formed upon specific detection of DNA/RNA target molecules (Circularization). Thereafter, circular PLPs are captured by biotinylated primers which are then captured on a microscope slide coated with streptavidin (Immobilization). Initiation of RCA reaction and production of tandemly repeated ssDNA products by introducing RCA amplification mixture a drop on a glass slide (RCA). RCPs are stained by hybridizing fluorescent tagged complementary DNA with RCPs. (Staining). Staining step is followed by imaging and DNA analysing steps for interpreting results. Adapted from (Björkesten *et al.*, 2020) with permission.**

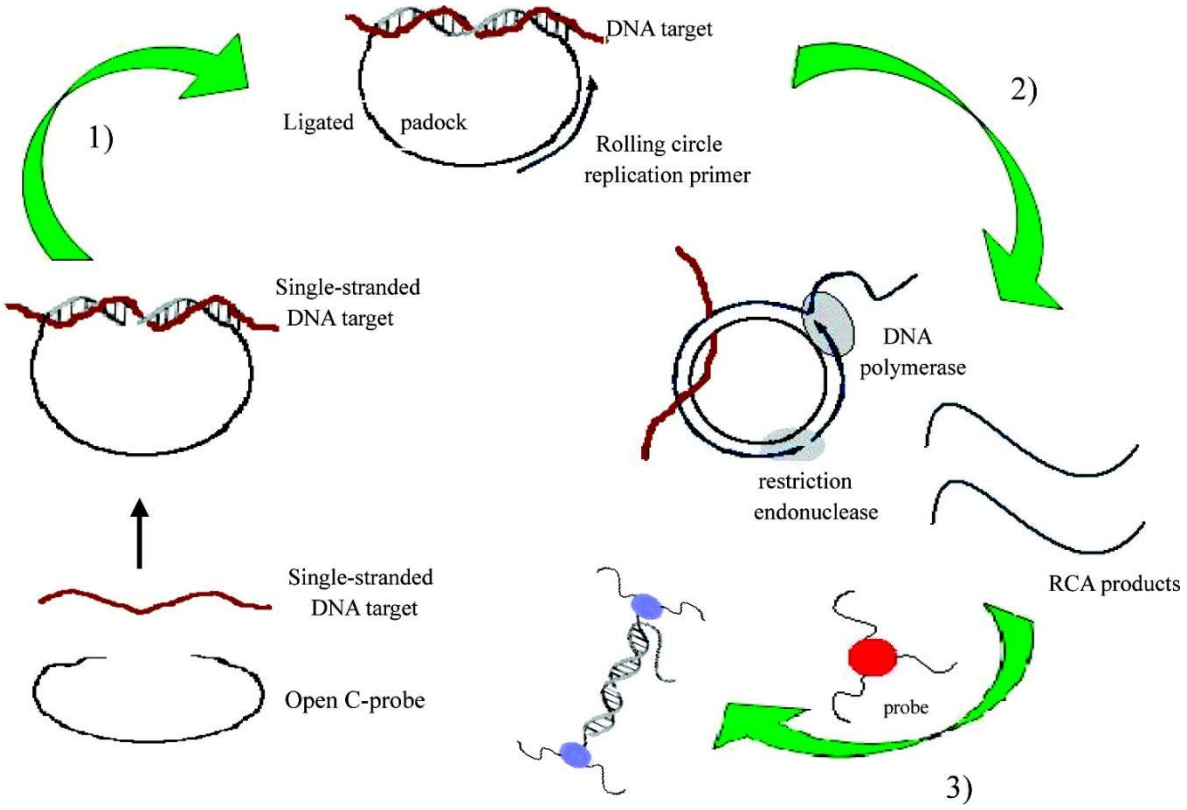

Figure 5.3 **Schematic representation of the RCA and AuNP assembly assay: (1) Specific hybridization of PLP and target which is followed with PLP hear to tail ligation (2) RCA DNA amplification and RCPs endonuclease digestion; (3) colorimetric detection through assembly AuNP aggregation. Adapted from (Li *et al.*, 2010) with permission.**

So far, this versatile technology has been combined with several platforms for signal magnification through DNA amplification for biosensing aims. This isothermal enzymatic reaction generates single strand DNA from short circular DNA template. The technique was first conducted to ultra sensitive detection of DNA targets, circular DNA viruses and genomic analyzing. Thereafter, conjugation of RCA with antibodies led to detection of single protein, protein-protein interaction and post-translational modifications through proximity ligation assay (PLA) strategy (Fig. 5.4) (Weibrecht *et al.*, 2010). Recently, RCA has been used to generate tandem sequences of DNAzymes and aptamers as detecting template for sensitive recognition of proteins and small molecules. Moreover, the repetitive nature of the RCA products is a good template to produce periodic nanoassembly. As a result, RCA has become a simple and exclusive technique for applications in a vast area of biotechnology including diagnosis, genomics, nanotechnology and biomaterial (Ali *et al.*, 2014, Mohsen *et al.*, 2016).

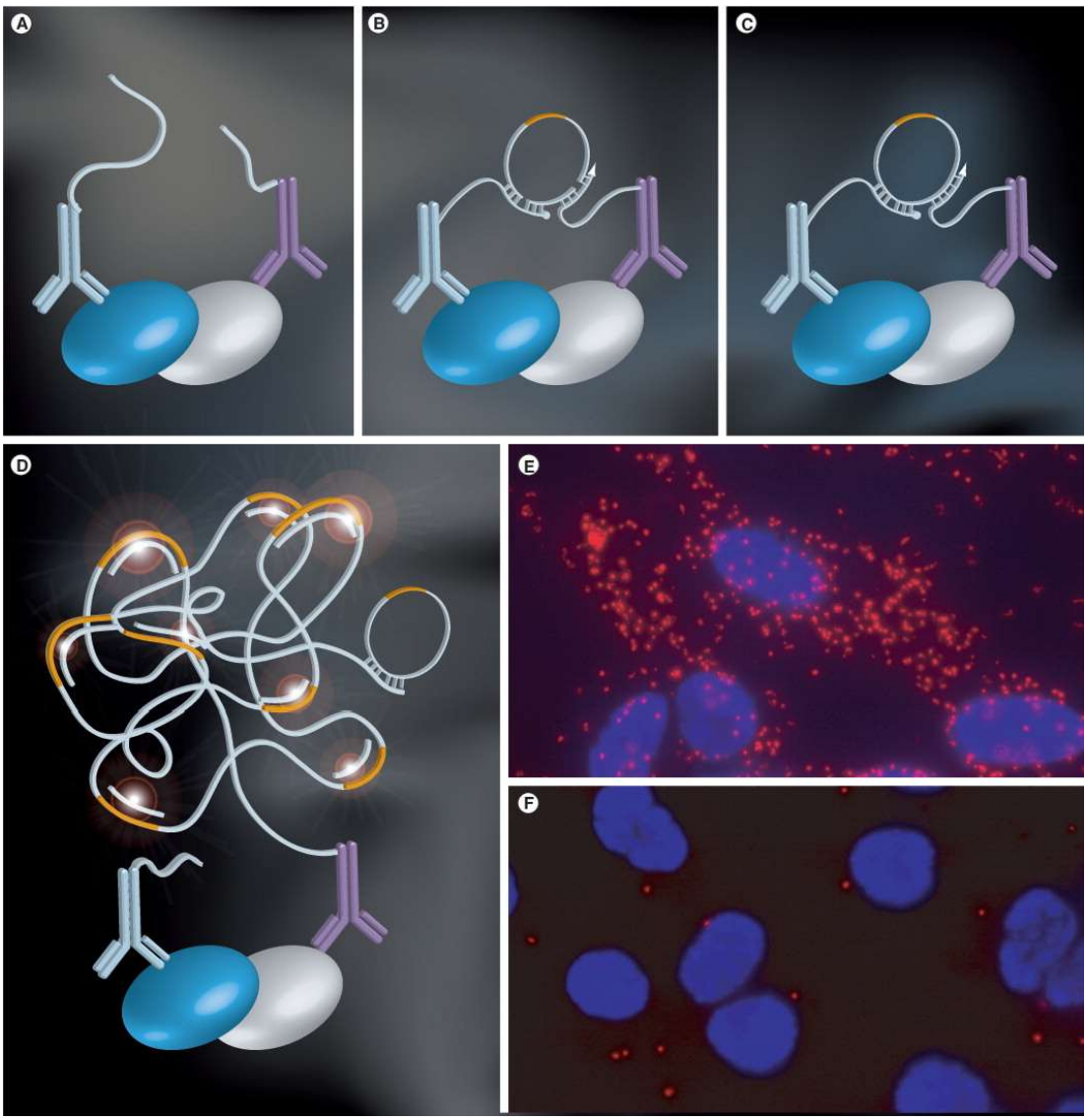

Figure 5.4 **Schematic illustration of PLA strategy. (A) By attaching two binding probes to similar target molecules in a protein mixture, the proximal probe oligonucleotides are placed side by side. (B) Then, the antibody-conjugated oligonucleotides can bind with two connector oligonucleotides, which (C) form a circular DNA template. (D) Thus the new DNA molecule can be amplified by RCA. The result of this amplification is a single and localized molecule of DNA that can be identified by the hybridization of complementary fluorescence-labeled complementary oligonucleotides. For example, this method has been used to detect post-translational changes in the individual PDGF-β receptor molecules in human fibroblast-stimulated PDGF-BB. Each bright spot indicates the detection of a phosphorylated receptor, the nuclei are gray. (F) Detection of phosphorylated PDGF-β receptors in unstimulated human fibroblasts. Adapted from (Weibrecht *et al.*, 2010) with permission.**

All in all, the overall aim of this thesis is using RCA as a powerful signal amplification technique for developing biosensors using different platforms including colorimetric and optical ones. In addition, as a part of this work a novel and simple *in-vitro* method was developed for linear and circular ssDNA generation due to rising applications of circular ssDNA in molecular biology

In the first objective of this work, a simple method was developed for colorimetric monitoring of RCA using phenol red as a pH sensitive dye. Although, the same colorimetric method was already developed for LAMP technique (Tanner *et al.*, 2015), in this work for the first time phenol red is employed for colorimetric monitoring of PLP-based RCA. Since PLP-based RCA is composed of ligation and amplification reactions, in this project for the first-time DNA ligation was performed in a ligation reaction mixture lacking Tris-HCl to be able to couple this colorimetric assay with PLP-based RCA. Moreover, in this study a novel colorimetric method was developed for specific monitoring of SNPs, highlighting the exceptional advantage of this assays compared to other isothermal DNA amplification techniques. Finally, the signal response of this assay was also validated in presence of real DNA target and samples containing complex matrix to confirm the performance the proposed assay in real situations.

In the second objective of this PhD thesis for the first time optical-fiber-based sensor (the μIMZI) has been applied for the real-time monitoring of isothermal DNA amplification. The proposed optical biosensor has the advantages of high sensitivity, analysis of analytes in volumes as low as picoliter (which indeed improves the sensitivity), as well as highly efficient optical fiber functionalization using click chemistry. An outstanding linearity ranging from 283 to 2 830 000 DNA target copies, was obtained by coupling RCA with μIMZI just within 30 min. In addition, the LOD as low as 6 copies was achieved using this strategy.

In third objective of this work by employing phosphor-derived modifications a novel and simple *in-vitro* linear and circular ssDNA preparation was introduced. Although, chemically modified nucleotides that are resistant to nucleases especially phosphorothioate bond modifications has already been reported for ssDNA preparation (Nikiforov *et al.*, 1994), In this study, phosphor-derived modifications including 5´ phosphorylation and phosphorothioate bonds modifications have been utilized for *in-vitro* production of linear or circular ssDNA. In this research we showed that although Lambda exonuclease enzyme has strong 5´ exonuclease activity on phosphorylated dsDNA, the digestion activity is completely repressed on phosphorothioate modified strand even though it has phosphorylation modifications. The protected phosphor group can be used for circular library preparation using ligase enzyme. This could highly simplify the process of circular ssDNA preparation since this method is not relied on gel and all steps could be done in just a

tube. It is worth to say that the performance of this method is also validated by doing 15 successive cycles of SELEX for selecting linear and circular aptamers against MERS-CoV spike protein.

As far as ASSURED definition is concerned, the proposed colorimetric method has advantages of affordability with final price of lower that 2 CAD per reaction, good selectivity, and also being rapid, user-friendly, equipment-free and deliverable to those people who need it. However, more optimizations are needed to get higher sensitivity proper for clinical proposes. This assay has also potential to be automated for ease of use and improvement of the simplicity of the technique. For the RCA-based μIMZI biosensor, although an ultra sensitive biosensor was developed by coupling two robust techniques, the proposed biosensor is not affordable and nor user-friendly and nor easily deliverable to the concerned group. Because, at least for now, such technique needs an expensive laser and skilled operators to perform this assay, this biosensor cannot be easily automated either. However, this sensor has the advantage of being robust and rapid. Indeed, it could measure a concentration as low as 280 copies of targets within just 30 mins.

6 CONCLUSION

RCA is a simple and robust isothermal DNA amplification technique that has a broad application in biosensing as well as clinical and point of care testing. The feasibility of the combination of the RCA with functional nucleic acids, especially aptamers, and other platforms namely ELISA, microfluidics, SPR (Surface plasmon resonance) and nanoparticles makes it possible to detect different types of targets (DNA, protein, virus, cells and small molecules) with high sensitivity (Ali *et al.*, 2014). Therefore, due to versatility and compatibility of this isothermal amplification method, in this PhD project, RCA was utilized as a powerful signal amplification method for biosensing purposes.

The focus of this Ph.D. project was developing RCA based biosensors for simple and sensitive monitoring of infectious disease using different platforms such as colorimetric and optical platforms. In addition, a new *in vitro* method for linear and circular ssDNA generation using phosphor-derived modification was developed. In case of first objective which is about colorimetric detection of H5N1 influenza virus using phenol red, several improvements in analytical parameters including a good linear range from 0.61 to 78.1 nM and improved contrast between positive controls (light orange color) and negative controls (pink) were obtained (chapter 2, Table 2.1). Such color contrast has not been achieved using other colorimetric dyes used for isothermal DNA amplification monitoring (Hamidi *et al.*, 2015a, Tanner *et al.*, 2015, Tomita *et al.*, 2008). Because of the isothermal nature of the RCA and the use of a colorimetric approach, this technique is proper for portable screening of infectious disease where there is no access to an equipped lab. In contrast, also as a part of this PhD thesis, an ultra-sensitive biosensor was developed by combining two robust techniques namely RCA and μIMZI. This picoliter size μIMZI had very high RI sensitivity of 14,000 nm per RI unit and showed a good linearity ranging from 9.4 aM and 94 pM of the H5N1 target with very low detection limit of 0.2 aM DNA. This ultra-sensitive μIMZI based RCA is also quite fast which is able to detect the concentration as low as 9.4 aM just after 30 mins. Such sensitive biosensors are proper to be used to screen infected patients that are asymptomatic because their virus load is very low. Therefore, the contagious people can be isolated in advance in order to slow down the spreading of the dangerous disease (the obvious example is COVID19 disease) as much as it is possible. In the final part of the project, a novel method for circular ssDNA preparation was devised and shown to work. Although several techniques have been already reported for this purpose, most of these techniques have several time-consuming steps which significantly increase the time required to perform SELEX, because

the latter typically required 15 iterations of the overall procedures, thus multiplies by that much the time required by any of the steps used in these iterations. Using simple phosphorothioate bond modifications as well as phosphorylation modification and using conventional Lambda exonuclease enzyme, the process to generate circular ssDNA was simplified and made faster. Unlike the other gel-based ssDNA preparation methods (Table 4.2), in this procedure all the steps including PCR, ssDNA generation using Lamda exonuclease, and ligation step using T4 ligase enzyme have been done just in a single tube, which would also make it easier for automation. Furthermore, using phosphorylated- phosphorothioated forward primer in PCR not only protects the primer from digestion during exonuclease treatment using Lamda enzyme but also the protected phosphor group can be used for ligation reaction. Moreover, this new technique is a good bridging method to connect PCR with RCA since RCA is based on the fundamental property of circular DNA. It is worth to note that the performance of the method has been validated by selecting linear and circular aptamer for MERS CoV spike protein during 15 cycles of SELEX.

7 PERSPECTIVES

The simplicity, efficiency, and isothermal nature of RCA makes this technique a robust molecular tool for methods development compared to conventional PCR method. For more simplification of molecular detection using RCA, it is possible to couple this isothermal amplification method with microfluidics systems in order to automate process of detection and offer instrumentation free devices. By using preprogrammed microfluidics systems, the whole process of the detection including PLP ligation step as well as RCA reaction can be fully automated. Thus, utilizing such strategy could highly minimize user intervention leading to a more rapid and precise detection process.

Protein-based detection has several advantages over nucleic acid-based detection because it allows rapid detection by excluding the arduous step of RNA/DNA extraction. Therefore, it is possible to select circularizable or circular aptamers to combine protein detection step using aptamer with signal magnification through RCA. The performance of methods described in chapter 4 is evaluated for circular aptamer selection via SELEX against spike protein of MERS CoV and hopefully after getting the selected aptamers, we can develop RCA based biosensors using circular aptamer not only for selective detection of the target but also as a template for signal amplification through RCA. To do this, the target molecule is captured using immobilized primary linear aptamer and circular aptamer to make aptamer based immune-sandwich (Fig. 7.1 A). Thereafter, the bound circular aptamer is used as a template for RCA reaction using specific primer for RCA reaction initiation (Fig. 7.1 B). This reaction can be monitored using SYBR Green as a fluorescence DNA intercalating dye for quantitative target detection (Fig. 7.1 C). This detection strategy can be more simplified with colorimetric dyes such as phenol red, HNB or calcein.

Furthermore, our proposed linear and circular ssDNA preparation technique can be used for other purposes such as PCR based PLP generation (Antson *et al.*, 2000), oligonucleotide microarray preparation (Gao *et al.*, 2003), circular aptamer selection (Brennan *et al.*, 2020, Li *et al.*, 2020, Liu *et al.*, 2019), labeled probe preparation (Tang *et al.*, 2006), coupling PCR with RCA method, linear and circular library for DNA sequencing (Gansauge *et al.*, 2013) as well as production of origami nanostructure (Hu *et al.*, 2018) and also long ssDNA donor for genome editing using clustered regularly interspaced short palindromic repeats (CRISPR) (Bai *et al.*, 2020).

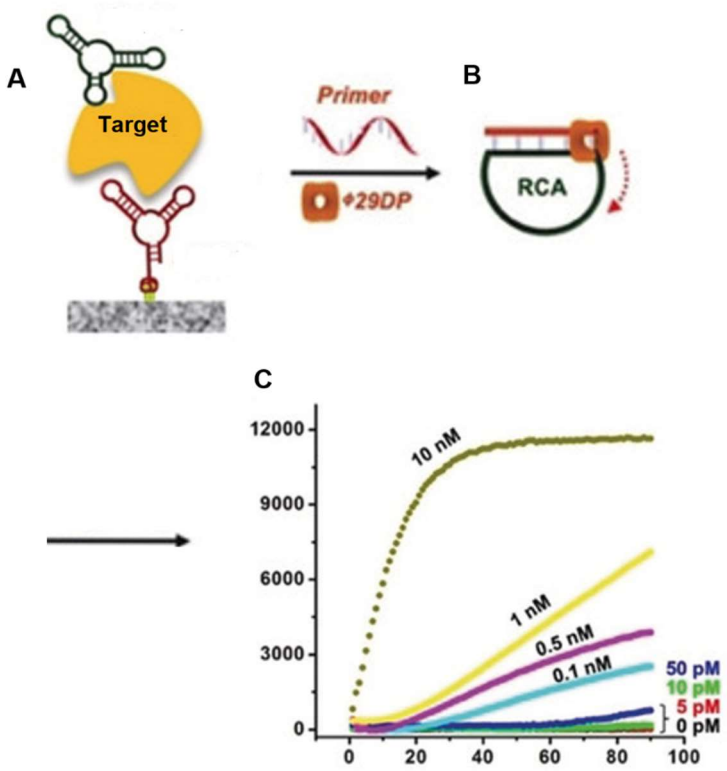

Figure 7.1 **Visual illustration of specific target detection using circular aptamer and RCA reaction. (A) immune-sandwich formation using immobilized linear aptamer and circular secondary aptamer. (B) RCA reaction initiation by introducing phi29 DNA polymerase and primer. (C) quantitative monitoring of RCA reaction using SYBR Green. Adapted from (Liu *et al.*, 2019) with permission.**

Moreover, by considering the fact that RCA can produce aptamer in multimer mode, it is possible to start to do positive and negative selections in the presence of the multimeric aptamers which is a novel strategy in selection process. Also using a multimeric library that have several binding sites is a good approach for selection of aptamers against cells or bacteria with several similar antigens on the surfaces to improve the affinity of the library toward such targets.

The other application of utilizing multimeric aptamer which is worth mentioning is developing multimeric aptamers that may show cooperative characteristics. It means that binding of one small target would facilitate the attachment of the other targets to the other binding sites of the aptamer. As well as this, using multimeric aptamers has been already used for facilitating and improving the process of drug delivery in cancer cells. This improves the killing ability of the multivalent aptamer by enhancing the loading capacity of the aptamer with drugs (Vorobyeva *et al.*, 2016) (Fig. 7.2).

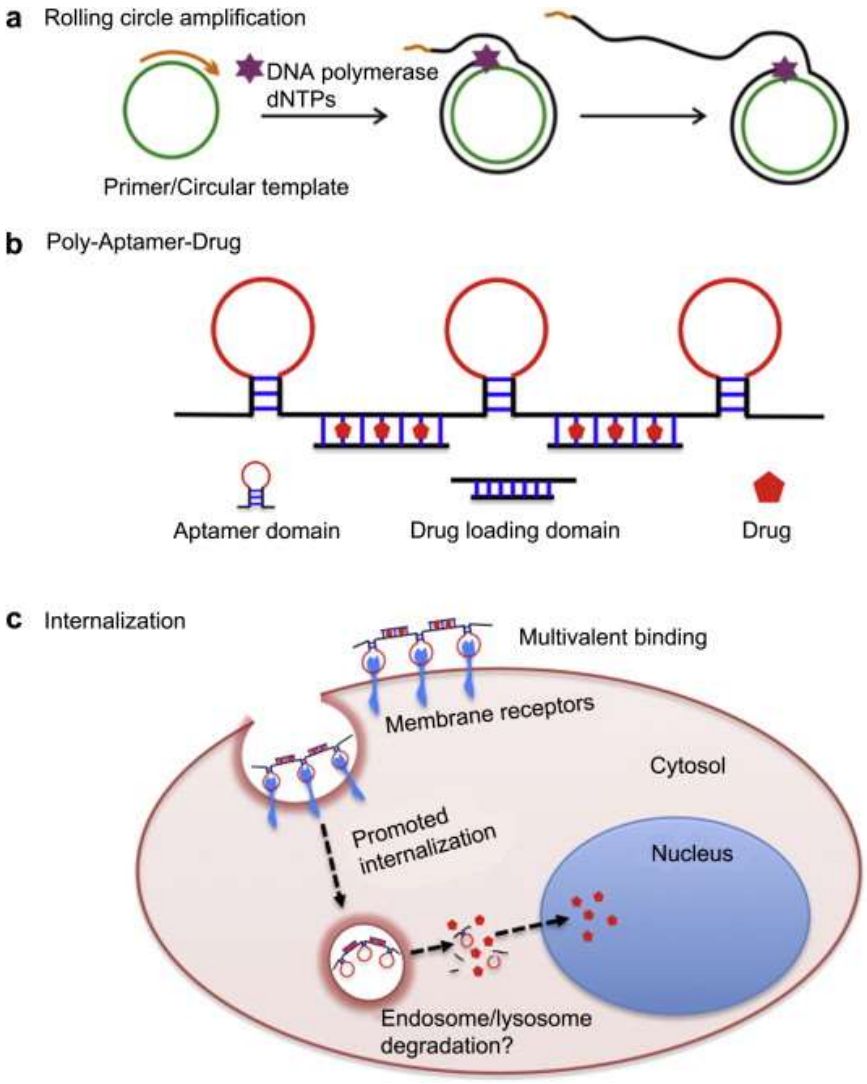

Figure 7.2 **Schematic concept of utilizing Poly-Aptamer-Drug for killing cancer cells.A) multivalent aptamer formation through RCA using circular template (green circle), primer for RCA initiation (orange line), phi29 DNA polymerase (purple star) and in the presence of dNTPs. B) Poly-Aptamer-Drug formation using a short complementary stand for drug loading. c) Specific binding of Poly-Aptamer-Drug to receptors of target cancer cell. multivalency effects caused by Poly-Aptamer-Drug highly improves cancerous cells during intake. Adapted from (Zhang *et al.*, 2013) with permission.**

All in all, RCA is a simple and robust isothermal DNA amplification technique that has a broad application in biosensing as well as clinical and point of care testing. The feasibility of the combination of the RCA with functional nucleic acids, especially aptamers, and other platforms namely ELISA, microfluidics, SPR and nanoparticles makes it possible to detect different types of targets (DNA, protein, virus, cells and small molecules) with high sensitivity (Ali *et al.*, 2014).

8 REFERENCES

Akter F, Mie M & Kobatake E (2011) Immuno-rolling circle amplification using a multibinding fusion protein. *Analytical Biochemistry* 416(2):174-179.

Al-Osail AM & Al-Wazzah MJ (2017) The history and epidemiology of Middle East respiratory syndrome corona virus. *Multidisciplinary respiratory medicine* 12(1):20.

Ali MM, Li F, Zhang Z, Zhang K, Kang D-K, Ankrum JA, Le XC & Zhao W (2014) Rolling circle amplification: a versatile tool for chemical biology, materials science and medicine. *Chemical Society Reviews* 43(10):3324-3341.

Antson D-O, Isaksson A, Landegren U & Nilsson M (2000) PCR-generated padlock probes detect single nucleotide variation in genomic DNA. *Nucleic acids research* 28(12):e58-e58.

Bai H, Liu L, An K, Lu X, Harrison M, Zhao Y, Yan R, Lu Z, Li S & Lin S (2020) CRISPR/Cas9-mediated precise genome modification by a long ssDNA template in zebrafish. *BMC genomics* 21(1):1-12.

Baner J, Nilsson M, Mendel-Hartvig M & Landegren U (1998) Signal amplification of padlock probes by rolling circle replication. *Nucleic acids research* 26(22):5073-5078.

Björkesten J, Patil S, Fredolini C, Lönn P & Landegren U (2020) A multiplex platform for digital measurement of circular DNA reaction products. *Nucleic Acids Research* 48(13):e73-e73.

Böhmer A, Schildgen V, Lüsebrink J, Ziegler S, Tillmann RL, Kleines M & Schildgen O (2009) Novel application for isothermal nucleic acid sequence-based amplification (NASBA). *Journal of virological methods* 158(1-2):199-201.

Brennan JD, Bialy RM, Ali MM & Li Y (2020) Protein-Mediated Suppression of Rolling Circle Amplification for Biosensing with an Aptamer-containing DNA Primer. *Chemistry–A European Journal*.

Chen C & Wang J (2020) Optical biosensors: an exhaustive and comprehensive review. *Analyst* 145(5):1605-1628.

Chen W, He B, Li C, Zhang X, Wu W, Yin X, Fan B, Fan X & Wang J (2007) Real-time RT-PCR for H5N1 avian influenza A virus detection. *Journal of Medical Microbiology* 56(5):603-607.

Cho I-H, Kim DH & Park S (2020) Electrochemical biosensors: perspective on functional nanomaterials for on-site analysis. *Biomaterials Research* 24(1):6.

Ciftci S, Neumann F, Abdurahman S, Appelberg KS, Mirazimi A, Nilsson M & Madaboosi N (2020) Digital Rolling Circle Amplification–Based Detection of Ebola and Other Tropical Viruses. *The Journal of Molecular Diagnostics* 22(2):272-283.

Citartan M, Tang T-H, Tan S-C & Gopinath SC (2011) Conditions optimized for the preparation of single-stranded DNA (ssDNA) employing lambda exonuclease digestion in generating DNA aptamer. *World Journal of Microbiology and Biotechnology* 27(5):1167-1173.

Craw P & Balachandran W (2012) Isothermal nucleic acid amplification technologies for point-of-care diagnostics: a critical review. *Lab on a Chip* 12(14):2469-2486.

Curtis KA, Rudolph DL & Owen SM (2009) Sequence-specific detection method for reverse transcription, loop-mediated isothermal amplification of HIV-1. *Journal of Medical Virology* 81(6):966-972.

Damborský P, Švitel J & Katrlík J (2016) Optical biosensors. *Essays in Biochemistry* 60(1):91-100.

Darmostuk M, Rimpelova S, Gbelcova H & Ruml T (2015) Current approaches in SELEX: An update to aptamer selection technology. *Biotechnology advances* 33(6):1141-1161.

Demidov VV (2002) Rolling-circle amplification in DNA diagnostics: the power of simplicity. *Expert review of molecular diagnostics* 2(6):542-548.

Donlagic D (2011) All-fiber micromachined microcell. *Optics letters* 36(16):3148-3150.

Eftimov TA, Janik M & Bock WJ (2019) Microcavity In-Line Mach–Zehnder Interferometers Fabricated in Single-Mode Fibers and Fiber Tapers for Visible (VIS) and Near-Infrared (NIR) Operation. *Journal of Lightwave Technology* 37(13):3351-3356.

Ellington AD & Szostak JW (1990) In vitro selection of RNA molecules that bind specific ligands. *nature* 346(6287):818.

Fan T, Mao Y, Sun Q, Liu F, Lin J-S, Liu Y, Cui J & Jiang Y (2018) Branched rolling circle amplification method for measuring serum circulating microRNA levels for early breast cancer detection. *Cancer science* 109(9):2897-2906.

Fouchier RAM, Munster V, Wallensten A, Bestebroer TM, Herfst S, Smith D, Rimmelzwaan GF, Olsen B & Osterhaus ADME (2005) Characterization of a Novel Influenza A Virus Hemagglutinin Subtype (H16) Obtained from Black-Headed Gulls. *Journal of Virology* 79(5):2814-2822.

Gansauge M-T & Meyer M (2013) Single-stranded DNA library preparation for the sequencing of ancient or damaged DNA. *Nature protocols* 8(4):737.

Gao H, Tao S, Wang D, Zhang C, Ma X, Cheng J & Zhou Y (2003) Comparison of different methods for preparing single stranded DNA for oligonucleotide microarray. *Analytical letters* 36(13):2849-2863.

Gill P & Ghaemi A (2008) Nucleic acid isothermal amplification technologies—a review. *Nucleosides, Nucleotides and Nucleic Acids* 27(3):224-243.

Goo NI & Kim DE (2016) Rolling circle amplification as isothermal gene amplification in molecular diagnostics. *BioChip Journal* 10(4):262-271.

Goto M, Honda E, Ogura A, Nomoto A & Hanaki K-I (2009) Short technical reports. *Biotechniques* 46:167-172.

Gracias KS & McKillip JL (2007) Nucleic acid sequence-based amplification (NASBA) in molecular bacteriology: a procedural guide. *Journal of Rapid Methods & Automation in Microbiology* 15(3):295-309.

Green NM (1990) Avidin and streptavidin. *Methods in enzymology* 184:51-67.

Gu L, Yan W, Liu L, Wang S, Zhang X & Lyu M (2018) Research Progress on Rolling Circle Amplification (RCA)-Based Biomedical Sensing. *Pharmaceuticals* 11(2):35.

Gyarmati P, Conze T, Zohari S, LeBlanc N, Nilsson M, Landegren U, Banér J & Belák S (2008) Simultaneous genotyping of all hemagglutinin and neuraminidase subtypes of avian influenza viruses by use of padlock probes. *Journal of clinical microbiology* 46(5):1747-1751.

Hamblin GD, Carneiro KMM, Fakhoury JF, Bujold KE & Sleiman HF (2012) Rolling Circle Amplification-Templated DNA Nanotubes Show Increased Stability and Cell Penetration Ability. *Journal of the American Chemical Society* 134(6):2888-2891.

Hamidi SV & Ghourchian H (2015a) Colorimetric monitoring of rolling circle amplification for detection of H 5 N 1 influenza virus using metal indicator. *Biosensors and Bioelectronics* 72:121-126.

Hamidi SV, Ghourchian H & Tavoosidana G (2015b) Real-time detection of H 5 N 1 influenza virus through hyperbranched rolling circle amplification. *Analyst* 140(5):1502-1509.

Hamidi SV & Perreault J (2019) Simple rolling circle amplification colorimetric assay based on pH for target DNA detection. *Talanta* 201:419-425.

Hao M, Qiao J & Qi H (2020) Current and Emerging Methods for the Synthesis of Single-Stranded DNA. *Genes* 11(2):116.

Hardenbol P, Baner J, Jain M, Nilsson M, Namsaraev EA, Karlin-Neumann GA, Fakhrai-Rad H, Ronaghi M, Willis TD, Landegren U & Davis RW (2003) Multiplexed genotyping with sequence-tagged molecular inversion probes. *Nature Biotechnology* 21(6):673-678.

Hardenbol P, Yu F, Belmont J, MacKenzie J, Bruckner C, Brundage T, Boudreau A, Chow S, Eberle J & Erbilgin A (2005) Highly multiplexed molecular inversion probe genotyping: over 10,000 targeted SNPs genotyped in a single tube assay. *Genome research* 15(2):269-275.

Hellyer TJ & Nadeau JG (2004) Strand displacement amplification: a versatile tool for molecular diagnostics. *Expert Review of Molecular Diagnostics* 4(2):251-261.

Hu Q, Wang S, Wang L, Gu H & Fan C (2018) DNA Nanostructure-Based Systems for Intelligent Delivery of Therapeutic Oligonucleotides. *Advanced healthcare materials* 7(20):1701153.

Hu T, Wang Y, Liao C & Wang D (2012) Miniaturized fiber in-line Mach–Zehnder interferometer based on inner air cavity for high-temperature sensing. *Optics letters* 37(24):5082-5084.

Huang P, Wang H, Cao Z, Jin H, Chi H, Zhao J, Yu B, Yan F, Hu X, Wu F, Jiao C, Hou P, Xu S, Zhao Y, Feng N, Wang J, Sun W, Wang T, Gao Y, Yang S & Xia X (2018) A Rapid and Specific Assay for the Detection of MERS-CoV. *Frontiers in Microbiology* 9(1101).

Huang W, Hsu H, Su J, Clapper J & Hsu J (2020) Room Temperature Isothermal Colorimetric Padlock Probe Rolling Circle Amplification for Viral RNA Detection. *bioRxiv* 10.1101/2020.06.12.128876:2020.2006.2012.128876.

Huang Y-Y, Hsu H-Y & Huang C-JC (2007) A protein detection technique by using surface plasmon resonance (SPR) with rolling circle amplification (RCA) and nanogold-modified tags. *Biosensors and Bioelectronics* 22(6):980-985.

Janik M (2019) *Development of rapid and real-time detection of pathogenic E. coli bacteria using microcavity in-line Mach-Zehnder interferometer (μIMZI)*. (Université du Québec en Outaouais).

Janik M, Hamidi SV, Koba M, Perreault J, Walsh R, Bock WJ & Śmietana M (2021) Real-time isothermal DNA amplification monitoring in picoliter volumes using an optical fiber sensor. *Lab on a Chip* 21(2):397-404.

Janik M, Myśliwiec A, Koba M, Celebańska A, Bock W & Śmietana M (2017) Sensitivity pattern of femtosecond laser mach-zehnder interferometers, as applied to small-scale refractive index sensing. *IEEE Sensors Journal* 17(11):3316-3322.

Jarvius J, Melin J, Göransson J, Stenberg J, Fredriksson S, Gonzalez-Rey C, Bertilsson S & Nilsson M (2006) Digital quantification using amplified single-molecule detection. *Nature methods* 3(9):725-727.

Jeong Y-J, Park K & Kim D-E (2009) Isothermal DNA amplification in vitro: the helicase-dependent amplification system. *Cellular and Molecular Life Sciences* 66(20):3325.

Jiang Y, Li S, Qiu Z, Le T, Zou S & Cao X (2019) Rolling circle amplification and its application in microfluidic systems for Escherichia coli O157: H7 detections. *Journal of Food Safety* 39(5):e12671.

Johne R, Müller H, Rector A, van Ranst M & Stevens H (2009) Rolling-circle amplification of viral DNA genomes using phi29 polymerase. *Trends in Microbiology* 17(5):205-211.

Ke R, Zorzet A, Göransson J, Lindegren G, Sharifi-Mood B, Chinikar S, Mardani M, Mirazimi A & Nilsson M (2011) Colorimetric Nucleic Acid Testing Assay for RNA Virus Detection Based on Circle-to-Circle Amplification of Padlock Probes. *Journal of Clinical Microbiology* 49(12):4279-4285.

Koch JE (2003) Cascade nucleic acid amplification reaction. Patent No. US 6,610,481 B2.

Koczula Katarzyna M & Gallotta A (2016) Lateral flow assays. *Essays in biochemistry* 60(1):111-120.

Krzywkowski T & Nilsson M (2018) Padlock Probes to Detect Single Nucleotide Polymorphisms. *RNA Detection: Methods and Protocols*, Gaspar I (Édit.) Springer New York, p 209-229.

Kuhn H, Demidov VV & Frank-Kamenetskii MD (2002) Rolling-circle amplification under topological constraints. *Nucleic acids research* 30(2):574-580.

Landegren U, Kaiser R, Sanders J & Hood L (1988) A ligase-mediated gene detection technique. *Science* 241(4869):1077-1080.

Larsson C, Koch J, Nygren A, Janssen G, Raap AK, Landegren U & Nilsson M (2004a) In situ genotyping individual DNA molecules by target-primed rolling-circle amplification of padlock probes. *Nature methods* 1(3):227-232.

Lee J, Icoz K, Roberts A, Ellington AD & Savran CA (2009) Diffractometric detection of proteins using microbead-based rolling circle amplification. *Analytical chemistry* 82(1):197-202.

Leonardo S, Toldrà A & Campàs M (2021) Biosensors Based on Isothermal DNA Amplification for Bacterial Detection in Food Safety and Environmental Monitoring. *Sensors* 21(2):602.

Lewin B (2004) Genes VIII. Upper Saddle River. *New Jeresy: Pearson Prentice Hall*.

Li F, Zhang H, Wang Z, Newbigging AM, Reid MS, Li X-F & Le XC (2014) Aptamers facilitating amplified detection of biomolecules. *Analytical chemistry* 87(1):274-292.

Li J, Deng T, Chu X, Yang R, Jiang J, Shen G & Yu R (2010) Rolling circle amplification combined with gold nanoparticle aggregates for highly sensitive identification of single-nucleotide polymorphisms. *Analytical chemistry* 82(7):2811-2816.

Li J, Mohammed-Elsabagh M, Paczkowski F & Li Y (2020) Circular Nucleic Acids: Discovery, Functions and Applications. *ChemBioChem 21(11): 1547-1566*.

Li X-H, Zhang X-L, Wu J, Lin N, Sun W-M, Chen M, Ou Q-S & Lin Z-Y (2019) Hyperbranched rolling circle amplification (HRCA)-based fluorescence biosensor for ultrasensitive and specific detection of single-nucleotide polymorphism genotyping associated with the therapy of chronic hepatitis B virus infection. *Talanta* 191:277-282.

Liang K, Zhai S, Zhang Z, Fu X, Shao J, Lin Z, Qiu B & Chen G-n (2014) Ultrasensitive colorimetric carcinoembryonic antigen biosensor based on hyperbranched rolling circle amplification. *Analyst* 139(17):4330-4334.

Liao C, Hu T & Wang D (2012) Optical fiber Fabry-Perot interferometer cavity fabricated by femtosecond laser micromachining and fusion splicing for refractive index sensing. *Optics express* 20(20):22813-22818.

Lin Y, Huang X, Zhang Y, Chen D, Wang J, Luo F, Guo L, Qiu B & Lin Z (2019) Electrochemiluminescence Biosensor for the Detection of the Folate Receptor in HeLa Cells Based on Hyperbranched Rolling Circle Amplification and Terminal Protection. *ChemElectroChem* 6(3):827-833.

Liu D, Daubendiek SL, Zillman MA, Ryan K & Kool ET (1996) Rolling circle DNA synthesis: small circular oligonucleotides as efficient templates for DNA polymerases. *Journal of the American Chemical Society* 118(7):1587-1594.

Liu M, Yin Q, Chang Y, Zhang Q, Brennan JD & Li Y (2019) In vitro selection of circular DNA aptamers for biosensing applications. *Angewandte Chemie International Edition* 58(24):8013-8017.

Lizardi PM, Huang X, Zhu Z, Bray-Ward P, Thomas DC & Ward DC (1998) Mutation detection and single-molecule counting using isothermal rolling-circle amplification. *Nature genetics* 19(3) 19(3):225-232.

Long Y, Zhou X & Xing D (2011) Sensitive and isothermal electrochemiluminescence gene-sensing of Listeria monocytogenes with hyperbranching rolling circle amplification technology. *Biosensors and Bioelectronics* 26(6):2897-2904.

Lutz S, Weber P, Focke M, Faltin B, Hoffmann J, Müller C, Mark D, Roth G, Munday P, Armes N, Piepenburg O, Zengerle R & von Stetten F (2010) Microfluidic lab-on-a-foil for nucleic acid analysis based on isothermal recombinase polymerase amplification (RPA). *Lab on a Chip* 10(7):887-893.

Mallikaratchy P (2017) Evolution of Complex Target SELEX to Identify Aptamers against Mammalian Cell-Surface Antigens. *Molecules* 22(2):215.

Marimuthu C, Tang T-H, Tominaga J, Tan S-C & Gopinath SC (2012) Single-stranded DNA (ssDNA) production in DNA aptamer generation. *Analyst* 137(6):1307-1315.

Mohsen MG & Kool ET (2016) The Discovery of Rolling Circle Amplification and Rolling Circle Transcription. *Accounts of chemical research* 49(11):2540-2550.

Mori Y & Notomi T (2009) Loop-mediated isothermal amplification (LAMP): a rapid, accurate, and cost-effective diagnostic method for infectious diseases. *Journal of infection and chemotherapy* 15(2):62-69.

Nallur G, Luo C, Fang L, Cooley S, Dave V, Lambert J, Kukanskis K, Kingsmore S, Lasken R & Schweitzer B (2001) Signal amplification by rolling circle amplification on DNA microarrays. *Nucleic acids research* 29(23):e118-e118.

Neumann F (2020) *Advancing isothermal nucleic acid amplification tests: Towards democratization of diagnostics*. (Department of Biochemistry and Biophysics, Stockholm University).

Neumann F, Hernández-Neuta I, Grabbe M, Madaboosi N, Albert J & Nilsson M (2018) Padlock Probe Assay for Detection and Subtyping of Seasonal Influenza. *Clinical Chemistry* 64(12):1704-1712.

Neumann T, Junker HD, Schmidt K & Sekul R (2007) SPR-based fragment screening: advantages and applications. *Current topics in medicinal chemistry* 7(16):1630-1642.

Nguyen AP & Downard KM (2013) Subtyping of influenza neuraminidase using mass spectrometry. *Analyst* 138(6):1787-1793.

Nikiforov TT, Rendle RB, Kotewicz ML & Rogers Y-H (1994) The use of phosphorothioate primers and exonuclease hydrolysis for the preparation of single-stranded PCR products and their detection by solid-phase hybridization. *Genome Research* 3(5):285-291.

Nilsson M, Gullberg M, Dahl F, Szuhai K & Raap AK (2002) Real-time monitoring of rolling-circle amplification using a modified molecular beacon design. *Nucleic Acids Research* 30(14):e66-e66.

Nilsson M, Malmgren H, Samiotaki M, Kwiatkowski M, Chowdhary B & Landegren U (1994) Padlock probes: circularizing oligonucleotides for localized DNA detection. *Science* 265(5181):2085-2088.

Obande GA & Banga Singh KK (2020) Current and Future Perspectives on Isothermal Nucleic Acid Amplification Technologies for Diagnosing Infections. *Infection and Drug Resistance* 13:455-483.

Payungporn S, Chutinimitkul S, Chaisingh A, Damrongwantanapokin S, Buranathai C, Amonsin A, Theamboonlers A & Poovorawan Y (2006) Single step multiplex real-time RT-PCR for H5N1 influenza A virus detection. *Journal of Virological Methods* 131(2):143-147.

Pevec S & Donlagic D (2014) High resolution, all-fiber, micro-machined sensor for simultaneous measurement of refractive index and temperature. *Optics express* 22(13):16241-16253.

Rector A, Tachezy R & Van Ranst M (2004) A sequence-independent strategy for detection and cloning of circular DNA virus genomes by using multiply primed rolling-circle amplification. *Journal of virology* 78(10):4993-4998.

Rosário-Ferreira N, Preto AJ, Melo R, Moreira IS & Brito RMM (2020) The Central Role of Non-Structural Protein 1 (NS1) in Influenza Biology and Infection. *International Journal of Molecular Sciences* 21(4):1511.

Sable R, Jambunathan N, Singh S, Pallerla S, Kousoulas KG & Jois S (2018) Proximity ligation assay to study protein–protein interactions of proteins on two different cells. *Biotechniques* 65(3):149-157.

Sefah K, Shangguan D, Xiong X, O'donoghue MB & Tan W (2010) Development of DNA aptamers using Cell-SELEX. *Nature protocols* 5(6):1169-1185.

Shen B, Li J, Cheng W, Yan Y, Tang R, Li Y, Ju H & Ding S (2015) Electrochemical aptasensor for highly sensitive determination of cocaine using a supramolecular aptamer and rolling circle amplification. *Microchimica Acta* 182(1-2):361-367.

Shi D, Huang J, Chuai Z, Chen D, Zhu X, Wang H, Peng J, Wu H, Huang Q & Fu W (2014) Isothermal and rapid detection of pathogenic microorganisms using a nano-rolling circle amplification-surface plasmon resonance biosensor. *Biosensors and Bioelectronics* 62:280-287.

Strömberg M, Göransson J, Gunnarsson K, Nilsson M, Svedlindh P & Strømme M (2008) Sensitive molecular diagnostics using volume-amplified magnetic nanobeads. *Nano Letters* 8(3):816-821.

Tang X, Morris SL, Langone JJ & Bockstahler LE (2006) Simple and effective method for generating single-stranded DNA targets and probes. *BioTechniques* 40(6):759-763.

Tanner NA, Zhang Y & Jr. TCE (2015) Visual detection of isothermal nucleic acid amplification using pH-sensitive dyes. *BioTechniques* 58(2):59-68.

Tomita N, Mori Y, Kanda H & Notomi T (2008) Loop-mediated isothermal amplification (LAMP) of gene sequences and simple visual detection of products. *Nature protocols* 3(5):877-882.

Tonyushkina K & Nichols JH (2009) Glucose meters: a review of technical challenges to obtaining accurate results. *Journal of Diabetes Science and Technology* 3(4):971-980.

Toyoshima Y, Nemoto K, Matsumoto S, Nakamura Y & Kiyotani K (2020) SARS-CoV-2 genomic variations associated with mortality rate of COVID-19. *Journal of Human Genetics* 65(12):1075-1082.

Tsouti V, Boutopoulos C, Zergioti I & Chatzandroulis S (2011) Capacitive microsystems for biological sensing. *Biosensors and Bioelectronics* 27(1):1-11.

Tuerk C & Gold L (1990) Systematic evolution of ligands by exponential enrichment: RNA ligands to bacteriophage T4 DNA polymerase. *Science* 249(4968):505-510.

Uyttendaele MR & Debevere JM (1999) LISTERIA | Listeria monocytogenes–Detection using NASBA (an Isothermal Nucleic Acid Amplification System). *Encyclopedia of Food Microbiology*, Robinson RK (Édit.) Elsevier, Oxford:1244-1251.

Vorobyeva M, Vorobjev P & Venyaminova A (2016) Multivalent aptamers: Versatile tools for diagnostic and therapeutic applications. *Molecules* 21(12):1613.

Wang J, Wang H, Wang H, He S, Li R, Deng Z, Liu X & Wang F (2019) Nonviolent Self-Catabolic DNAzyme Nanosponges for Smart Anticancer Drug Delivery. *ACS nano* 13(5): 5852–5863

Wang L, Tram K, Ali MM, Salena BJ, Li J & Li Y (2014) Arrest of Rolling Circle Amplification by Protein-Binding DNA Aptamers. *Chemistry-A European Journal* 20(9):2420-2424.

Wang N, Shang J, Jiang S & Du L (2020) Subunit Vaccines Against Emerging Pathogenic Human Coronaviruses. *Frontiers in Microbiology* 11(298).

Wastling SL, Picozzi K, Kakembo AS & Welburn SC (2010) LAMP for human African trypanosomiasis: a comparative study of detection formats. *PLOS Neglected Tropical Diseases* 4(11):e865.

Wei T, Han Y, Li Y, Tsai H-L & Xiao H (2008) Temperature-insensitive miniaturized fiber inline Fabry-Perot interferometer for highly sensitive refractive index measurement. *Optics Express* 16(8):5764-5769.

Weibrecht I, Leuchowius K-J, Clausson C-M, Conze T, Jarvius M, Howell WM, Kamali-Moghaddam M & Söderberg O (2010) Proximity ligation assays: a recent addition to the proteomics toolbox. *Expert review of proteomics* 7(3):401-409.

Wharam SD, Hall MJ & Wilson WH (2007) Detection of virus mRNA within infected host cells using an isothermal nucleic acid amplification assay: marine cyanophage gene expression within Synechococcus sp. *Virology journal* 4(1):1-8.

Wu Z-S, Zhou H, Zhang S, Shen G & Yu R (2010) Electrochemical aptameric recognition system for a sensitive protein assay based on specific target binding-induced rolling circle amplification. *Analytical chemistry* 82(6):2282-2289.

Xiang Y, Deng K, Xia H, Yao C, Chen Q, Zhang L, Liu Z & Fu W (2013) Isothermal detection of multiple point mutations by a surface plasmon resonance biosensor with Au nanoparticles enhanced surface-anchored rolling circle amplification. *Biosensors and Bioelectronics* 49:442-449.

Xu L, Duan J, Chen J, Ding S & Cheng W (2021) Recent advances in rolling circle amplification-based biosensing strategies-A review. *Analytica Chimica Acta* 1148:238187.

Yang L, Fung CW, Cho EJ & Ellington AD (2007) Real-time rolling circle amplification for protein detection. *Analytical chemistry* 79(9):3320-3329.

Zhang Z, Ali MM, Eckert MA, Kang D-K, Chen YY, Sender LS, Fruman DA & Zhao W (2013) A polyvalent aptamer system for targeted drug delivery. *Biomaterials* 34(37):9728-9735.

Zhao W, Ali MM, Brook MA & Li Y (2008) Rolling circle amplification: applications in nanotechnology and biodetection with functional nucleic acids. *Angewandte Chemie International Edition* 47(34):6330-6337.

Zhao Y, Zhao H, Lv R-q & Zhao J (2019) Review of optical fiber Mach–Zehnder interferometers with micro-cavity fabricated by femtosecond laser and sensing applications. *Optics and Lasers in Engineering* 117:7-20.

Zhou L, Ou L-J, Chu X, Shen G-L & Yu R-Q (2007) Aptamer-based rolling circle amplification: a platform for electrochemical detection of protein. *Analytical chemistry* 79(19):7492-7500.

9 APPENDIX 1 (SUPPLEMENTARY INFORMATION OF PUBLICATIONS)

Supplementary materials for:

Simple rolling circle amplification colorimetric assay based on pH for target DNA detection

Seyed Vahid Hamidi and Jonathan Perreault

INRS, Centre INRS – Institut Armand-Frappier, 531 boul. des Prairies, Laval, Québec, Canada.

Table 2.S1 Sequences of the oligonucleotides that have been used in the project.

H_5N_1 PLP [13,14]	5′P*GGATGATCTGAATTTTCTCAAA*CCCGGTCAACTTCAAGCTCCTAAGCCTTGACGAA CCGCTTTGCCTGACTGAATGCAGCGTAGGTATCGAC*TTCGGACCAAGAACTTTTGG3′*
M13 PLP	5′P*GTCATAGCTGTTTCCTGTGTG*CCCGGTCAACTTCAAGCTCCTAAGCCTTGACGAAC CGCTTTGCCTGACTGAATGCAGCGTAGGTATCGAC*TGAGCTCGAATTCGTAATCATG*3′
RCA forward primer [13, 14]	5′GCTTAGGAGCTTGAAGTTGAC3′
RCA reverse primer [13, 14]	5′GCTTTGCCTGACTGAATGCAG3′
H_5N_1 target [13, 14]	5′TTTGAGAAAATTCAGATCATCCCCAAAAGTTCTTGGTCCGA3′
H_5N_1 target (SNP)	5′TTTGAGAAAATTCAGATCATCCGCAAAAGTTCTTGGTCCGA3′
M13 target	5′AATTTCACACAGGAAACAGCTATGACCATGATTACGAATTCGAGCTCGGTAC3′
PCR forward primer	5′CACAGGAAACAGCTATGAC3′
PCR reverse primer	5′GAGCTCGAATTCGTAATCAT3′

P at the 5′ ends of PLPs indicate phosphorylation. For PLP and target sequences, bases in *italic* correspond to those involved in hybridization between PLP and target.

Supplementary materials for:

Real-time isothermal DNA amplification monitoring in picoliter volumes using optical fiber sensor.

Monika Janik[1],[2],*, ǂ, Seyed Vahid Hamidi[3], ǂ, Marcin Koba1,[4], Jonathan Perreault[3], Ryan Walsh[3], Wojtek J. Bock[5], Mateusz Śmietana[1]

[1]Warsaw University of Technology, Institute of Microelectronics and Optoelectronics, Koszykowa 75, 00-662, Warszawa, Poland

[2]Gdansk University of Technology, Faculty of Electronics, Telecommunications and Informatics, Department of Metrology and Optoelectronics, Narutowicza 11/12, 80-233 Gdansk

[3] INRS Centre Armand-Frappier Santé Biotechnologie, 531 boulevards des Prairies Laval (QC) Canada

[4]National Institute of Telecommunications, Szachowa 1, 04-894, Warszawa, Poland

[5]Photonic Research Centre, University of Quebec in Outaouais, 101 rue Saint-Jean-Bosco, Gatineau (QC), Canada

ǂThese two authors contributed equally as first authors in this article.

Experimental work.

To visualize the presence of DNA resulting from RCA reactions we have performed another test using SYBR Green that confirmed our functionalization, amplification, and thus detection method.

RCA reaction on a glass slide

Glass slides were functionalized with DBCO modified primers using the same procedure used to functionalize the optical fibers with the following exceptions, the 2 hours curing step at 105°C was omitted, RCA reactions were performed in a final volume of 30 µL by including different concentrations of c-PLP, L-PLP (linear PLP), and no PLP (depending on the reaction) with a final concentration of 416 µM deoxyribonucleotide triphosphate (dNTP) (Thermo Fisher Scientific, USA), 1X Phi29 DNA polymerase buffer (NEB), 30 µg bovine serum albumin – BSA (NEB), 8 units of Phi29 DNA polymerase (NEB) and a final concentration of 1x SYBR Green dye (Invitrogen, USA) which becomes fluorescent upon binding dsDNA. The reactions were placed on functionalized glass slides at room temperature for 90 mins and then glass surfaces were

scanned with a Typhoon FLA 9500 biomolecular imager (GE Healthcare) to visualize the presence of the dsDNA resulting from the HRCA reactions.

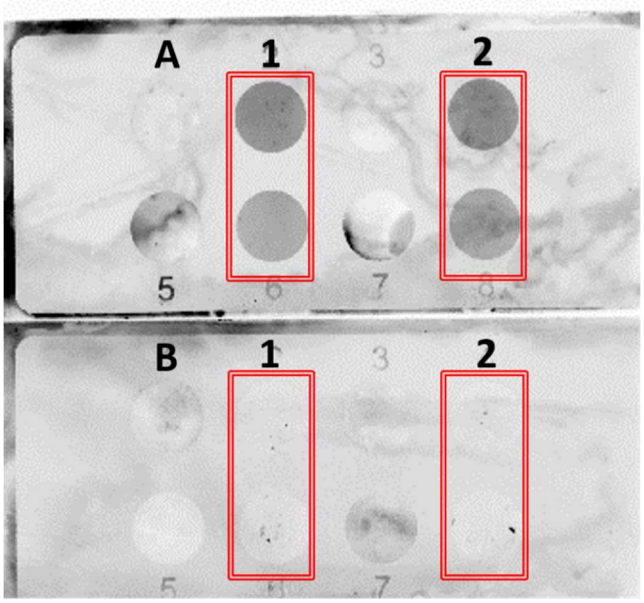

Figure 3.S1 **Visualization of the RCA reaction on a glass slide using SYBR Green. (A) Positive controls. A1 and A2, RCA reaction in the presence of 50 nM and 10 nM of c-PLP, respectively. (B) Negative controls. B1 and B2: RCA reaction in the absence of PLP and the presence of 50 nM of L-PLP (noncircularized PLP), respectively.**

Supplementary materials for:

Simple in-vitro single stranded linear and circular DNA preparation and validation via SELEX using through phosphor-derived modifications

Seyed Vahid Hamidi and Jonathan Perreault*

INRS Centre Armand-Frappier Santé Biotechnologie, 531 boulevards des Prairies Laval (QC) Canada.

Table 4.S1 Oligonucleotide sequences used in this study.

PCR and RCA forward primers	5′-AACGCCTATGTCTCGTTGAAGCAGC3′
	5′-P-AACGCCTATGTCTCGTTGAAGCAGC-3′
	5′-A*A*C*G*C*CTATGTCTCGTTGAAGCAGC-3′
	5′-P-A*A*C*G*C*CTATGTCTCGTTGAAGCAGC-3′
	5′-P-T*A*C*G*C*CTATGTCTCGTTGAAGCAGC-3′
PCR and RCA reverse primer	5′-P-TTGCCGGTGACAGACTGCTTGCATA-3′
	5′-P-CTGCCGGTGACAGACTGCTTGCATA-3′
Template/library	5′-AACGCCTATGTCTCGTTGAAGCAGCNNNNNNNNNNNNNNNNNNNNNNNNNNNNNNNNNNNNNNNNNNNNTATGCAAGCAGTCTGTCACCGGCAA-3′
	5′-P-AACGCCTATGTCTCGTTGAAGCAGCNNNNNNNNNNNNNNNNNNNNNNNNNNNNNNNNNNNNNNNNNNNNTATGCAAGCAGTCTGTCACCGGCAA-3′
Complementary strands	5′-GCTGCTTCAACGAGACATAGGCGTTTTGCCGGTGACAGACTGCTTGCATA-3′
	5′-GCTTCAACGAGACATAGGCGTTTTGCCGGTGACAGACTGCTT-3′
	5′-CAACGAGACATAGGCGTTTTGCCGGTGACAGACTG-3′
	5′-CAACGAGACATAGGCGTACTGCCGGTGACAGACTG-3′
Complementary strands with additional T	5′-GCTGCTTCAACGAGACATAGGCGTTTTTGCCGGTGACAGACTGCTTGCATA-3′
	5′-GCTTCAACGAGACATAGGCGTTTTTGCCGGTGACAGACTGCTT-3′
	5′-CAACGAGACATAGGCGTTTTTGCCGGTGACAGACTG-3′
	5′-CAACGAGACATAGGCGTATCTGCCGGTGACAGACTG-3′
Labeled complementary strand	Cy5-ACATAGGCGTT

P indicates phosphorylation modifications
***shows phosphorothioate bond modifications**

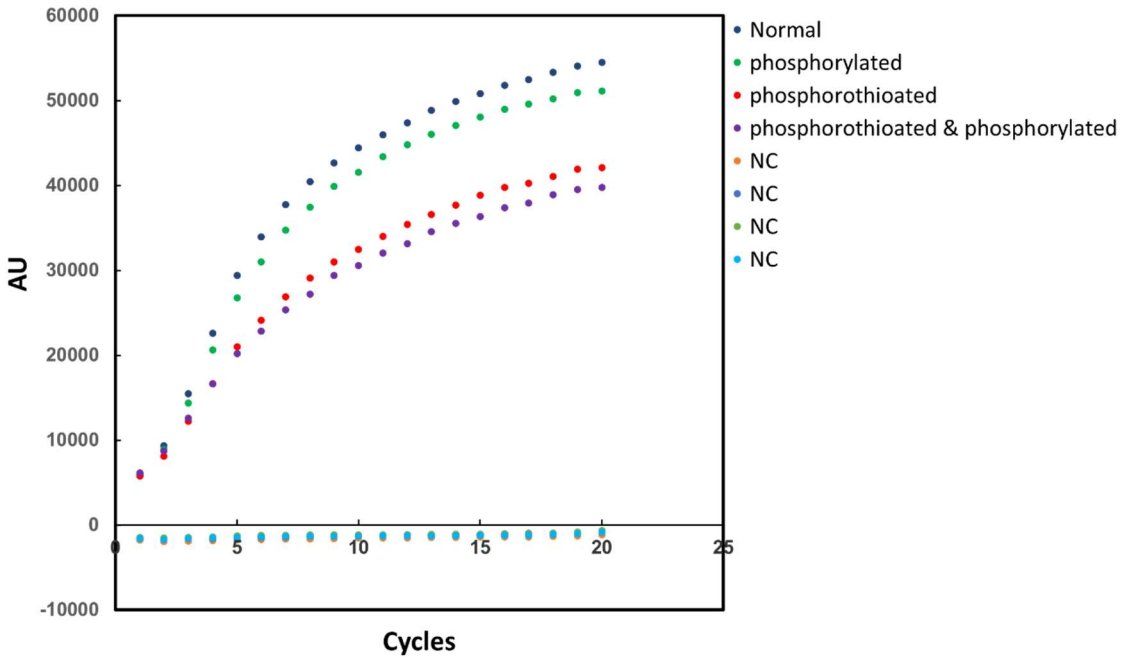

Figure 4.S1 **Real-time monitoring of modified PCR primers using qPCR technique. Primers used are as indicated in the legend within the figure, NC are the corresponding negative controls.**

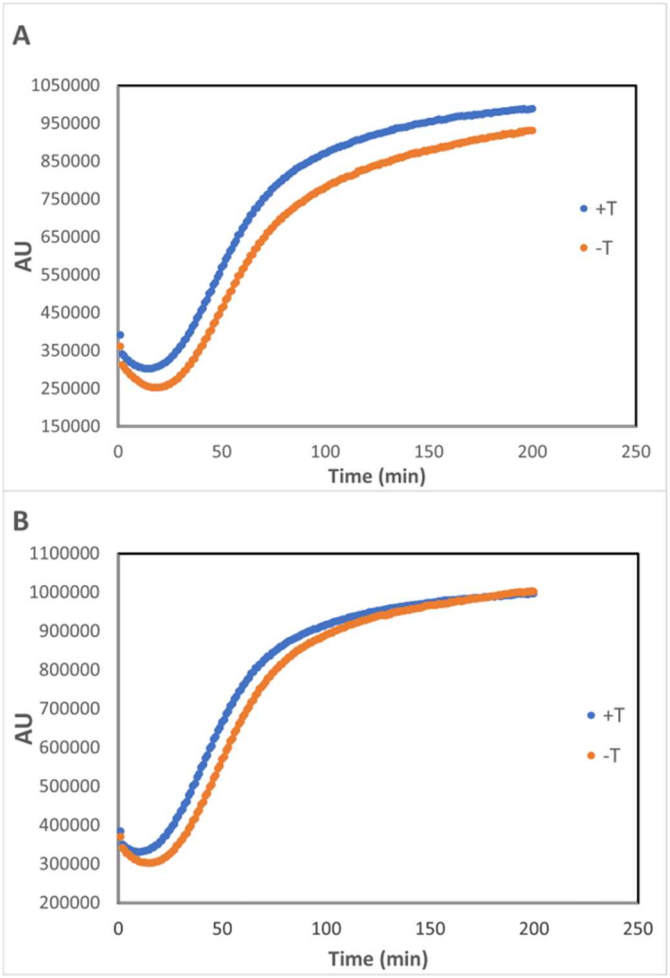

Figure 4.S2 **HRCA reaction using circularized ssPCRP with and without additional T. (A) Monitoring of HRCA reaction via circularized ssPCRP sealed by T4 DNA ligase using specific complementary strand. (B) HRCA reaction through circular ssPCRP sealed by Taq DNA ligase and specific complementary strand.**

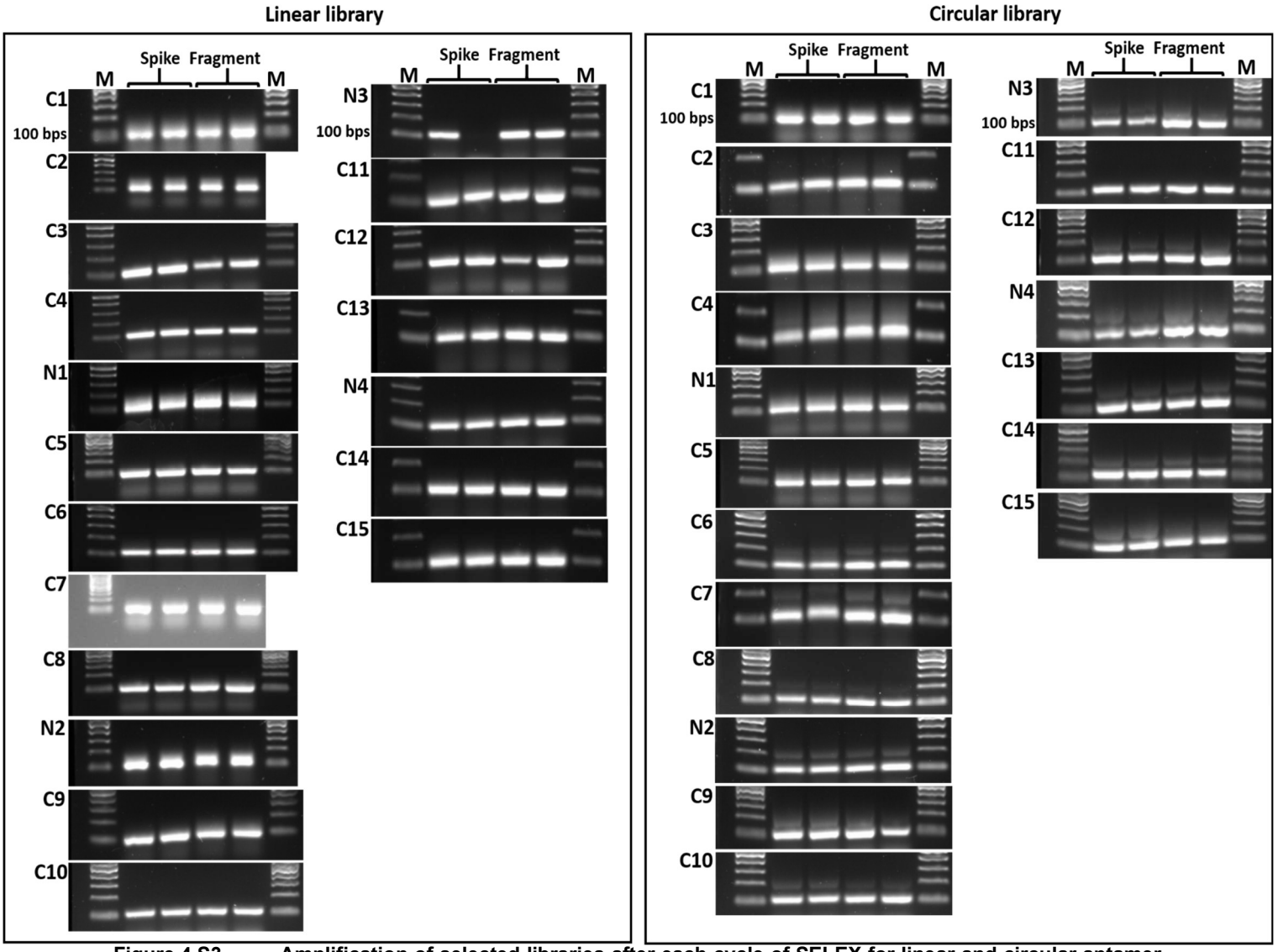

Figure 4.S3 **Amplification of selected libraries after each cycle of SELEX for linear and circular aptamer selection targeting MERS-CoV spike protein. M, C and N refer to ladder, SELEX cycle, and negative selection respectively. The reason why additional bands are seen in PCR amplification products of circular libraries, especially generations 6, 7, N2 is that it is likely two ssPCRs were hybridized with two complementary strands during ligation process and thus dimers were produced during ssPCRs circularization reaction. PCR products are shown in duplicate for each full spike or RBD because during each SELEX round one PCR product was used for the next SELEX round and the other one was kept as a backup in case something went wrong during the SELEX process, both are shown.**

Table 4.S2 Detailed conditions used for circular and linear aptamer selection against MERS CoV spike protein.

Target	Library	Rounds	Incubation time (min)	No of washes	Added target (µl)	Washing time (min)
Full spike & fragment (RBD)	Linear & circular	C1	120	1	200	30
		C2	120	1	20	30
		C3	120	1	20	30
		C4	120	1	20	30
		N1	30	-	10 (beads)	-
		C5	105	1	20	30
		C6	90	1	20	30
		C7	75	1	20	45
		C8	60	1	20	45
		N2	60	-	15 (beads)	-
		C9	45	2	20	45
		C10	30	2	15	45
		N3	30	-	10 (lysozyme)	-
		C11	30	3	15	60
		C12	30	2	10	60
		C13	30	3	10	60
		N4	60	-	15 (lysozyme)	-
		C14	10	3	10	60
		C15	5	2	5	60

10 APPENDIX 2 (PERMISSIONS)

Fig. 1.1 Order Number: 5039540102553

Fig. 1.2 The IEEE does not require individuals working on a thesis to obtain a formal reuse license.

Fig. 1.4 Order Number: 5039551510273

Fig. 1.6 Order Number: 5043280306424

Fig. 1.7 Order Number: 5039590086854

Fig. 1.7 If you are not the author of this article and you wish to reproduce material from it in a third-party non-RSC publication you must formally request permission using Copyright Clearance Center.

Fig. 1.8 Order Number: 5039590466686

Fig. 1.10 Order Number: 5039610689186

Fig. 1.12 & Fig. 1.13 Order Number: 5039611106365

Fig. 1.14 PERMISSION/LICENSE IS GRANTED FOR YOUR ORDER AT NO CHARGE.

Fig. 1.15 PERMISSION/LICENSE IS GRANTED FOR YOUR ORDER AT NO CHARGE.

Fig. 1.16 & Fig. 1.17 Order Number: 5039630745852

Fig. 1.18 & Fig. 1.19 Order number 1108655

Fig. 1.20 Order Number: 5039640354360

Fig. 1.21 PERMISSION/LICENSE IS GRANTED FOR YOUR ORDER AT NO CHARGE.

Fig. 1.22 & Fig. 7.1 Order Number: 5039641147123

Fig. 1.23 & Fig. 1.24 No special permission is required to reuse all or part of article published by MDPI, including figures and tables.

Table 1.1 Order Number 5150970565948

Table 1.2 Order Number: 1148322

Fig. 2.1 to 2.7, Table 2.1, Table 2.S1 Please note that, as the author of this Elsevier article, you retain the right to include it in a thesis or dissertation, provided it is not published commercially. Permission is not required, but please ensure that you reference the journal as the original source.

Fig. 3.1 to 3.7, Table 3.1, Table 3.S1 Authors contributing to RSC publications (journal articles, books or book chapters) do not need to formally request permission to reproduce material contained in this article provided that the correct acknowledgement is given with the reproduced material.

Fig. 5.1 This is an open access article distributed under the terms of the Creative Common CC BY license, which permits unrestricted use, distribution, and reproduction in any medium, provided the original work is properly cited. You are not required to obtain permission to reuse this article.

Fig. 5.2 PERMISSION/LICENSE IS GRANTED FOR YOUR ORDER AT NO CHARGE

Fig. 5.3 Taylor & Francis is pleased to offer reuses of its content for a thesis or dissertation free of charge contingent on resubmission of permission request if work is published.

Fig. 5.4 Under this (PLOS ONE) Open Access license, you as the author agree that anyone can reuse your article in whole or part for any purpose, for free, even for commercial purposes. Anyone may copy, distribute, or reuse the content as long as the author and original source are properly cited. This facilitates freedom in re-use and also ensures that PLOS content can be mined without barriers for the needs of research.

Fig. 7.2 Order Number: 5039651092576